DRAFT VERSION 1.005
July 1, 2008

Surface meteorology and Solar Energy (SSE) Release 6.0 Methodology

I. Introduction

II. What's New

III. Overview of Underlying NASA Data and Parameters in SSE Release 6.0

IV. All Sky Horizontal Surface Insolation

V. All Sky Horizontal Diffuse and Direct Normal Radiation

VI. Clear Sky Total, Horizontal Diffuse and Direct Normal Radiation

VII. All Sky Monthly Tilted Surface Insolation

VIII. Meteorological Parameters
- **A. Global Temperatures**
  - **i. Climate Zone**
  - **ii. Heating/Cooling Degree Days**
- **B. Surface Pressure**
- **C. Humidity**
- **D. Precipitation**

IX. Wind Speed Parameters

X. References

I. Introduction

NASA, through its' Earth science research program has long supported satellite systems and research providing data important to the study of climate and climate processes. These data include long-term estimates of meteorological quantities and surface solar energy fluxes. These satellite and modeled based products have also been shown to be accurate enough to provide reliable solar and meteorological resource data over regions where surface measurements are sparse or nonexistent, and offer two unique features – the data is global and, in general, contiguous in time. These two important characteristics, however, tend to generate very large data archives which can be intimidating for commercial users, particularly new users with little experience or resources to explore these large data sets. Moreover the data products contained in the various NASA archives are often in formats that present challenges to new users. Accordingly, NASA's Earth Applied Sciences program has provided the means to make these data available for government and public sector usage. To foster the usage of the global solar and meteorological data, NASA supported, and continues to support, the development of the Surface meteorology and Solar Energy (SSE) dataset which has been formulated specifically for photovoltaic and renewable energy system design needs. Of equal important is the access to these data; to this end the SSE parameters are available via a user friendly web-based portal designed based on user needs.

The original SSE data-delivery web site, intended to provide easy access to parameters needed in the renewable energy industry (e.g. solar and wind energy), was released to the public in 1997. The solar and meteorological data contained in this first release was based on the 1993 NASA/World Climate Research Program Version 1.1 Surface Radiation Budget (SRB) science data and TOVS data from the International Satellite Cloud Climatology Project (ISCCP). This initial design approach proved to be of limited value because of the use of "traditional" scientific terminology that was not compatible with terminology/parameters used in the energy industry to design renewable energy power systems. After additional consultation with industry, Release 2 SSE was made public in 1999 with parameters specifically tailored to the needs of the renewable energy community. Subsequent releases of SSE - SSE-Release 3.0 in 2000, SSE-Release 4.0 in 2003, SSE-Release 5.0 in 2005, and now SSE-Release 6.0 in 2008 – have continued to build upon an interactive dialog with potential customers resulting in updated parameters using revised NASA data as well as inclusion of new parameters as requested by the user community.

The Prediction Of Worldwide Energy Resource (POWER) project was initiated in 2003 both to improve subsequent releases of SSE, and to create new datasets applicable to other industries from new satellite observations and the accompanying results from forecast modeling. The POWER web interface (http://power.larc.nasa.gov) currently encompasses the SSE data set, tailored for the renewable energy industry, as well as parameters tailored for the sustainable buildings community, and the bio-energy/agricultural industries. In general, the underlying data behind the parameters used by each of these industries is the same – solar radiation and meteorology, including surface and air temperatures, moisture, and winds.

The purpose of this document is to provide data users of POWER/SSE Release 6.0 insight into the underlying source for the solar and meteorological data sets, and to provide additional information relative to the various industry specific parameters, their limitations, and estimated accuracies based on information available to NASA at the time of this document. The intent is to provide information that will enable new and/or long time users to make decisions concerning the suitability of the POWER/SSE data for his or her project in a particular region of the globe. And finally, it is noted that SSE Release 6.0 and this document is focused primarily on parameters of interest to the renewable energy industry, although there are many parameters common to both the SSE and Sustainable Buildings components of POWER, and the underlying solar and meteorological data for all three POWER components is the derived from common data sources.

In general, meteorology and solar radiation for SSE Release 6.0 were obtained from the NASA Science Mission Directorate's satellite and re-analysis research programs. Parameters based upon the solar and/or meteorology data were derived and validated based on recommendations from partners in the energy industry. Release 6.0

extends the temporal coverage of the solar and meteorological data from approximately 11 years to 22 plus years (e.g. July 1983 through June 2005) with improved NASA data, and includes new parameters and validation studies.

The remainder of this section provides a summary of the estimates of the levels of uncertainty for insolation (solar radiation), temperature, surface pressure, relative humidity, and wind speed through comparisons with ground measurement data. A more detained description of the parameters and the procedures used to estimate their uncertainties is given in the subsequent section of the document.

It is generally considered that quality ground-measured data are more accurate than satellite-derived values. However, measurement uncertainties from calibration drift, operational uncertainties, or data gaps are unknown or unreported for most ground site data sets. In 1989, the World Climate Research Program estimated that most routine-operation solar-radiation ground sites had "end-to-end" uncertainties from 6 to 12%. Specialized high quality research sites are hopefully more accurate by a factor of two.

SSE estimates have been compared to ground site data on a global basis. Radiation parameters were compared to data from the Baseline Surface Radiation Network (BSRN) (Table I.1). Meteorological parameters were compared to data from the National Climate Data Center (NCDC) (Table I.2). The SSE Release 6.0 wind speeds have been carried over from SSE Release 4 because newer data sets do not provide enough information about vegetation/surface types. The RETScreen Weather Database (RETScreen 2005) was used to test uncertainties in the SSE Release 4 wind speeds (Table I.3).

Table I-1: Regression analysis of SSE versus BSRN monthly averaged values for the time period July 1983 through June 2006

Parameter	Region	Bias (%)	RMSE (%)
Horizontal Insolation	Global	-0.01	10.25
	60° Poleward	-1.18	34.37
	60° Equatorward	0.29	8.71
Horizontal Diffuse Radiation	Global	7.49	29.34
	60° Poleward	11.29	54.14
	60° Equatorward	6.86	22.78
Direct Normal Radiation	Global	-4.06	22.73
	60° Poleward	-15.66	33.12
	60° Equatorward	2.40	20.93

Table I-2: Linear least squares regression analysis of SSE versus NCDC monthly averaged values for the time period 1983 through 2006					
Parameter	**Slope**	**Intercept**	**R^2**	**RMSE**	**Bias**
Tmax (°C)	0.99	-1.58	0.95	3.12	-1.83
Tmin (°C)	1.02	0.10	0.95	2.46	0.24
Tavg (°C)	1.02	-0.78	0.96	2.13	-0.58
Tdew (°C)	0.96	-0.80	0.95	2.46	-1.07
RH (%)	0.79	12.72	0.56	9.40	-1.92
Heating Degree Days (degree days)	1.02	12.47	0.93	77.20	17.28
Cooling Degree Days (degree days)	0.86	2.36	0.92	28.90	-5.65
Atmospheric Pressure (hPa)	0.89	102.16	0.74	27.33	-10.20

Table I-3: Estimated uncertainty for monthly averaged wind speed for the time period July 1983 through June 1993			
Parameter	**Method**	**Bias**	**RMSE**
Wind Speed at 10 meters for terrain similar to airports (m/s)	RETScreen Weather Database (documented 10-m height airport sites)	-0.2	1.3
	RETScreen Weather Database (unknown-height airport sites)	-0.0	1.3

II. What's New

Relative to the previous version of SSE (i.e. Release 5.1), SSE Release 6.0 has been updated in four basic ways: (1) the solar data in Release 6.0 now spans the 22 years from July 1, 1983 through June 31, 2005, and the meteorological data spans the time period from January 1, 1983 – December 31, 2005, versus the nominal 10 years of coverage in Release 5.1; (2) the solar radiation data is derived from an improved inversion algorithm which provides an overall improvement in the estimation of the surface solar radiation of about 2.8%; (3) the basic temperature data and parameters are based upon the higher spatial resolution Goddard Earth Observing System model version 4 (GEOS-4) versus GEOS-1; and (4) additional parameters of interest to the renewable energy community have been included.

III. Overview of Underlying NASA Data and Parameters in SSE Release 6.0

SSE Release 6.0 (SSE 6.0) contains more than 200 primary and derived solar, meteorology and cloud related parameters. The solar radiation parameters are derived from solar data spanning the 22 year period from July 1, 1983 through June 31, 2005. Parameters based upon meteorological data are derived from data spanning the period from January 1, 1983 – December 31, 2005. Table III.1 gives an overview of the various NASA programs from which the underlying solar and meteorological data are obtained. Table III.2 shows an explicit list of the data used to derive the parameters currently available through SSE 6.0. Table III.3 shows an overview

list of most of the parameters available through SSE 6.0. The parameters listed in Table III.3 are available globally on a 1-degree grid which is selectable by the user. Typically the value of the parameter is given in a tabular format as a monthly average over the 22-year time span July 1983 – June 2005.

<table>
<tr><th colspan="5">Table III-1. POWER/SSE Release 6.0 Data Flow/Sources</th></tr>
<tr><th colspan="4">Programs Contributing to POWER/SSE Release 6.0</th><th>POWER/SSE Release 6.0</th></tr>
<tr><td>NASA/ISCCP & CERES/MODIS: TOA Radiance, Clouds, and Surface Parameters</td><td rowspan="4">⇨</td><td rowspan="4">NASA GEWEX/SRB Release 3.0: Global estimates of the short and long wavelength solar radiation at earth's surface</td><td rowspan="4">⇨</td><td rowspan="6">(See Table 2 for explicit list of data from underlying projects)</td></tr>
<tr><td>NCAR MATCH: Aerosols</td></tr>
<tr><td>TOMS/TOVS: Ozone</td></tr>
<tr><td>NASA/GMAO GEOS-4: Atmospheric temperature and humidity profiles and surface parameters.</td></tr>
<tr><td colspan="3">NASA/GMAO GEOS-1: Winds at 1st layer above the earth's surface</td><td rowspan="2">⇨</td></tr>
<tr><td colspan="3">NASA/TRMM and NOAA/GPCP: Surface precipitation</td></tr>
</table>

The underlying solar and cloud related data (Table III.1) are obtained from the Surface Radiation Budget (SRB) portion of NASA's Global Energy and Water Cycle Experiment (GEWEX). The current SRB archive is Release 3.0 (http://eosweb.larc.nasa.gov/PRODOCS/srb/table_srb.html). The underlying meteorological data are obtained from NASA's Global Model and Assimilation Office (GMAO), Goddard Earth Observing System model version 4 (GEOS-4), and precipitation parameters are obtained from the Global Precipitation Climate Project (GPCP) and the Tropical Rainfall Measurement Mission (TRMM). The wind data is based upon the NASA/GMAO GEOS version 1 (GEOS-1).

The right most column of Table III.2 enumerates the basic parameters that are extracted from the SRB 3.0 archive, the GMAO programs (GEOS-1 & 4), and the NASA/TRMM and NOAA/GPCP programs.

Table III-2. Basic solar and meteorological data used in POWER/SSE Release 6.0		
Contributing Programs (see Table III.1)		**POWER/SSE Archive.**
NASA GEWEX/SRB Release 3.0: Global estimates of the solar and thermal infrared wavelength radiation at earth's surface and top of atmosphere		**Daily averaged parameters for July 1, 1983 through June 30, 2005:** 1. Top of atmosphere insolation 2. Shortwave (solar, 0.2 - 4.0 μm) insolation incident on a horizontal surface at the Earth's surface 3. Longwave (thermal infrared, 4.0 - 100 μm) radiative flux incident on a horizontal surface at the Earth's surface 4. Clear sky insolation on a horizontal surface at the Earth's surface
NASA GMAO GEOS-4: Air temperatures and moisture near the surface and through the atmosphere		**Monthly averaged parameters for July 1, 1983 through June 30, 2005:** 1. Cloud amount at available (0, 3, 6, 9, 12, 15, 18, 21) UT times 2. Frequency of cloud amount at 0, 3, 6, 9, 12, 15, 18, and 21 UT 3. Average insolation at available (0, 3, 6, 9, 12, 15, 18, 21) UT times 4. Average insolation at available (0, 3, 6, 9, 12, 15, 18, 21) UT times (Number of clear sky days (cloud amount < 10%). 5. Surface Albedo 6. Total column precipitable water 7. Minimum available insolation over consecutive-day period (1, 3, 7, 14, and 21 days) 8. Maximum available insolation over consecutive-day period (1, 3, 7, 14, and 21 days) **GEOS-4 3-hourly synoptic parameters (January 1, 1983 – December 31, 2005):** 1. Air temperature at 2m and 10m above the Earth's surface 2. Air pressure 3. Specific humidity 4. Earth's surface temperature **GEOS-1 3-hourly synoptic lowest layer wind speed**. **Daily averaged surface precipitation (January 1, 1997 – Present)**
NASA GMAO GEOS-1: Winds at 50m above earth's surface		
NASA/TRMM and NOAA/GPCP: Surface precipitation		

Table III-3. Overview of parameters available in POWER/SSE Release 6.0

1. Parameters for Solar Cooking:

- Average insolation
- Midday insolation
- Clear sky insolation
- Clear sky days

2. Parameters for Sizing and Pointing of Solar Panels and for Solar Thermal Applications:

- Insolation on horizontal surface (Average, Min, Max)
- Diffuse radiation on horizontal surface (Average, Min, Max)
- Direct normal radiation (Average, Min, Max)
- Insolation at 3-hourly intervals
- Insolation clearness index, K (Average, Min, Max)
- Insolation normalized clearness index
- Clear sky insolation
- Clear sky insolation clearness index
- Clear sky insolation normalized clearness index
- Downward Longwave Radiative Flux

3. Solar Geometry:

- Solar Noon
- Daylight Hours
- Daylight average of hourly cosine solar zenith angles
- Cosine solar zenith angle at mid-time between sunrise and solar noon
- Declination
- Sunset Hour Angle
- Maximum solar angle relative to the horizon
- Hourly solar angles relative to the horizon
- Hourly solar azimuth angles

4. Parameters for Tilted Solar Panels:

- Radiation on equator-pointed tilted surfaces
- Minimum radiation for equator-pointed tilted surfaces
- Maximum radiation for equator-pointed tilted surfaces

5. Parameters for Sizing Battery or other Energy-storage Systems:

- Minimum available insolation as % of average values over consecutive-day period
- Horizontal surface deficits below expected values over consecutive-day period
- Equivalent number of NO-SUN days over consecutive-day period

6. Parameters for Sizing Surplus-product Storage Systems:

- Available surplus as % of average values over consecutive-day period

7. Diurnal Cloud Information:

- Daylight cloud amount
- Cloud amount at 3-hourly intervals
- Frequency of cloud amount at 3-hourly intervals

8. Meteorology (Temperature):

- Air Temperature at 10 m
- Daily Temperature Range at 10 m
- Cooling Degree Days above 18 °C
- Heating Degree Days below 18 °C
- Arctic Heating Degree Days below 10 °C
- Arctic Heating Degree Days below 0 °C
- Earth Skin Temperature
- Daily Mean Earth Temperature (Min, Max, Amplitude)
- Frost Days
- Dew/Frost Point Temperature at 10 m
- Air Temperature at 3-hourly intervals

9. Meteorology (Wind):

- Wind Speed at 50 m (Average, Min, Max)
- Percent of time for ranges of Wind Speed at 50 m
- Wind Speed at 50 m for 3-hourly intervals
- Wind Direction at 50 m
- Wind Direction at 50 m for 3-hourly intervals
- Wind Speed at 10 m for terrain similar to airports

10. Meteorology (Moisture, pressure):

- Relative Humidity
- Humidity Ratio (i.e. Specific Humidity)
- Surface Pressure
- Total Column Precipitable Water
- Precipitation

11. Supporting Information

- Top of Atmosphere Insolation
- Surface Albedo

While it is not the purpose of this document to discuss in detail the process by which either the basic solar data (i.e. SRB Release 3.0), the meteorological data (i.e. GEOS-4), or precipitation data (GPCP/TRMM) are derived, we will provide herein an overview perspective on the process for each of these data sets with particular emphasis on how these data are used in SSE Release 6.0. More detailed descriptions of the SRB, GEOS-4, and GPCP/TRMM data can be found in documentation and publications enumerated on their respective online web sites at http://eosweb.larc.nasa.gov/PRODOCS/srb/table_srb.html, http://gmao.gsfc.nasa.gov/index.php, http://precip.gsfc.nasa.gov, and http://disc.sci.gsfc.nasa.gov/precipitation/.

IV. All Sky Horizontal Surface Insolation:

The solar radiation and cloud parameters contained in SSE 6.0 are obtained directly or derived from parameters available in the SRB Release 3.0 archive (http://eosweb.larc.nasa.gov/PRODOCS/srb/table_srb.html). Figure IV.1 illustrates the major components/processes associated with the Earth's Energy Budget, and Figure IV.2 provides a brief schematic illustration of the process through which the surface solar radiation, or horizontal surface insolation [in industry terms], is inferred from satellite observations.

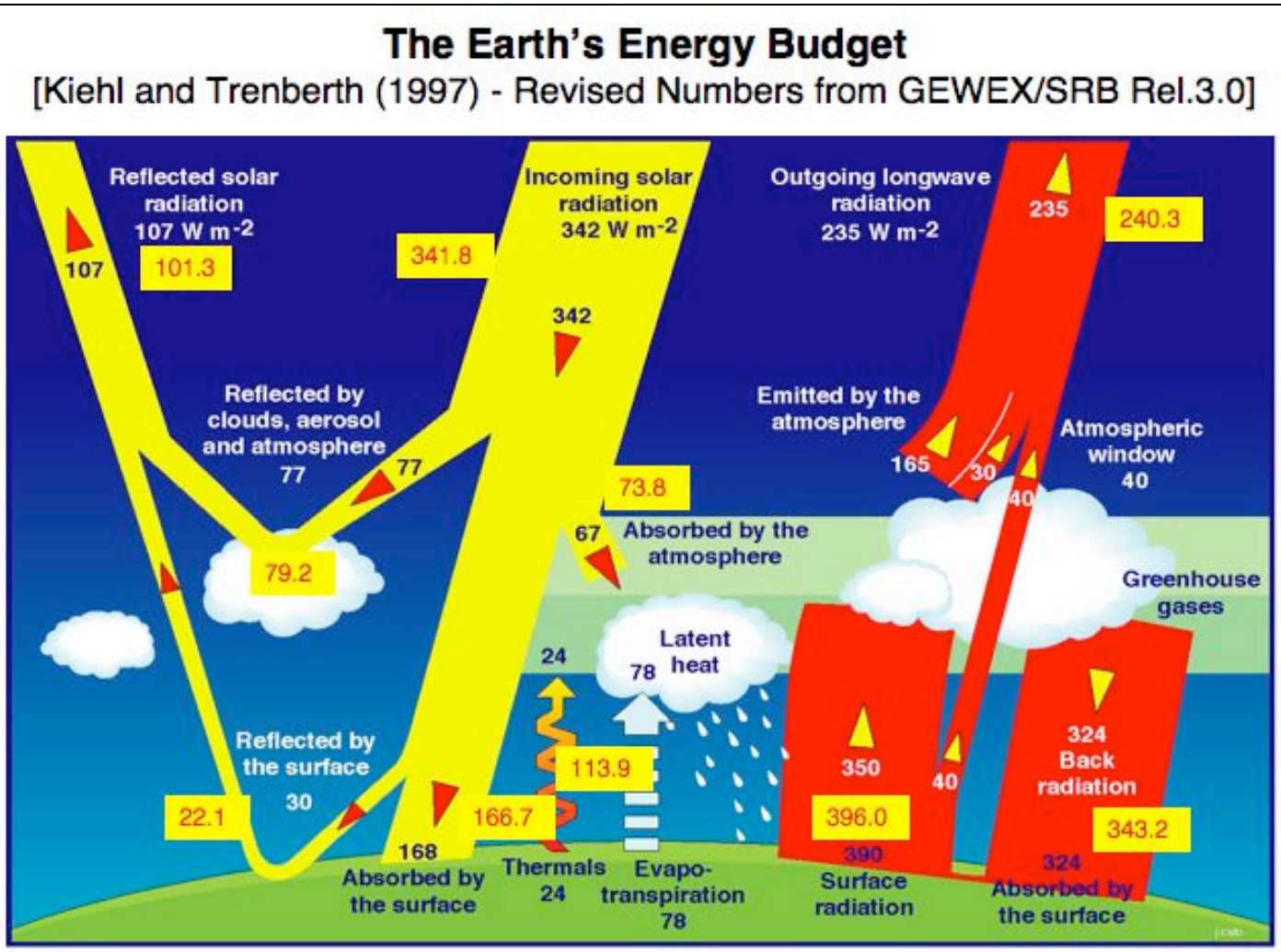

Figure IV-1. The major components/processes associated with the Earth's Energy Budget. The values in the yellow rectangles are based upon the updated solar and thermal infrared radiation estimates in SRB Release 3.0. (Note that all units are in W/m^2; multiplying W/m^2 by 0.024 yields kWh/day/m^2, and by 0.0864 yields MJ/day/m^2.)

Figure IV.1 values in the yellow rectangles are based upon the updated solar and thermal infrared radiation estimates in SRB Release 3.0. These values are based on the 23 year annual global averaged radiative fluxes

with year-to-year annual average variability of +/- 4 W/m^2 in the solar wavelengths and +/- 2 W/m^2 in the thermal infrared (longwave) flux estimates. The most recent satellite based measurements of the incoming solar radiation disagree with previous measurements and indicate this value should be closer 340.3 W/m^2 providing another source of uncertainty.

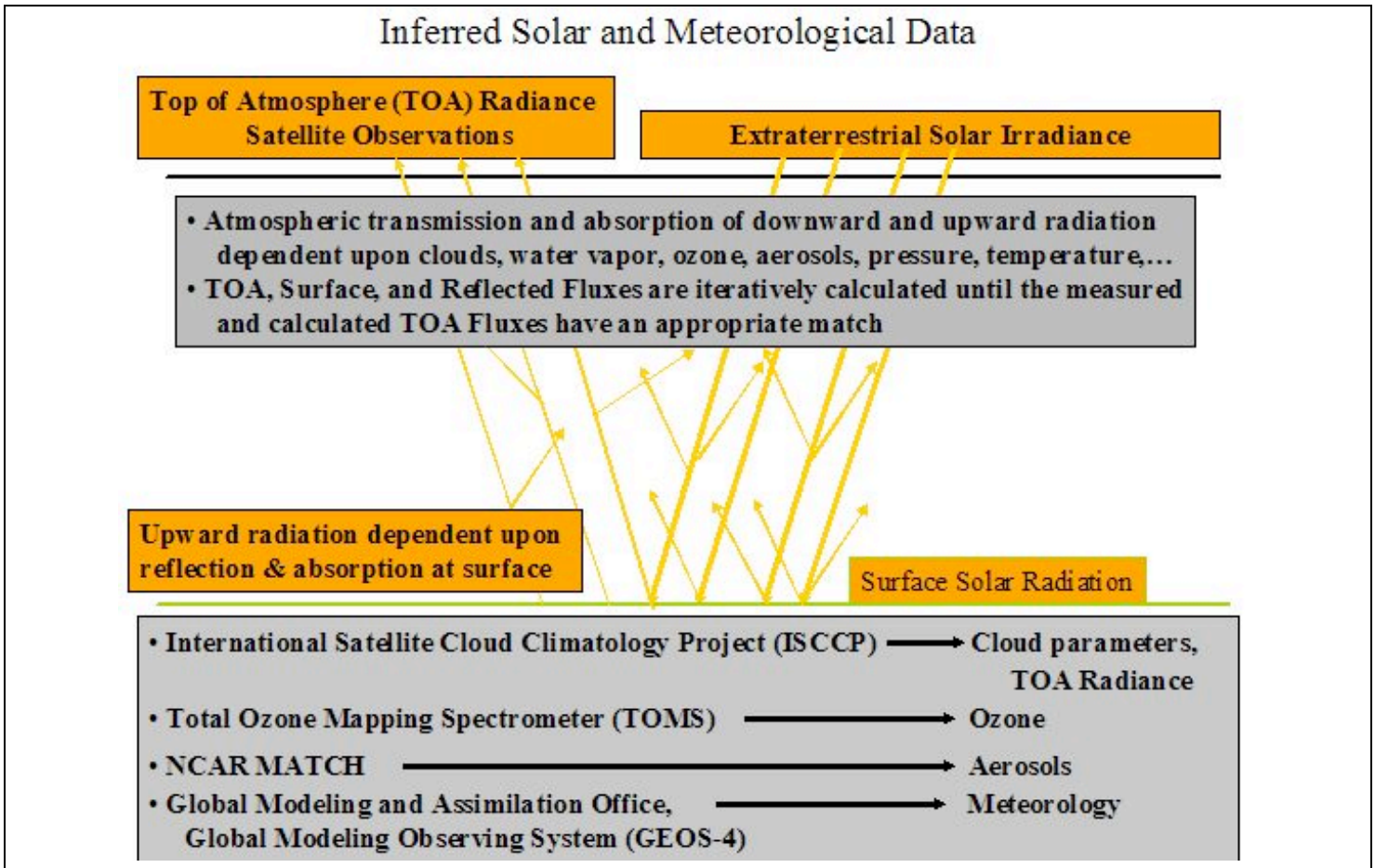

Figure IV-2. Schematic showing the salient features of the process through which the SRB project infers surface solar radiation form satellite observations.

The basic, underlying satellite observations are the top of atmosphere (TOA) radiances consisting of the upwelling thermal radiation from the earth's surface and atmosphere (i.e. long wave radiation) plus solar radiation scattered from the earth's surface and atmosphere (i.e. short wave radiation). Very succinctly, the extraterrestrial solar radiation and the TOA are measured quantities, and the surface solar radiation is the desired quantity.

The process of inferring the surface solar insolation from satellite observations involves the use of a radiative transfer model consisting of a modeled atmosphere and a mathematical model and/or parameterization of the scattering and absorption processes illustrated in Figure IV.1 and IV.2. Within this radiative transfer model a calculative TOA radiance is iteratively compared to the measured TOA radiance. The overall process typically entails iterations on a parameter within the model, such as the aerosol distribution, until the measure TOA and calculated TOA radiances agree to within some acceptable margin of error. The resulting surface insolation, among other parameters, is calculated on each iteration and is one of the output parameters available from the SRB data archive. All SRB parameters are output on a 1^0 by 1^0 global grid at 3-hourly temporal resolution for each day of each month.

A close examination of Figures IV.1 and IV.2, suggest that the above cryptic description of the process employed in the SRB project to estimate the global distribution of solar insolation from satellite observations is,

at best, a gross simplification of a very complex atmospheric process. Within the radiative transfer model, atmospheric transmission, absorption, and scattering, dependent upon the horizontal and vertical distribution of clouds, water vapor, ozone, and atmospheric state variables (temperature and pressure), as well as surface interactions must be accurately modeled or known. Inputs to the model used by the SRB project are listed in the bottom portion of Figure IV.2 and in the left most column of Table III-1.

The cloud parameters and TOA radiances are from the International Satellite Cloud Climatology Project (ISCCP) DX data product (http://eosweb.larc.nasa.gov/PRODOCS/isccp/table_isccp.html). The ISCCP project provides global 3-hourly snapshots of the clouds and the TOA radiance compiled from an array of satellite platforms (i.e. GMS-1 through 8; METEOSAT-2 through 5; NOAA-7 through 14). Within the SRB project, the ISCCP DX data are augmented by data from the Earth Radiation Budget Energy (ERBE - http://eosweb.larc.nasa.gov/PRODOCS/erbe/table_erbe.html), the Clouds and the Earth's Radiant Energy System (CERES - http://eosweb.larc.nasa.gov/PRODOCS/ceres/table_ceres.html), and Multi-angle Imaging Spectro-Radiometer (MISR - http://eosweb.larc.nasa.gov/PRODOCS/misr/data.html) projects. The current ISCCP DX data product covers the time period July 1, 1983 – June 30, 2005. Subsequent updates by ISCCP are planned.

Supporting observations relative to the composition of the atmosphere consist of global ozone obtained from the Total Ozone Mapping Spectrometer (TOMS - http://toms.gsfc.nasa.gov/ozone/ozone_v8.html) and from TIROS Operational Vertical Sounder (TOVS - http://daac.gsfc.nasa.gov/data/datapool/TOVS/index.html); the distribution of aerosols from the NCAR Model of Atmospheric Transport and Chemistry project (MATCH - http://www.cgd.ucar.edu/cms/match/new_website/); and meteorology, including atmospheric moisture, temperature, and pressure, from the Global Modeling and Assimilation Office (GMAO - http://gmao.gsfc.nasa.gov/), Global Modeling Observation System version 4 (GEOS-4).

Data products obtained from the SRB archive are listed in Table III.2. The data products listed are generally available through the SRB data archive although in some instances the product may be bundled with a number of other parameters.

The solar data in the SRB Release 3.0 and subsequently in SSE Release 6 have been tested/validation against research quality observation from the Baseline Surface Radiation Network (BSRN). Figure IV.3 shows the location of ground stations within the BSRN networks/archives. Results and examples of comparisons of solar radiation parameters in SSE Release 6.0 with ground observation from the BSRN network are given below.

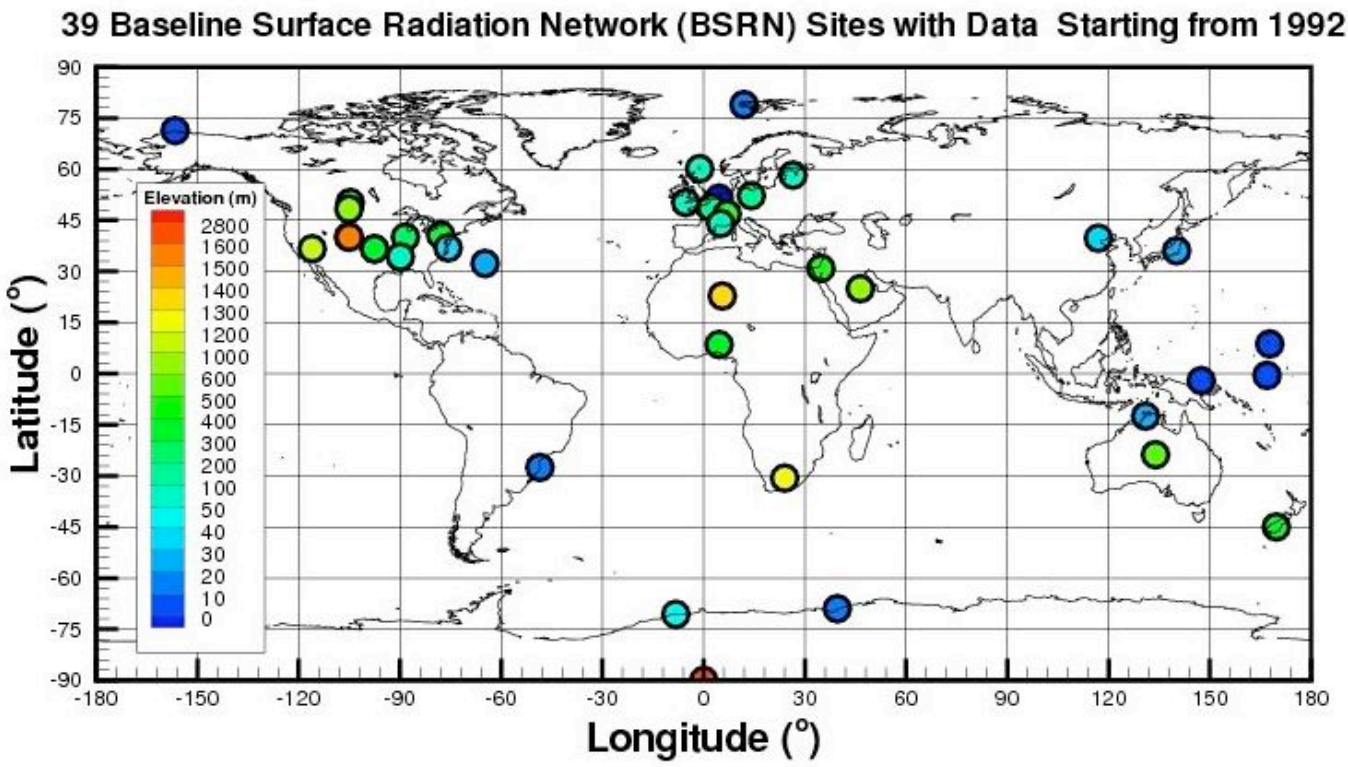

Figure IV-3. Location of ground stations in the Baseline Surface Radiation Network (BSRN).

The total (i.e. diffuse plus direct) surface insolation observed at ground site in the BSRN network (Figure IV-3) have been compared to insolation values from the SRB release 3.0 archive. Figure IV-4 shows the scatter plot and corresponding statistics for the BSRN vs the SRB 3-hourly insolation values for the time period January 1, 1992 – June 30, 2006. We note here that the 3-hourly SRB values are the initial values estimated through the retrieval process described in Section III. The 3-hourly values are used to calculate the daily total insolation shown in Figure IV-5 and the monthly averages shown in Figure IV-6. The 3-hourly values are available through the Atmospheric Science Data Center (ASDC – http://eosweb.larc.nasa.gov). The daily and monthly insolation values are available through SSE Release 6.

Correlation and accuracy parameters for each scatter plots (Figures IV-4 – IV-6) are given in the legend box in each figure. Note that the correlation and accuracy parameters are given for all sites (e.g. Global), for the BSRN sites regions above 60^0 latitude, north and south, and for BSRN sites below 60^0 latitude, north and south. The Bias is the difference between the mean (μ) of the respective solar radiation values for SRB and BSRN. RMS is the root mean square difference between the respective SRB and BSRN values. The correlation coefficient between the SRB and BSRN values is given by ρ, the variance in the SRB values is given by σ, and N is number of SRB:BSRN pairs for each latitude region.

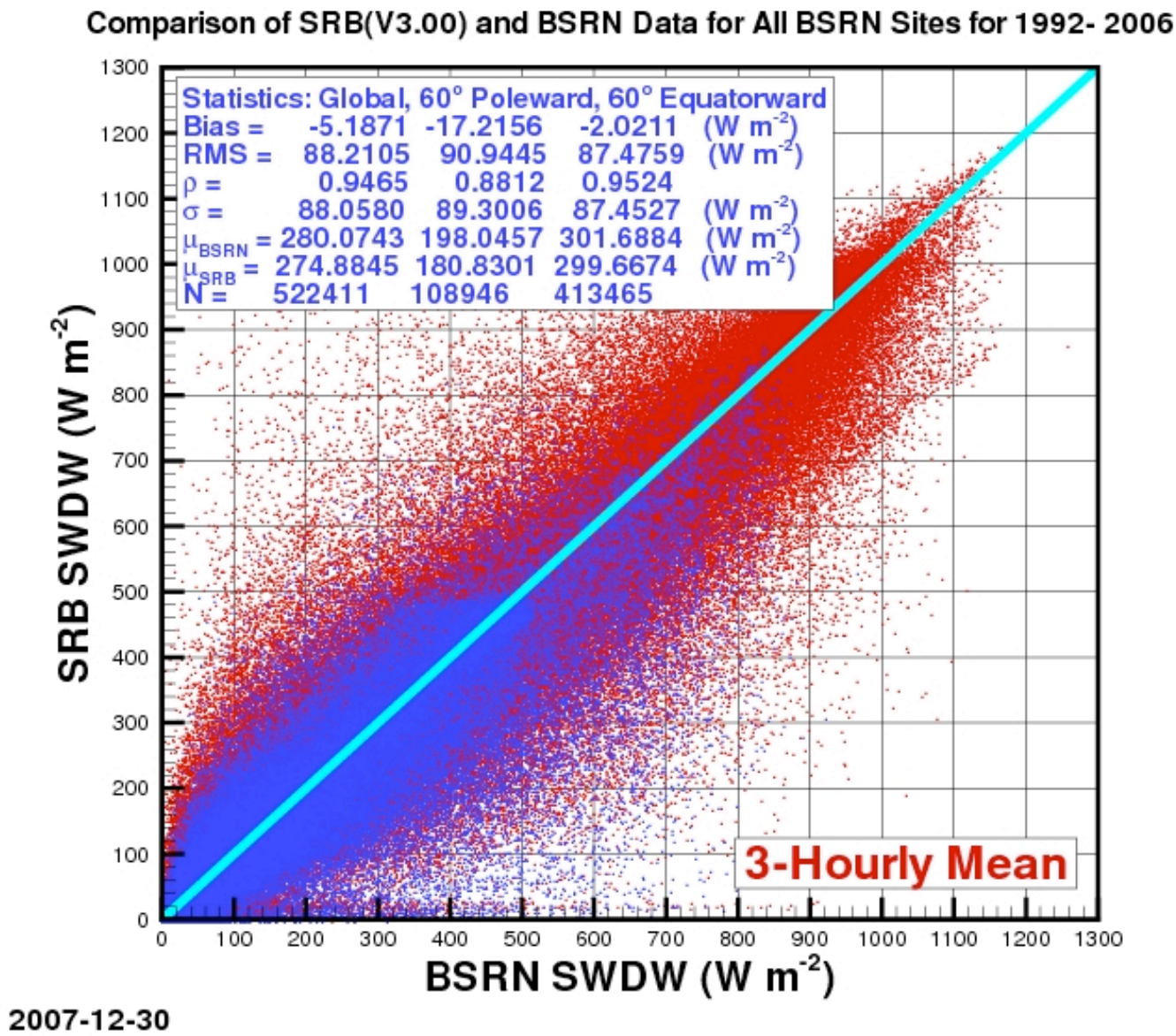

Figure IV-4. Scatter plot of 3-hourly total surface solar radiation observed at BSRN ground sites versus 3-hourly values from the SRB Release 3.0 archive. These 3-hourly are used to calculate the daily total insolation and monthly values that are provided in SSE Release 6.0. (Note that solar insolation is in W/m^2; multiplying W/m^2 by 0.024 yields kWh/day/m^2, and by 0.0864 yields MJ/day/m^2.)

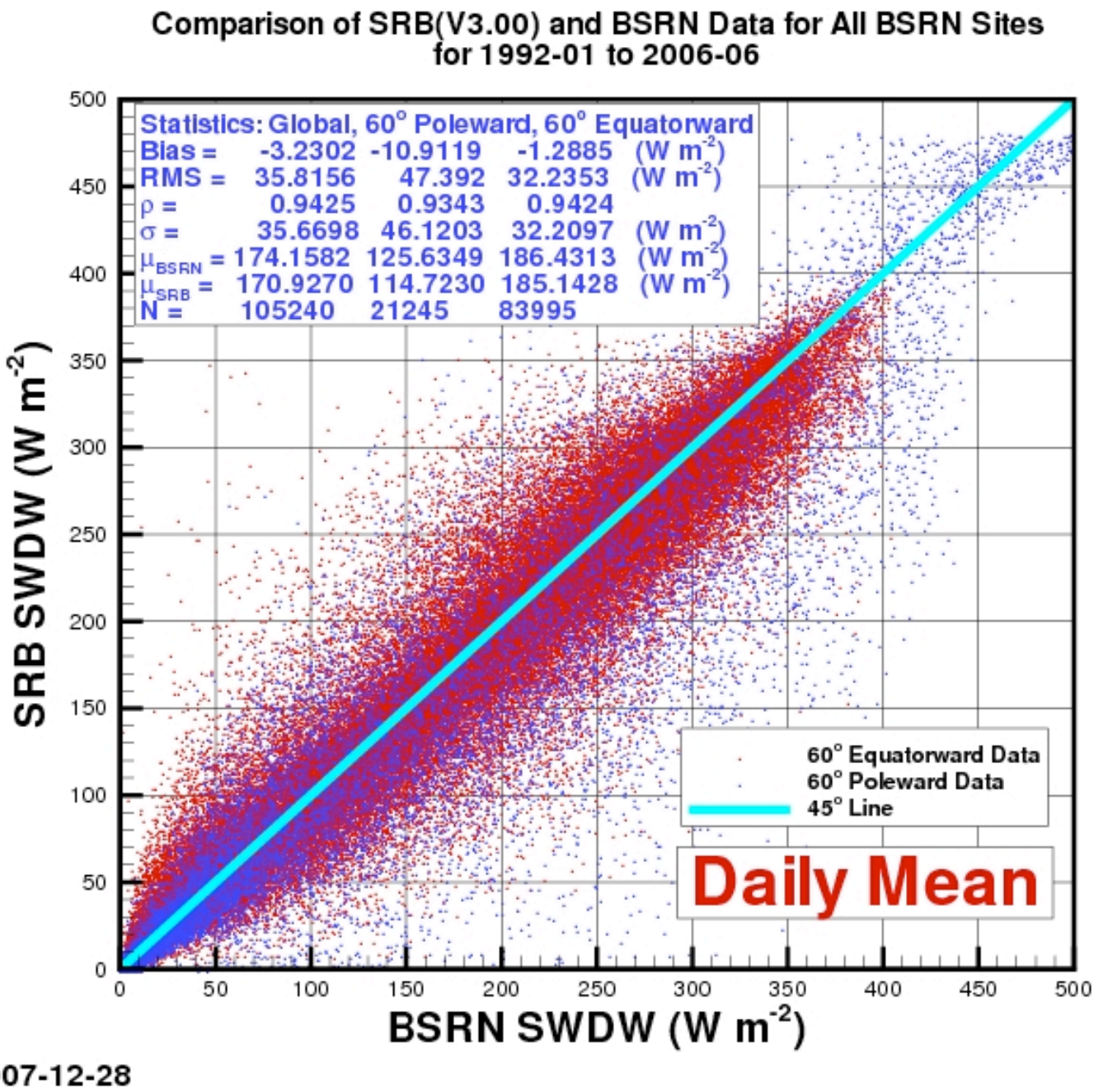

Figure IV-5. Scatter plot of daily total surface solar radiation observed at BSRN ground sites versus daily values from the SRB Release 3.0 archive. These daily are used to calculate the monthly averages that are provided in SSE Release 6.0. (Note that solar insolation is in W/m^2; multiplying W/m^2 by 0.024 yields kWh/day/m^2, and by 0.0864 yields MJ/day/m^2.)

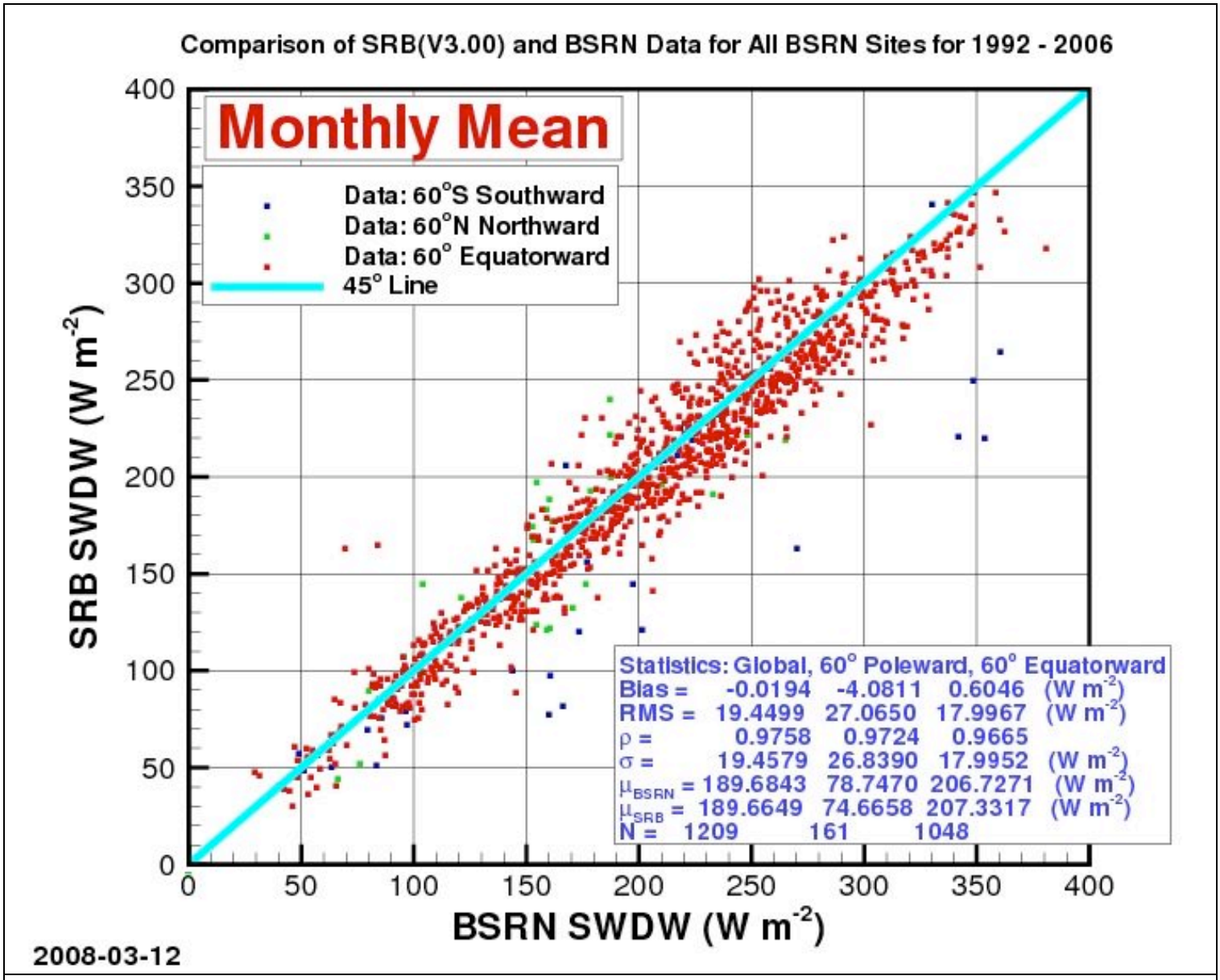

Figure IV-6. Scatter plot of monthly total surface solar radiation observed at BSRN ground sites versus monthly values from the SRB Release 3.0 archive. The daily values illustrated in figure IV-5 are used to calculate the monthly averages. The bias differs from the daily value due to differences in sampling requirements. (Note that solar insolation is in W/m^2; multiplying W/m^2 by 0.024 yields kWh/day/m^2, and by 0.0864 yields MJ/day/m^2.)

V. All Sky Horizontal Diffuse and Direct Normal Radiation:

Estimates of all sky horizontal diffuse, $(H^{All})_{Diff}$, and direct normal radiation, $(H^{All})_{DNR}$, are often needed for hardware system design parameters such as solar panel tilt, solar concentrator size, day lighting, as well as agricultural and hydrology applications. From an observational perspective, $(H^{All})_{Diff}$ at the surface of the earth is that radiation remaining with $(H^{All})_{DNR}$ from the sun's beam blocked by a shadow band or tracking disk. $(H^{All})_{Diff}$ is typically measured using a sun tracking pyrheliometer with a shadow band or disk to block the direct normal radiation from the sun. Similarly, from an observational perspective, $(H^{All})_{DNR}$ is the amount of solar radiation from the direction of the sun, and is typically measured using a pyrheliometer tracking the sun through out the day.

These measurements are difficult to make and consequently are generally only available at high quality observational sites such as those in the BSRN network. In order to use the global estimates of the total surface solar radiation, H^{All}, from SRB Release 3.0 (see previous section) to provide global estimates of $(H^{All})_{Diff}$ and $(H^{All})_{DNR}$, we have developed a set of polynomial equations for the ratio of $[(H^{All})_{Diff}]/[H^{All}]$ using ground based observations from the BSRN network. We extended methods employed by RETScreen (RETScreen 2005) to estimate $(H^{All})_{DNR}$ based on site observations from the BSRN network.

In the remainder of this section we outline the techniques for $[H^{All})_{Diff}]$ and $[(H^{All})_{DNR}]$ available in SSE Release 6.0 and present results of comparative studies with ground site observations, which serve to validate the resulting $[H^{All})_{Diff}]$ and $[(H^{All})_{DNR}]$ and provide a measure of the overall accuracy of our global results.

***All Sky Monthly Averaged Diffuse Radiation* $[(H^{All})_{Diff}]$:** As just noted, measurements of $(H^{All})_{Diff}$, $(H^{All})_{DNR}$, and H^{All} are made at the ground stations in the BSRN network. We used this observational data to develop the set of polynomial equations given below relating the ratio $[(H^{All})_{Diff}]/[H^{All}]$ to the clearness index KT = $[H^{All}]/[H^{TOA}]$. We note that the top of atmosphere solar radiation, H^{TOA}, is known from satellite observations.

For latitudes between 0 and 45 degrees North and South:

$[(H^{All})_{Diff}]/[H^{All}]$ =

0.96268 - 1.45200*KT + 0.27365*KT^2 + (0.04279*KT^3 + 0.000246*SSHA + 0.001189*NHSA

For latitudes between 45 and 90 degrees North and South:

If SSHA = 0 - 81.4 deg:

$[(H^{All})_{Diff}]/[H^{All}]$ =1.441-(3.6839*KT)+(6.4927*KT^2)-(4.147*KT^3)+(0.0008*SSHA)-(0.008175*NHSA)

If SSHA = 81.4 - 100 deg:

$[(H^{All})_{Diff}]/[H^{All}]$ =1.6821-(2.5866*KT)+(2.373*KT^2)-(0.5294*KT^3)-(0.00277*SSHA)-(0.004233*NHSA)

If SSHA = 100 - 125 deg:

$[(H^{All})_{Diff}]/[H^{All}]$ =0.3498+(3.8035*KT)-(11.765*KT^2)+(9.1748*KT^3)+(0.001575*SSHA)-(0.002837*NHSA)

If SSHA = 125 - 150 deg:

$[(H^{All})_{Diff}]/[H^{All}]$ =1.6586-(4.412*KT)+(5.8*KT^2)-(3.1223*KT^3)+(0.000144*SSHA)-(0.000829*NHSA)

If SSHA = 150 - 180 deg:

$[(H^{All})_{Diff}]/[H^{All}]$ = 0.6563-(2.893*KT)+(4.594*KT^2)-(3.23*KT^3)+(0.004*SSHA)-(0.0023*NHSA)

where:

KT = $[H^{All}]/[H^{TOA}]$

SSHA = sunset hour angle in degrees

NHSA = noon solar angle from the horizon in degrees

The above set of polynomial equations relate the ratio of monthly averaged horizontal diffuse radiation for all sky conditions to the monthly averaged total solar radiation for all sky conditions { $[(H^{All})_{Diff}]/[H^{All}]$ } to the clearness index KT = $[H^{All}]/[H^{TOA}]$. In Figure V-1 the monthly averaged diffuse radiation for all sky conditions computed from measured values at the BSRN sites (designated as BSRN SWDF) is compared to values computed from the monthly averaged total insolation obtained from SRB Release 3.0 (designated as SRB SWDF). Correlation and accuracy parameters are given in the legend box. Note that the correlation and accuracy parameters are given for all sites (e.g. Global), for the BSRN sites regions above 60^0 latitude, north and south, and for BSRN sites below 60^0 latitude, north and south. The Bias is the difference between the mean (μ) of the respective solar radiation values for SRB and BSRN. RMS is the root mean square difference between the respective SRB and BSRN values. The correlation coefficient between the SRB and BSRN values

is given by ρ, the variance in the SRB values is given by σ, and N is number of SRB:BSRN pairs for each latitude region.

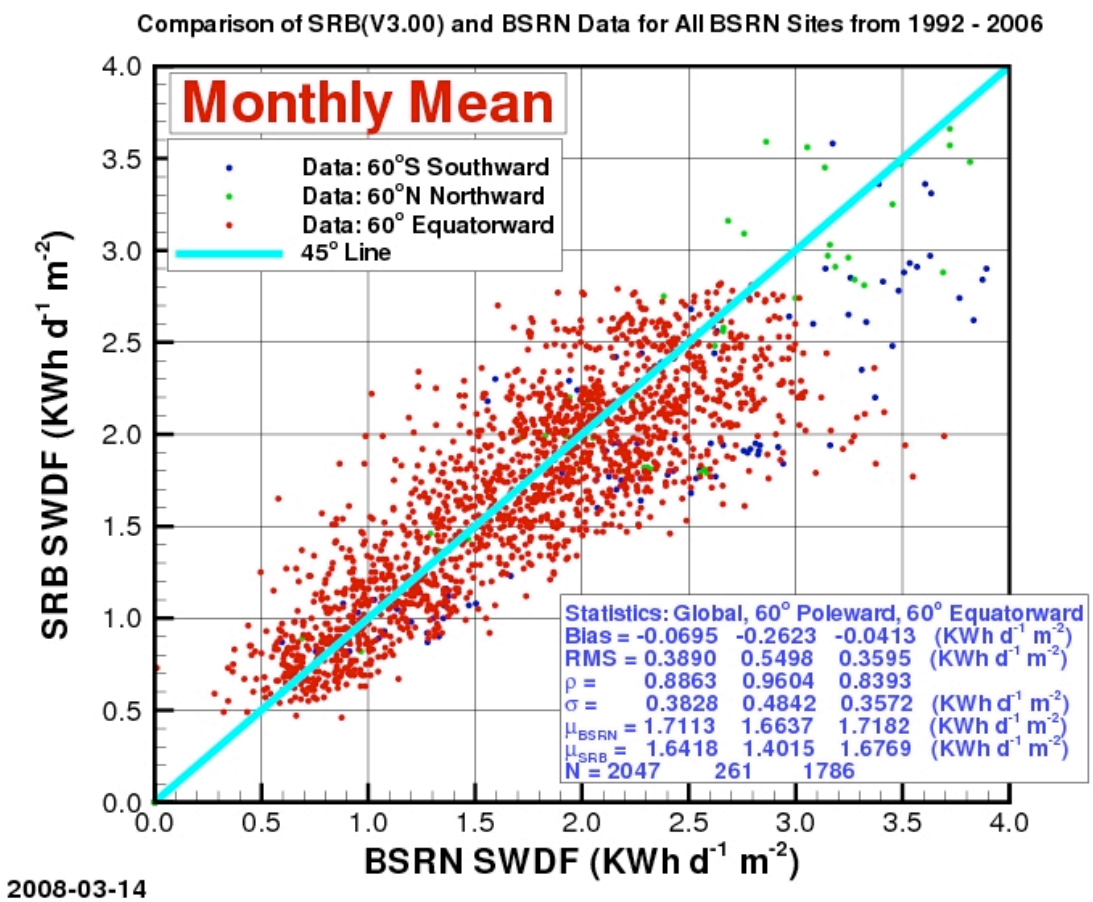

Figure V-1. Scatter plot of the monthly averaged horizontal diffuse radiation calculated from BSRN observations and the monthly averaged horizontal diffuse radiation derived from SRB-Release 3.0 data. (Note that solar radiation is in KWh/day/m^2; multiplying KWh/day/m^2 by 41.67 yields W/m^2, and by 3.6 yields MJ/day/m^2.)

All Sky Monthly Averaged Direct Normal Radiation:

$[(H^{All})_{DNR}] = ([H^{All}] - [(H^{All})_{Diff}])/ COS(THMT)$

where:

THMT is the solar zenith angle at the mid-time between sunrise and solar noon (Gupta, et al. 2001) for the "monthly average day" (Klein 1977).

$COS(THMT) = f + g\,[(g - f)/ 2g]^{1/2}$

H^{All} = Total of direct beam solar radiation and diffuse atmospheric radiation falling on a horizontal surface at the earth's surface

$(H^{All})_{Diff}$ = diffuse atmospheric radiation falling on a horizontal surface at the earth's surface

f = sin(latitude) sin(solar declination)

g = cos(latitude) cos(solar declination)

If the Sunset Hour Angle = 180 degrees, then COS(THMT) = f.

Figure V-2 compares the monthly averaged direct normal radiation for all sky conditions computed from BSRN ground observations (designated as BSRN SWDN) to monthly averaged $(H^{All})_{DNR}$ calculated from SRB-R 3.0 (designated as SRB SWDN in Figure V-2).

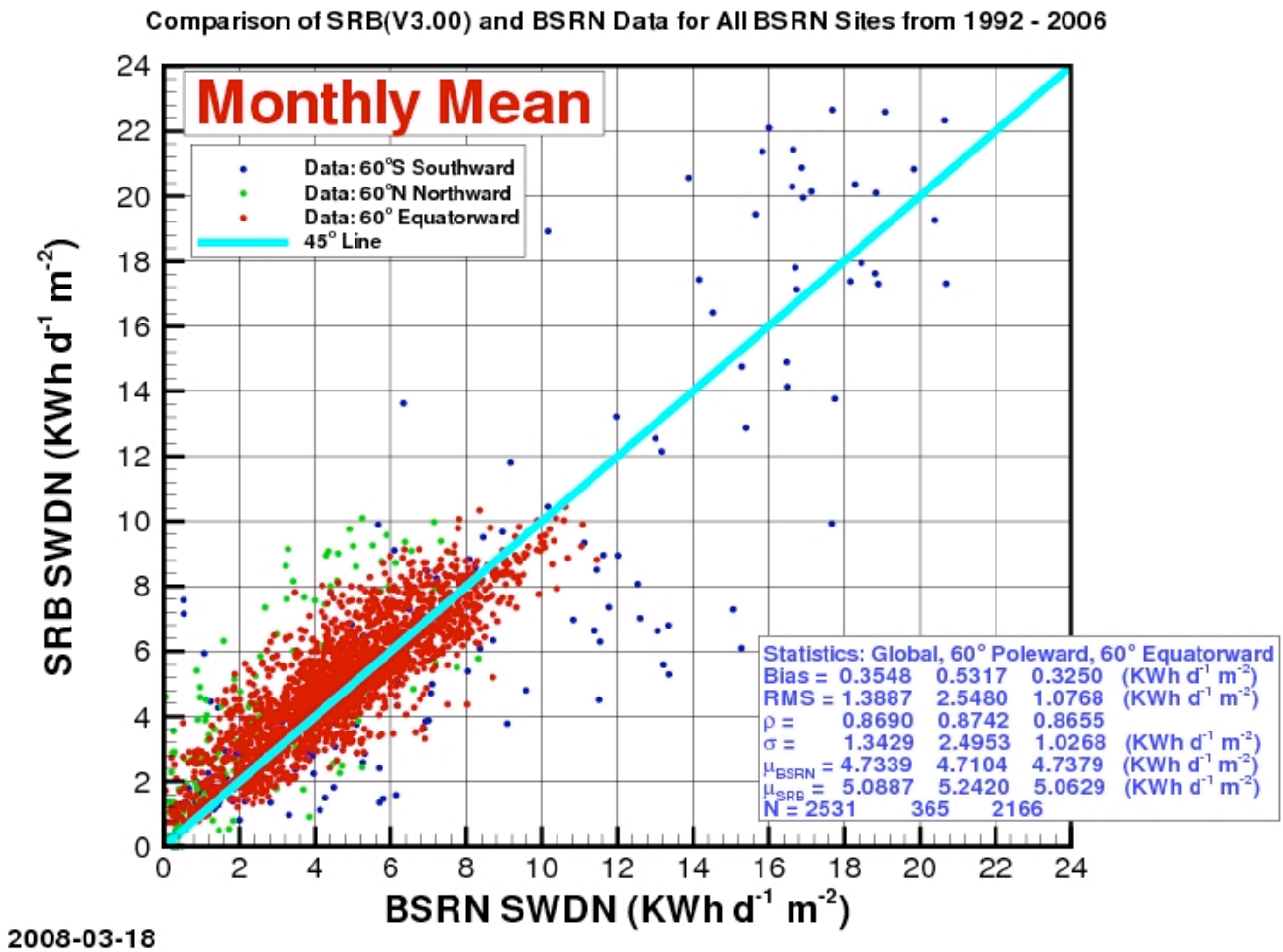

Figure V-2. Scatter plot of the monthly averaged direct normal radiation determined from BSRN ground observations and the monthly average of direct normal radiation derived from SRB-Release 3.0 data. (Note that solar radiation is in KWh/day/m^2; multiplying KWh/day/m^2 by 41.67 yields W/m^2, and by 3.6 yields MJ/day/m^2.)

Correlation and accuracy parameters for each scatter plot are given in the legend box in each figure. Note that the correlation and accuracy parameters are given for all sites (e.g. Global), for the BSRN sites regions above 60^0 latitude, north and south, and for BSRN sites below 60^0 latitude, north and south. The Bias is the difference between the mean (μ) of the respective solar radiation values for SRB and BSRN. RMS is the root mean square difference between the respective SRB and BSRN values. The correlation coefficient between the SRB and BSRN values is given by ρ, the variance in the SRB values is given by σ, and N is number of SRB:BSRN pairs for each latitude region.

VI. Clear Sky Total, Horizontal Diffuse and Direct Normal Radiation.

Our methods for clear sky conditions have been developed specifically in response to the needs of the buildings and solar industries. We have employed explicit equations that can be implemented in either spreadsheets or design software programs for both preliminary and final design purposes, and have concentrated our efforts for calculating and validating $[(H^{Clear})_{Diff}]$ and $[(H^{Clear})_{DNR}]$ for clear sky conditions. We have performed several investigations to create new methods and validate the resulting $[(H^{Clear})_{Diff}]$ and $[(H^{Clear})_{DNR}]$. Our goal has been to provide equations and maps for various buildings, agricultural and solar energy parameters applicable for the entire globe.

In the remainder of this section we outline the techniques use to calculate the values of $[H^{Clear})_{Diff}]$ and $[(H^{Clear})_{DNR}]$ available in SSE Release 6.0, and present results of comparative studies with ground site observations that validate the resulting $[H^{Clear})_{Diff}]$ and $[(H^{Clear})_{DNR}]$ and provide a measure of the overall accuracy of our global results.

Clear Sky Total: The clear sky total insolation, (H^{Clear}), was obtained from the SRB Release 3.0 archive. (http://eosweb.larc.nasa.gov/PRODOCS/srb/table_srb.html)

Clear Sky Monthly Averaged Diffuse Radiation $[H^{Clear})_{Diff}]$**:** Using the methodology described in Erbs, et al (1982), the following cubic polynomial equation was found to best fit ground observations from the BSRN network for clear sky conditions.

$$[(H^{Clear})_{Diff}] = [0.90873 - 2.08587*KT + 2.32668*(KT^2) - 1.22061(KT^3)]* [(H^{Clear})]$$

where:

$[(H^{Clear})]$ = Total shortwave radiation at the earth's surface for clear sky conditions

$KT = [(H^{Clear})]/[H^{TOA}]$

Clear Sky Monthly Averaged Direct Normal Radiation**:** $[(H^{Clear})_{DNR}]$**:** The clear sky direct normal radiation $[(H^{Clear})_{DNR}]$ is calculated from the above NASA THMT method (Gupta, et al. 2001

$$[(H^{Clear})_{DNR}]= [H^{clear} - (H^{Clear})_{Diff}]/ COS(THMT)$$

where:

$[(H^{Clear})]$ = Total shortwave radiation at the earth's surface for clear sky conditions

THMT is the solar zenith angle at the mid-time between sunrise and solar noon for the "monthly average day"

$COS(THMT) = f + g\ [(g - f)/ 2g]^{1/2}$

H^{clear} = Total of direct beam solar radiation and diffuse atmospheric radiation falling on a horizontal surface at the earth's surface

$(H^{Clear})_{Diff}$ = diffuse atmospheric radiation falling on a horizontal surface at the earth's surface

f = sin(latitude) sin(solar declination)

g = cos(latitude) cos(solar declination)

If the Sunset Hour Angle = 180 degrees, then COS(THMT) = f.

In the previous paragraphs, the monthly clear sky diffuse radiation on a horizontal surface, $[H^{Clear})_{Diff}]$, was related to the clearness index, KT and the total clear sky insolation, $[(H^{Clear})]$ through a cubic polynomial equation. Similarly, the monthly averaged clear sky direct normal radiation was related to the difference between the monthly averaged clear sky total radiation and the monthly averaged clear sky diffuse radiation divided by COS(THMT).

In this remainder of this section we compare, for clear sky conditions, the monthly averaged total insolation obtained from SRB Release 3.0 (Figure VI-2), the monthly averaged horizontal diffuse radiation (Figure VI-3), and direct normal radiation values (Figure VI-4) calculated from the SRB values to ground observations from the BSRN network (Figure VI-1).

For these comparisons it was necessary to ensure that the ground observations and the satellite derived solar radiation values are for equivalent clear sky conditions. Fortunately, observational data from a number of BSRN ground sites (see Figure VI-1) and the satellite observational data provide information related to cloud cover for each observational period. Recall in Section III and in Table III-2, it was noted that cloud parameters from the NASA ISCCP were used to infer the solar radiation in the SRB Release 3.0 archive. Parameters within the ISCCP data provide a measure of the clearness for each satellite observation use in the SRB-

inversion algorithms. Similarly, observations from upward viewing cameras at the 27 BSRN sites shown in Figure VI-1 provided a measure of cloud cover for each ground observational period. The comparison data shown in Figures VI-2,-3, and -4 used the ground cameras and the ISCCP data to matched clearness conditions. In particular, the comparisons shown below use clearness criteria defined such that clouds in the field of view of the upward viewing camera and the field of view from the ISCCP satellites must both be respectively less that 10%, 15%, and 20%.

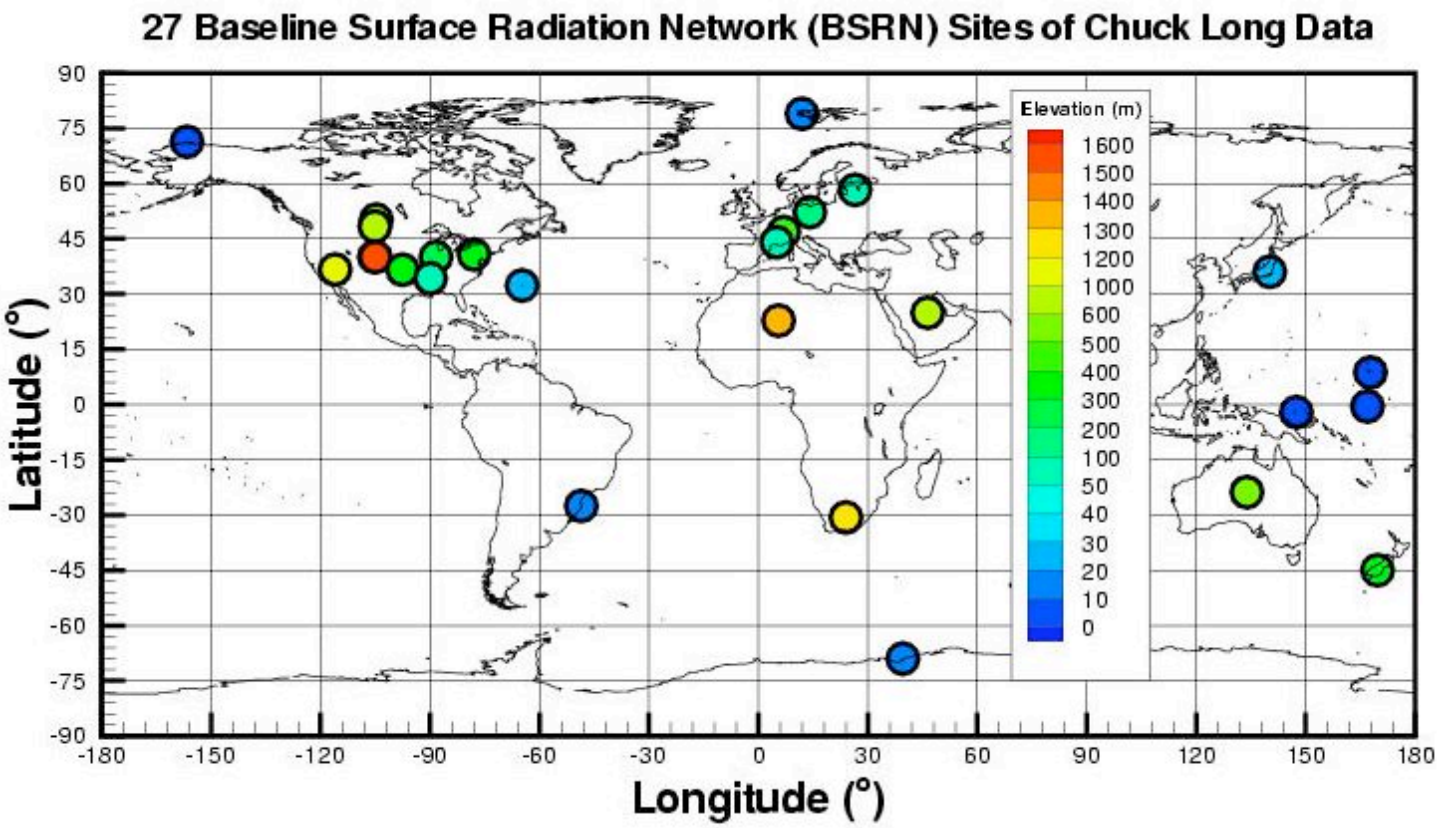

Figure VI-1. Location of ground stations in the Baseline Surface Radiation Network (BSRN) with upward viewing cameras.

Note that for the scatter plots in Figures VI-2, -3, and -4 the comparison statistics are given for the entire globe (i.e. Global), for latitudes north and south of 60^0 (i.e. 60^0 Poleward), and for latitudes from 60^0 S to 60^0 N (i.e. 60^0 Equatorward). The Bias is the difference between the mean (μ) of the respective solar radiation values for SRB and BSRN. RMS is the root mean square difference between the respective SRB and BSRN values. The correlation coefficient between the SRB and BSRN values is given by ρ, the variance in the SRB values is given by σ, and N is number of SRB:BSRN month pairs for each latitude region.

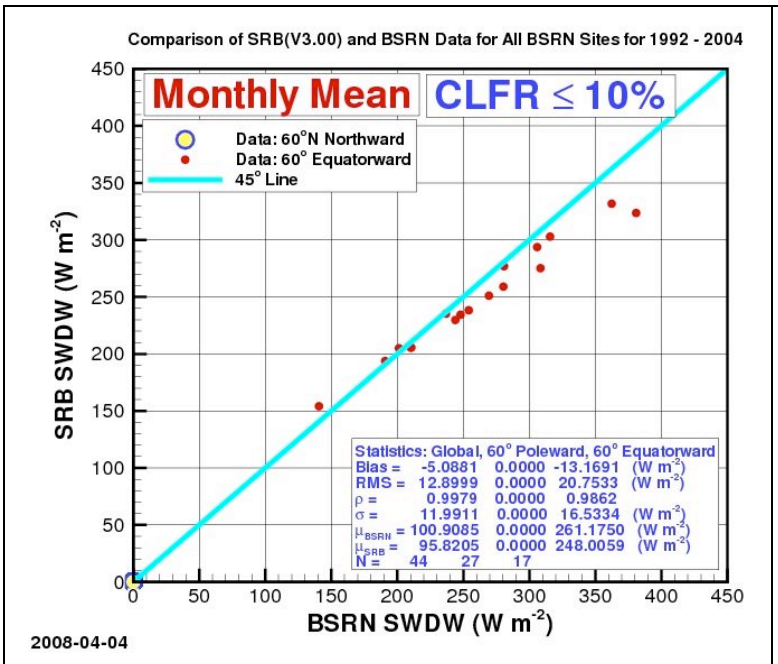

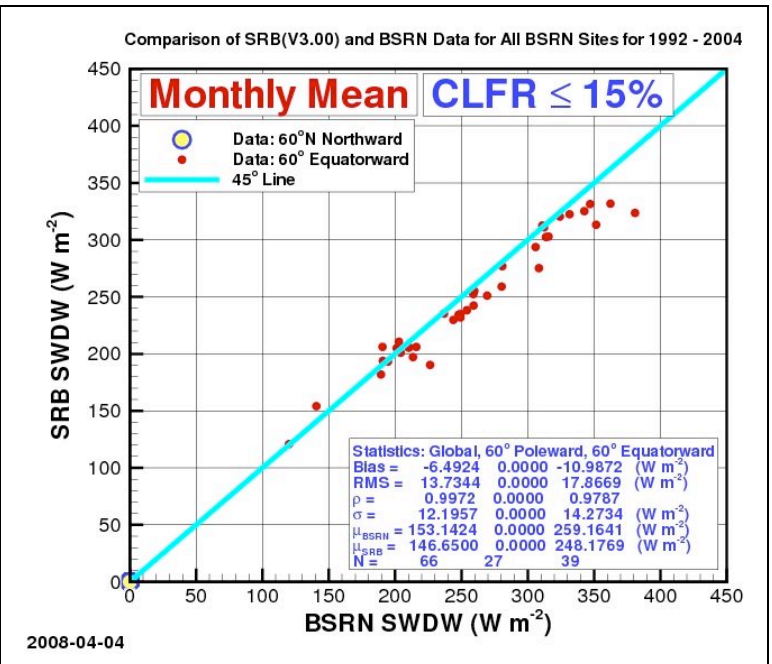

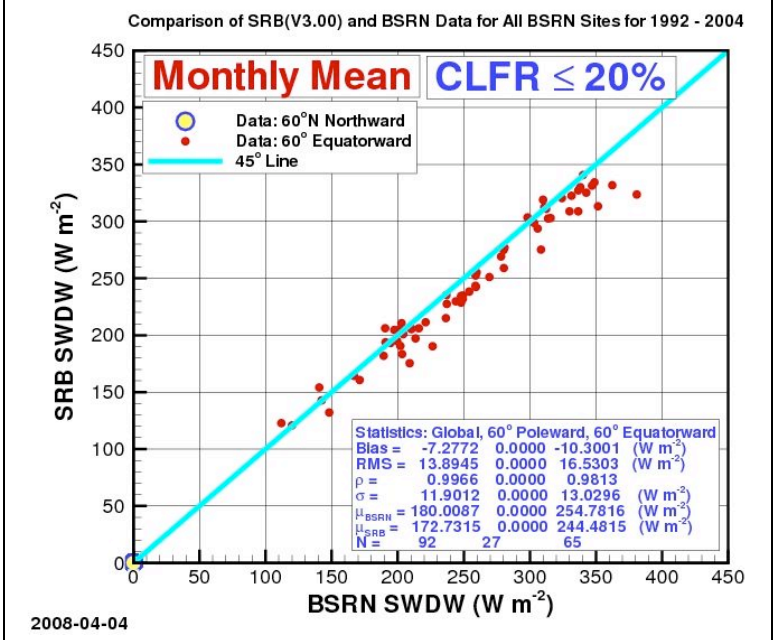

Figure VI-2. Scatter plots of the monthly averaged clear sky total solar radiation derived from observations at BSRN ground sites and monthly averaged values calculated from SRB Release 6.0. The top left panel is for less that 10% cloud cover in field-of-view of both the upward viewing ground and downward viewing satellite cameras; the top right panel is for less that 15% cover and the bottom left panel is for less that 20% cover.

The comparison statistics are given for the entire globe (i.e. Global), for latitudes north and south of 60^0 (i.e. 60^0 Poleward), and for latitudes from 60^0 S to 60^0 N (i.e. 60^0 Equatorward). The Bias is the difference between the mean (μ) of the respective solar radiation values for SRB and BSRN. RMS is the root mean square difference between the respective SRB and BSRN values. The correlation coefficient between the SRB and BSRN values is given by ρ, the variance in the SRB values is given by σ, and N is number of SRB:BSRN month pairs for each latitude region**.** (Note that solar radiation is in W/m^2; multiplying W/m^2 by 0.024 yields kWh/day/m^2, and by 0.0864 yields MJ/day/m^2.)

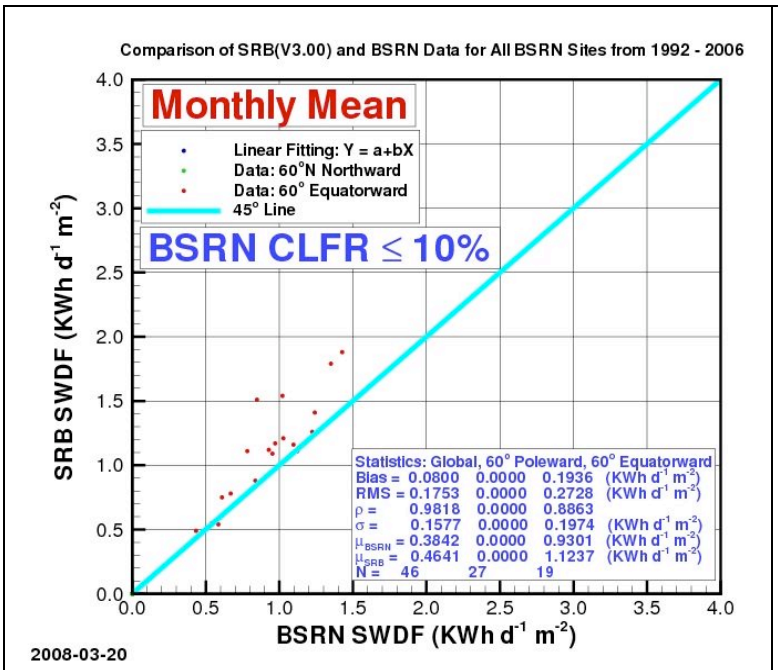

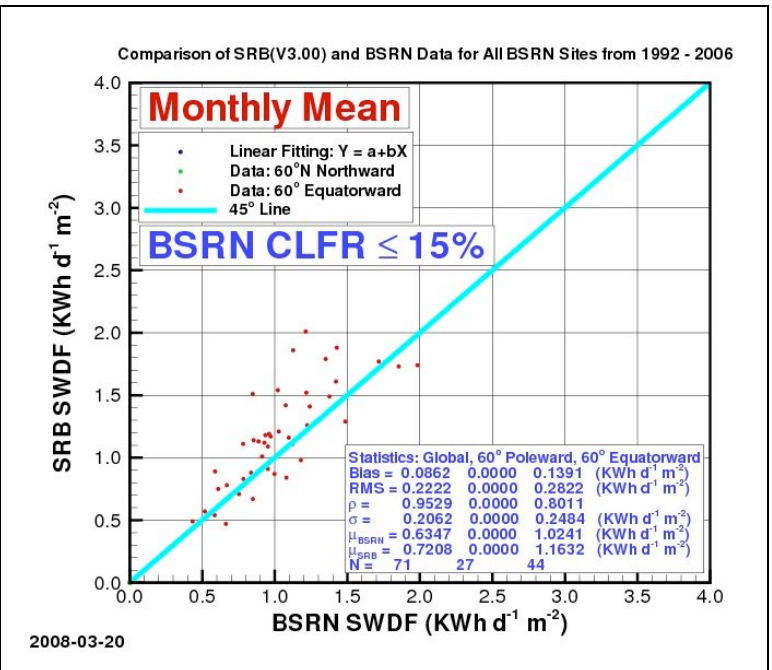

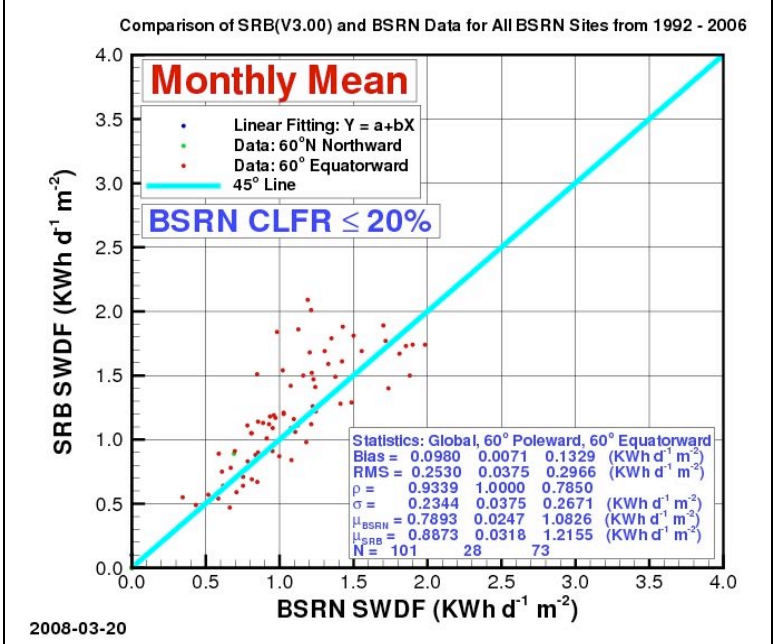

Figure VI-3. Scatter plots of the monthly averaged clear sky diffuse radiation derived from observations at BSRN ground sites and monthly averaged values calculated from SRB Release 6.0 using equations discussed in this section. The top left panel is for less that 10% cloud cover in field-of-view of both the upward viewing ground and downward viewing satellite cameras; the top right panel is for less that 15% cover and the bottom left panel is for less that 20% cover.

The comparison statistics are given for the entire globe (i.e. Global), for latitudes north and south of 60^0 (i.e. 60^0 Poleward), and for latitudes from 60^0 S to 60^0 N (i.e. 60^0 Equatorward). The Bias is the difference between the mean (μ) of the respective solar radiation values for SRB and BSRN. RMS is the root mean square difference between the respective SRB and BSRN values. The correlation coefficient between the SRB and BSRN values is given by ρ, the variance in the SRB values is given by σ, and N is number of SRB:BSRN month pairs for each latitude region. (Note that the solar radiation unit is kWh/day/m^2; multiplying kWh/day/m^2 by 3.6 yields MJ/day/m^2, and by 41.67 yields W/m^2.)

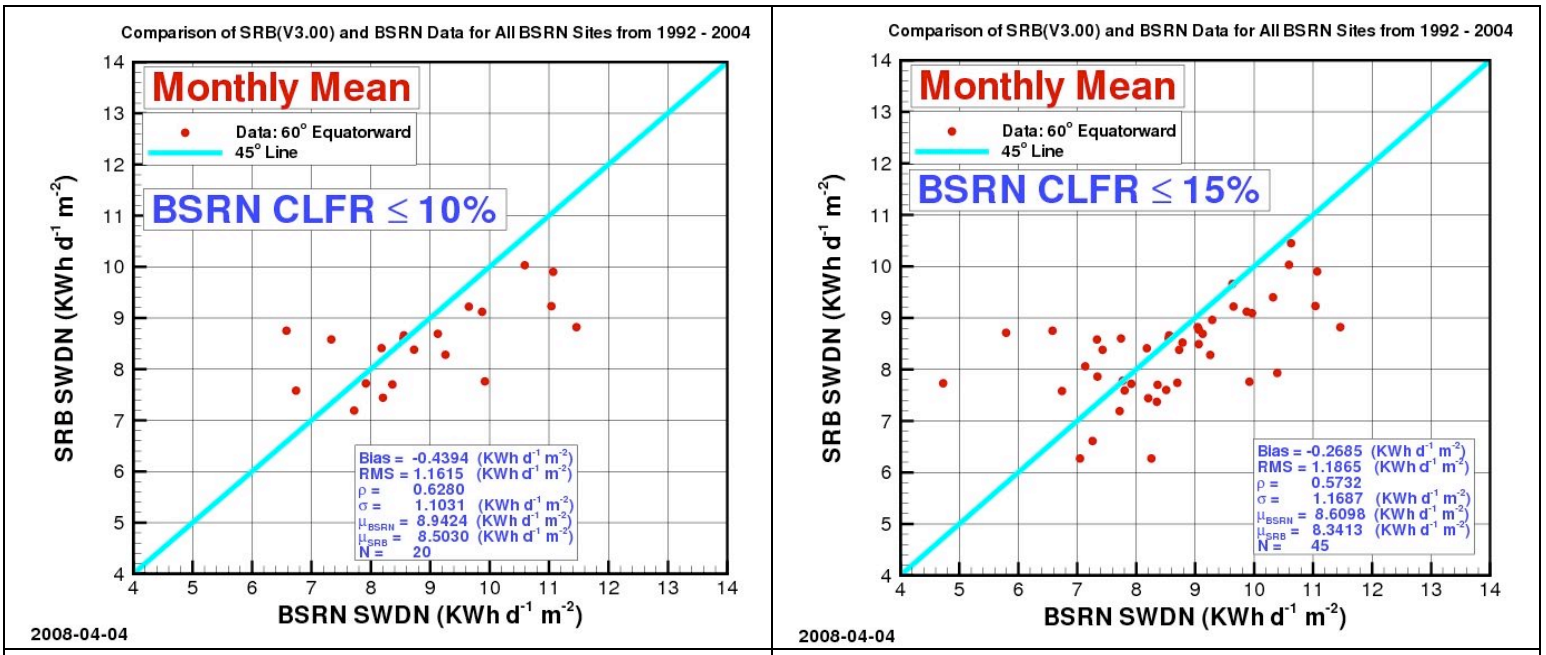

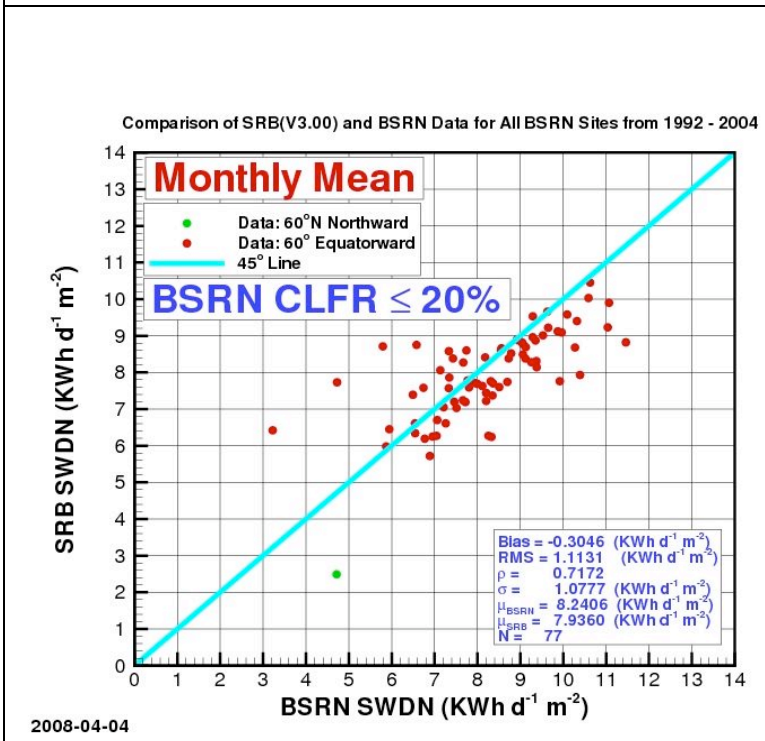

Figure VI-4. Scatter plots of the monthly averaged clear sky direct normal radiation derived from observations at BSRN ground sites and monthly averaged values calculated from SRB Release 6.0 using equations discussed in this section. The top left panel is for less that 10% cloud cover in field-of-view of both the upward viewing ground and downward viewing satellite cameras; the top right panel is for less that 15% cover and the bottom left panel is for less that 20% cover.

The Bias is the difference between the mean (μ) of the respective solar radiation values for SRB and BSRN. RMS is the root mean square difference between the respective SRB and BSRN values. The correlation coefficient between the SRB and BSRN values is given by ρ, the variance in the SRB values is given by σ, and N is number of SRB:BSRN month pairs for each latitude region. (Note that the solar radiation unit is kWh/day/m^2; multiplying kWh/day/m^2 by 3.6 yields MJ/day/m^2, and by 41.67 yields W/m^2.)

VII. All Sky Monthly Tilted Surface Insolation

The calculation of the insolation impinging on a tilted surface in SSE Release 6.0 basically follows the method employed by RETScreen (RETScreen 2005). The major difference is that the diffuse radiation in the SSE Release 6.0 is derived from the equations described in Section V. In the remainder of this section we briefly outline the RETScreen method and provide a comparison of the SSE and RETScreen tilted surface insolation. The RETScreen method uses the "monthly average day" hourly calculation procedures where the equations developed by Collares-Pereira and Rabl (1979) and Liu and Jordan (1960) are used respectively for the "monthly average day" hourly insolation and the "monthly average day" hourly diffuse radiation.

First, we describe the method of estimating the hourly horizontal surface insolation (H_h) and horizontal diffuse (H_{dh}) for daylight hours between 30 minutes after sunrise to 30 minutes before sunset during the "monthly average day". The "monthly average day" is the day in the month whose declination is closest to the average declination for that month (Klein 1977). Table VII.1 lists the date and average declination for each month.

Table VII.1. List of the day in the month whose solar declination is closest to the average declination for that month

Month	Date in month	Declination	Month	Date in month	Declination
January	17	-20.9	July	17	21.2
February	16	-13.0	August	16	13.5
March	16	-2.4	September	15	2.2
April	15	9.4	October	15	-9.6
May	15	18.8	November	14	-18.9
June	11	23.1	December	10	-23.0

$H_h = r_t H$

$H_{dh} = r_d H_d$

where:

H is the monthly average horizontal surface insolation from the SSE data set.

H_d is the monthly average horizontal diffuse from the method described in section V.

solar declination = 23.45*sin[6.303*{(284 + n)/365}]

where:

n = day number of year, 1 = January 1

$\omega_s = \cos^{-1}$[-tan (solar declination)*tan(latitude)], (+ = west relative to solar noon)

where:

ω_s = sunset hour angle

$A = 0.409 + 0.5016 \sin[\omega_s - (\pi/3)]$

$B = 0.6609 - 0.4767 \sin[\omega_s - (\pi/3)]$

$r_t = (\pi/24)*(A + B\cos\omega)*[(\cos\omega - \cos\omega_s)/(\sin\omega_s - \omega_s \cos\omega_s)]$ from Collares-Pereira and Rabl.

where:

ω = solar hour angle for each daylight hour relative to solar noon between sunrise plus 30 minutes and sunset minus 30 minutes. The sun is displaced 15° from the local meridian for each hour from local solar noon.

$r_d = (\pi/24)*[(\cos\omega - \cos\omega_s)/(\sin\omega_s - \omega_s \cos\omega_s)]$ from Liu and Jordan.

Next, we describe the method of estimating hourly total radiation on a tilted surface (H_{th}) as outlined in the RETScreen tilted surface method. The equation, in general terms, is:

H_{th} = solar beam component + sky diffuse component + surface/sky reflectance component

The solution is as follows:

$\cos\theta_{zh}$ = cos(latitude) cos(solar declination) $\cos\omega$ + sin(latitude) sin(solar declination)

$\cos\theta_h = \cos\theta_{zh} \cos\beta_h + (1 - \cos\theta_{zh})(1 - \cos\beta_h)(\cos(\gamma_{sh} - \gamma_h))$

where:

β_h = hourly slope of the PV array relative to a horizontal surface. β_h is constant for fixed panels or panels in a vertical- axis tracking system. $\beta_h = \theta_z$ for panels in a two-axis tracking system. Values for other types of tracking systems are given in Braun and Mitchell (1983).

$\gamma_{sh} = \sin^{-1}$ [($\sin\omega$ cos(solar declination))/$\sin\theta_{zh}$]

= hourly solar azimuth angle; angle between the line of sight of the Sun into the horizontal surface and the local meridian. Azimuth is zero facing the equator, positive west, and negative east.

γ_h = hourly surface azimuth of the tilted surface; angle between the projection of the normal to the surface into the horizontal surface and the local meridian. Azimuth is zero facing the equator, positive west, and negative east. γ_h is constant for fixed surfaces. $\gamma_h = \gamma_{sh}$ for both vertical- and two-axis tracking systems. See Braun and Mitchell (1983) for other types of tracking systems.

$H_{th} = (H_h - H_{dh})(\cos\theta_h/\cos\theta_{zh}) + H_{dh}[(1+\cos\beta_h)/2] + H_h*\rho_s[(1-\cos\beta_h)/2]$

where:

ρ_s = surface reflectance or albedo is assumed to be 0.2 if temperature is above 0^oC or 0.7 if temperature is below -5^oC. Linear interpolation is used for temperatures between these values.

Finally, monthly average tilted surface insolation (H_t) is estimated by summing hourly values of H_{th} over the "monthly average day". It was recognized that such a procedure would be less accurate than using quality "day-by-day" site measurements, but RETScreen validation studies indicate that the "monthly average day" hourly calculation procedures give tilted surface results ranging within 3.9% to 8.9% of "day-by-day" hourly methods.

Reliable measurements of the solar radiation on tilted surfaces are not available for comparison with either the SSE Release 6.0 or RETScreen tilted surface insolation values. Accordingly, Table VII-2 summarizes the agreement in terms of the Bias and RMSE between the two methods, and the parameters (i.e. slope, intercept, and R^2) characterizing the linear least square fit to the RETScreen values (x-axis) to SSE Release 6.0 values (y-axis) when both the RETScreen and SSE methods have the same horizontal insolation as inputs. Recall that the major difference between the two methods involves the determination of the diffuse radiation, and note that the results from the two methods are in good agreement.

Table VII-2 Summary results from a comparison of the insolation on a tilted surface calculated by RETScreen and SSE Release 6.0 using the same monthly averaged insolation on a horizontal surface

Location	Lat x Long	Tilt Angle	Titled-Bias	Titled-RMSE	Titled-Slope	Titled-In'cept	Titled-R2
Ottawa Int'l Airport, Ontario. Canada	45.3N x 75.7W	45	0.47	0.56	1.17	-1.19	0.94
Berverlodge,Alberta,CN	55.2N x 119.4W	40	0.30	0.36	1.09	-0.65	0.99
Castlegar AP, British Cl, CN	49.3N x 117.6W	49	0.35	0.45	1.24	-1.43	0.99
Totonto Int'l AP, Ontario, CN	43.7N x 79.6W	43	0.06	0.09	1.02	-0.12	1.00
Burmingham,AL	33.6N x 86.8W	48	0.06	0.07	1.05	-0.29	1.00
Dodge City, KS	37.8N x 100.0W	37	0.04	0.07	1.01	-0.11	0.99
Covington, KY	39.1N x 84.7W	39	0.03	0.05	1.00	-0.03	1.00
San Francisco, CA	37.6N x 122.4W	37	0.03	0.05	1.00	-0.01	1.00
San Jose, Costa Rica	10.0N x 84.2W	25	-0.09	0.24	0.79	1.08	0.93
Boulogne Sur Seine, France	50.7N x 1.6E	35	0.15	0.18	1.06	-0.36	1.00
Riyadh (Saud-AFB), Saudi Arabia	24.7N x 46.7E	39	0.09	0.11	1.07	-0.51	0.99
Tabuk (Saud-AFB),Saudi Arabia	28.4N x 36.6E	43	0.07	0.09	1.09	-0.59	0.97
Beer-Sheva/Teyman,Israel	31.2N x 34.8E	46	0.05	0.09	0.98	0.07	0.99
Jerusalem/Atarot, Israel	31.5N x 35.2E	46	0.10	0.12	0.99	-0.05	0.99
Naha (Civ/JASDF), Japan	26.2N x 127.7E	41	0.07	0.08	1.00	-0.08	1.00
Brasila, Brasil	15.8S x 47.9W	30	-0.09	0.24	0.83	1.02	0.94
Antofagasta, Chile	23.4S x 70.5W	38	0.08	0.10	1.01	-0.13	1.00
Arica/Chacallute, Chile	18.4S x 70.5W	33	-0.20	0.49	1.14	-0.50	0.90
Pretoria (Met), S. Africa	25.7S x 28.2E	40	0.06	0.09	1.02	-0.19	0.98
Pietersburg (SAAF), S. Africa	23.9S x 29.5E	38	0.07	0.09	0.99	-0.03	0.98
Johannesburg, S. Africa	26.1S x 28.2E	41	0.04	0.07	1.06	-0.38	0.99
Canberra, Australlia	35.3S x 149.2E	35	0.04	0.06	0.99	0.00	1.00
		AVE =	**0.06**	**0.19**	**1.00**	**-0.03**	**0.94**
		STD =	**0.15**	**0.16**	**0.14**	**0.86**	**0.15**

VIII. Meteorological Parameters

An important input to the SRB radiative transfer model is the global distribution of atmospheric state variables obtained from NASA's Global Model and Assimilation Office (GMAO), Goddard Earth Observing System global assimilation model version 4 (GEOS-4) (http://gmao.gsfc.nasa.gov/systems/geos4/). Briefly, the meteorological parameters emerging from the GEOS-4 model are estimated via "An atmospheric analysis performed within a data assimilation context [that] seeks to combine in some "optimal" fashion the information from irregularly distributed atmospheric observations with a model state obtained from a forecast initialized from a previous analysis." (Bloom, et al., 2005). The model seeks to assimilate and optimize observational data and model estimates of atmospheric variables. Types of observations used in the GEOS-4 analysis include (1) land surface observations of surface pressure; (2) ocean surface observations of sea level pressure and winds; (3) sea level winds inferred from backscatter returns from space-borne radars; (4) conventional upper-air data from rawinsondes (e.g., height, temperature, wind and moisture); (5) additional sources of upper-air data include drop sondes, pilot balloons, and aircraft winds; and (6) remotely sensed information from satellites (e.g., height and moisture profiles, total precipitable water, and single level cloud motion vector winds obtained from geostationary satellite images). Emerging from the GEOS-4 analysis are 3-hourly global estimates of the vertical distribution of a range of atmospheric parameters.

The GEOS-4 data products are initially output on a 1^0 by 1.25^0 grid with 50 atmospheric levels, on 3-hourly time steps (e.g. 0, 3, 6, 9, 12, 15, 18, and 21 GMT). For use by the SRB retrieval, the GEOS-4 products are bi-linearly interpolated to a 1^0 by 1^0 grid. As a result of the GEOS-4 data being an integral component of the SRB retrieval process, it is readily available to the POWER/SSE project. Table III-2 lists the basic parameters that the POWER/SSE project obtains from GEOS-4.

***A. Validation of Daily Mean and Daily Maximum and Minimum Temperatures*:**
In addition to the analysis reported by the NASA's Global Model and Assimilation Office (GMAO) (Bloom, et al.), the POWER/SSE project initiated a study focused on determining the accuracy of the GEOS-4 meteorological parameters in terms of the applications within the POWER/SSE project. In particular, the GEOS-4 temperatures (minimum, maximum and daily averaged air and dew point), relative humidity, and surface pressure have been explicitly compared to global data obtained from the National Climate Data Center (NCDC - http://www.ncdc.noaa.gov/oa/ncdc.html) global "Summary of the Day" (gsod) files, and to observations from other high quality networks such as the Surface Radiation (SURFRAD - http://www.srrb.noaa.gov/surfrad/index.html), Atmospheric Radiation Measurement (ARM - http://www.arm.gov/), as well as observations from automated weather data networks such as the High Plains Regional Climate Center (HPRCC - http://www.hprcc.unl.edu/index.php).

In this section we will focus primarily on the analysis of the GEOS-4 daily maximum and minimum temperatures, and the daily mean temperature using observations reported in the NCDC –gsod files, with only summary comments regarding results from the other observational networks noted above. The GEOS-4 re-analysis model outputs meteorological parameters at 3-hourly increments (e.g. 0, 3, 6, 9, 12, 15, 18, and 21 Z) on a global 1^0 by 1.25^0 grid at 50 pressure levels. This 1^0 by 1.25^0 grid is bi-linearly interpolated to a 1^0 by 1^0 grid to match the SRB Release 6.0 solar radiation values. The local daily maximum (Tmax) and minimum (Tmin) temperature, and the local daily mean (Tave) temperature at 2 meters above the surface were obtained from the GEOS-4 3-hourly data. The GEOS-4 meteorological data spans the time period from January 1, 1983 –through near real time. However, our comparative analysis has used observational data from January 1, 1983 - through December 31, 2006.

The observational data reported in the NCDC – gsod files are hourly observations, typically beginning at 0Z, and from globally distributed ground stations. For the analysis reported herein, the daily Tmin, Tmax, and Tave at each observational station in the NCDC files were derived from the hourly observations filtered by an "85%" selection criteria applied to the observations reported for each station. Namely, only data from NCDC stations reporting 85% or greater of the possible 1-hourly observations per day and 85% or greater of the possible days per month were used to determine the daily Tmin, Tmax, and Tave included in comparisons with the GEOS-4 derived data. Figure VIII-A.1 illustrates the global distribution of the surface stations remaining in the NCDC data files for 1983 and 2004 after applying our 85% selection criteria. Note that the number of stations more that doubled from 1983 (e.g. 1104 stations) to 2004 (e.g. 2704 stations), and that majority of the stations are located in the northern hemisphere.

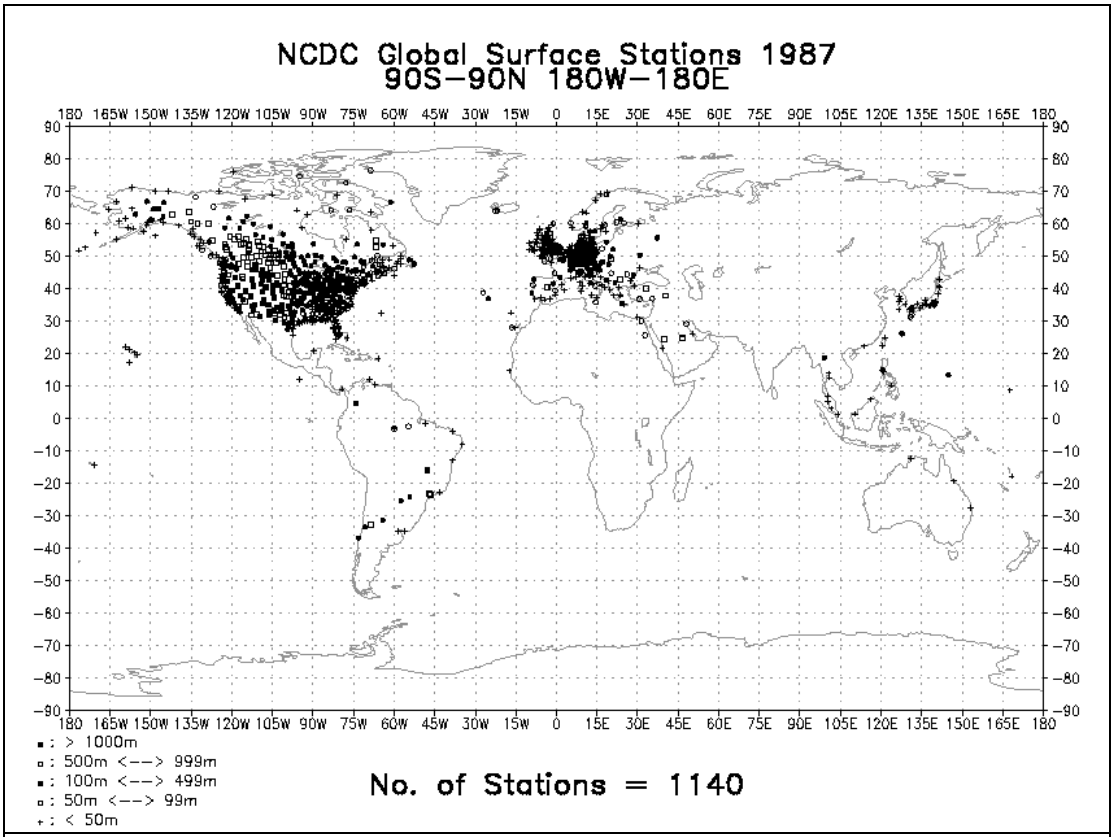

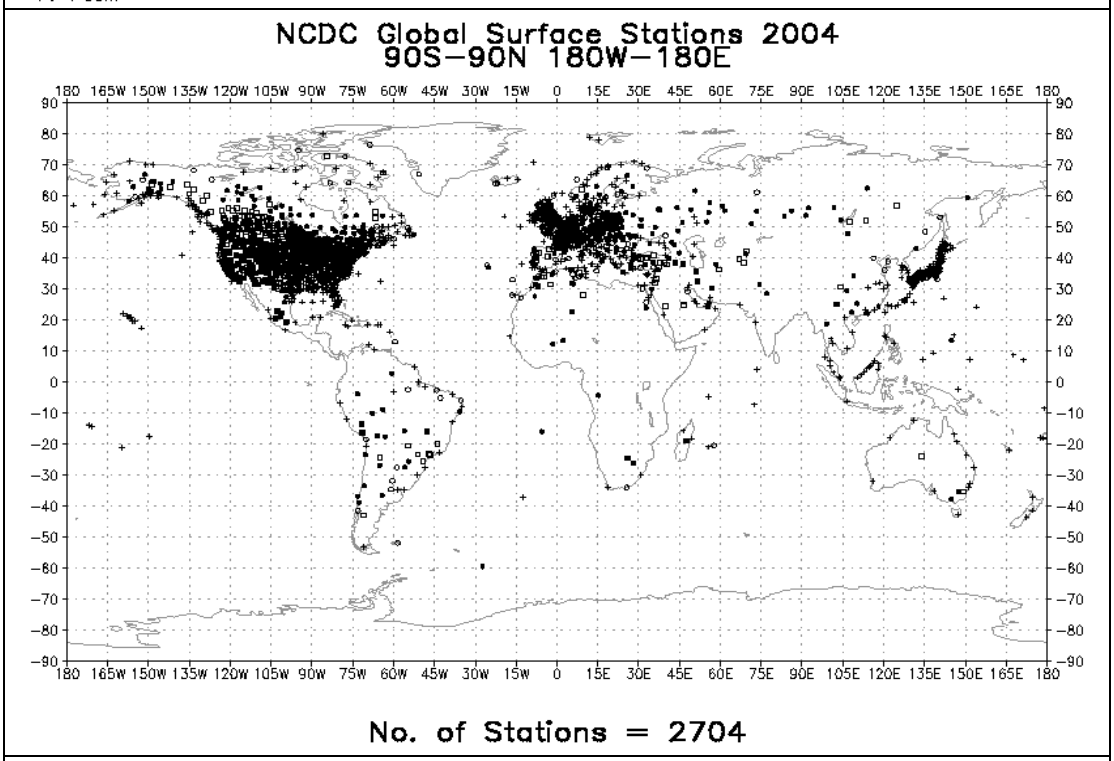

Figure VIII-A.1: Top (a) and bottom (b) figures show distribution of NCDC stations meeting 85% selection criteria for 1987 and 2004, respectively.

Unless specifically noted otherwise, all air temperature validations have used GEOS-4 values and ground observations at an elevation of 2 meters above the earth's surface. We also note again that all values in POWER/SSE Release 6.0 (e.g. solar and meteorological) represent the average over a 1° latitude by 1° longitude grid cell. Figures VIII-A.2a, -A.2b, and –A.2c are, respectively, scatter plots of Tave, Tmax, and Tmin derived from ground observations in the NCDC files versus GEOS-4 values for the years 1987 and 2004. These plots illustrate the agreement typically observed for all the years 1983 through 2005. In the upper left

corner of each figure are the parameters for the linear least squares regression fit to theses data, along with the mean Bias and RMSE between the GEOS-4 and NCDC observations. The mean Bias and RMSE are given as:

$$\text{Bias} = \sum_j \{\sum_i \{[(T_i^j)_{GEOS4} - (T_i^j)_{NCDC}]\}\}/N$$

$$\text{RMSE} = \{\sum_j \{\sum_i \{[(T_i^j)_{GEOS4} - (T_i^j)_{NCDC}]^2/N\}\}\}^{1/2},$$

where, $\sum_i$ is summation over all days meeting the 85% selection criteria, $\sum_j$ indicates the sum over all stations, $(T_i^j)_{NCDC}$ is the temperature on day i for station j, and $(T_i^j)_{GEOS4}$ is the GEOS-4 temperature corresponding to the overlapping GEOS-4 1-degree cell for day i and station j, and N is the number of matching pairs of NCDC and GEOS-4 values. For the year 1987, 1139 stations passed our 85% selection criteria yielding 415,645 matching pairs on NCDC/GEOS-4 values; for 2004, 2697 stations passed yielding 987,451 matching pairs of NCDC/GEOS-4 temperature values. The color bar along the right side of the scatter plot provides a measure of the distribution of the NCDC/GEOS-4 temperature pairs. For example, in Figure III-A.2a, each data point shown in dark blue represents a 1-degree cell with 1 to 765 matching temperature pairs, and all of the 1-degree cells shown in dark blue contain 15.15% of the total number of ground site points. Likewise, the darkest orange color represent 1-degree cells for which there are from 6120 to 6885 matching temperature pairs, and taken as a group all of the 1-degree cells represented by orange contain 10.61% if the total number of matching ground site points. Thus, for the data shown in Figure VIII-A.2a, approximately 85% of matching temperature pairs (i.e. excluding the data represented by the dark blue color) is "tightly" grouped along the 1:1 correlation line.

In general the scatter plots shown in Figure VIII-A.2, and indeed for all the years from 1983 through 2006, exhibit good agreements between the GEOS-4 data and ground observations. Notice however that for both the 1987 and 2004 data, on a global basis, the GEOS-4 Tmax bias is cooler (e.g. -1.9 C in 1987 and -1.8 C in 2004), the GEOS-4 Tmin bias is warmer (e.g. 0.4 ^{o} C in 1987 and 0.2 ^{o} C in 2004), and that GEOS-4 Tave bias is cooler (e.g. -0.5 ^{o} C in 1987, and -0.6 ^{o} C in 2004) relative to values reported by the NCDC stations. Similar trends in the respective biases between GEOS-4 and NCDC observations were noted for each year from 1983 – 2006 (see Table VIII-A.1 below). The ensemble average for the years 1983 – 2006 yields a GEOS-4 Tmax which is 1.82^{o} C cooler than observed at NCDC ground Sites, a Tmin about 0.27^{o} C warmer, and a Tave about 0.55^{o} C cooler. Similar trends are also observed for measurements from other meteorological networks. For example, using the US National Weather Service Cooperative Observer Program (COOP) observations, White, et al (2008) found the mean values of GEOS-4 Tmax, Tmin, and Tave to be respectively 2.4^{o} C cooler, Tmin 1.1^{o} C warmer, and 0.7 ^{o} C cooler that the COOP values.

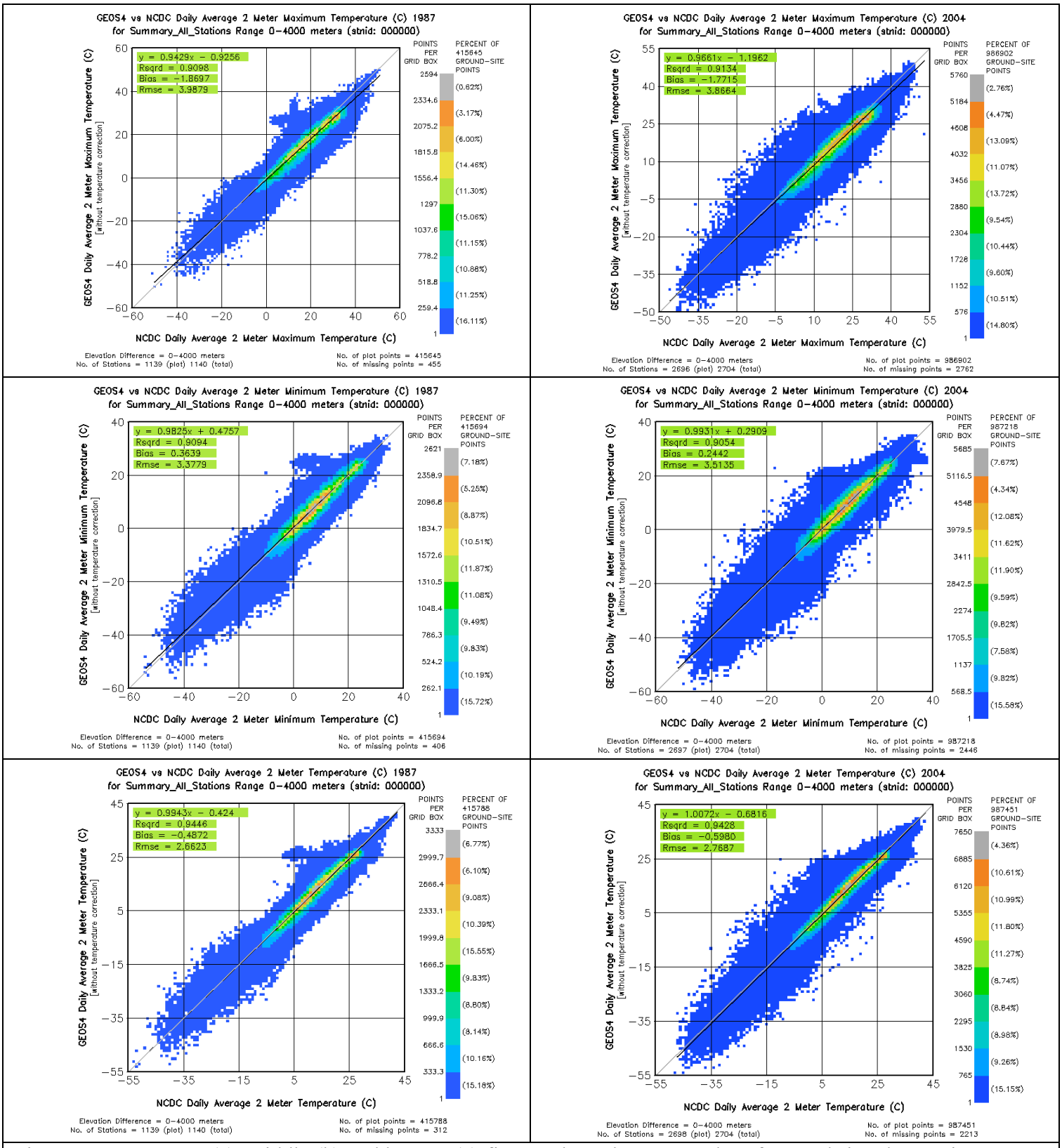

Figure VIII-A.2. Top (a), middle (b) and bottom (c) figures show the scatter plot of ground site observations versus GEOS-4 values of Tmax, Tmin, and Tave for the years 1987 and 2004. The color bar in each figure indicates the number and percentage of ground stations that are included within each color range. (WRS)

Table VIII-A.1.Comparison of NCDC and GEOS-4 Temperatures with no corrections to GEOS-4 values.															
	Tmax					Tmin					Tave				
Year	Slope	Intercept (C)	R^2	RMSE (C)	Bias (C)	Slope	Intercept (C)	R^2	RMSE (C)	Bias (C)	Slope	Intercept (C)	R^2	RMSE (C)	Bias (C)
2006	0.97	-1.28	0.92	3.88	-1.72	1.00	0.09	0.90	3.59	0.11	1.02	-0.79	0.94	2.82	-0.59
2005	0.97	-1.40	0.92	4.00	-1.92	0.99	0.20	0.91	3.57	0.16	1.01	-0.81	0.95	2.81	-0.67
2004	0.97	-1.20	0.91	3.86	-1.78	0.99	0.28	0.91	3.50	0.24	1.01	-0.69	0.94	2.76	-0.60
2003	0.95	-0.91	0.91	3.96	-1.74	0.99	0.46	0.91	3.49	0.38	1.00	-0.47	0.94	2.82	-0.53
2002	0.94	-0.88	0.91	4.06	-1.94	0.98	0.47	0.90	3.55	0.30	0.98	-0.48	0.94	2.85	-0.66
2001	0.97	-1.69	0.92	4.00	-2.20	1.00	0.10	0.90	3.62	0.11	1.01	-0.97	0.95	2.78	-0.81
2000	0.97	-1.17	0.91	3.84	-1.67	1.00	0.25	0.91	3.50	0.27	1.01	-0.65	0.94	2.77	-0.52
1999	0.97	-1.25	0.91	3.80	-1.78	0.99	0.47	0.91	3.37	0.39	1.00	-0.60	0.95	2.63	-0.54
1998	0.98	-1.29	0.92	3.67	-1.71	0.99	0.11	0.91	3.27	0.07	1.01	-0.81	0.94	2.62	-0.68
1997	0.97	-1.20	0.92	3.64	-1.66	0.99	-0.01	0.91	3.30	-0.05	1.00	-0.72	0.95	2.67	-0.68
1996	0.95	-0.71	0.91	3.67	-1.56	0.98	0.27	0.91	3.31	0.15	0.99	-0.46	0.94	2.66	-0.55
1995	0.97	-1.44	0.92	3.93	-1.91	1.00	0.32	0.92	3.44	0.29	1.01	-0.69	0.95	2.69	-0.60
1994	0.98	-1.58	0.92	4.08	-1.93	1.00	-0.01	0.91	3.55	-0.04	1.01	-0.82	0.95	2.85	-0.71
1993	0.96	-1.22	0.92	3.93	-1.80	0.99	0.22	0.92	3.40	0.16	1.00	-0.51	0.95	2.68	-0.52
1992	0.95	-0.92	0.91	3.90	-1.70	0.98	0.43	0.90	3.46	0.33	1.00	-0.43	0.94	2.67	-0.43
1991	0.95	-1.05	0.91	4.14	-1.89	0.99	0.35	0.91	3.45	0.27	1.00	-0.45	0.94	2.80	-0.49
1990	0.95	-1.12	0.90	4.18	-1.94	0.99	0.40	0.91	3.49	0.35	1.00	-0.44	0.94	2.79	-0.49
1989	0.96	-1.18	0.91	4.15	-1.91	0.99	0.48	0.92	3.50	0.42	0.99	-0.40	0.95	2.79	-0.46
1988	0.95	-1.11	0.91	4.03	-1.90	0.99	0.55	0.91	3.38	0.47	1.00	-0.38	0.95	2.63	-0.42
1987	0.94	-0.93	0.91	3.99	-1.87	0.98	0.48	0.91	3.38	0.36	0.99	-0.42	0.94	2.66	-0.49
1986	0.95	-1.02	0.91	4.05	-1.88	0.98	0.52	0.91	3.37	0.39	0.99	-0.35	0.94	2.70	-0.45
1985	0.96	-1.11	0.92	4.03	-1.84	0.99	0.38	0.92	3.58	0.32	0.99	-0.44	0.95	2.83	-0.49
1984	0.96	-1.07	0.91	4.00	-1.79	1.00	0.44	0.91	3.46	0.41	1.00	-0.45	0.94	2.79	-0.47
1983	0.96	-1.19	0.91	4.02	-1.78	0.99	0.41	0.91	3.44	0.34	1.00	-0.49	0.94	2.82	-0.52
Average	**0.96**	**-1.16**	**0.91**	**3.95**	**-1.82**	**0.99**	**0.32**	**0.91**	**3.46**	**0.26**	**1.00**	**-0.57**	**0.94**	**2.75**	**-0.56**
STDEV	**0.01**	**0.22**	**0.01**	**0.15**	**0.13**	**0.01**	**0.17**	**0.01**	**0.10**	**0.14**	**0.01**	**0.17**	**0.00**	**0.08**	**0.10**

Figures VIII-A.3a and VIII-A.3b, showing the differences between the 2004 yearly mean values of Tmin and Tmax for the NCDC and the corresponding GEOS-4, suggest at least one factor contributing to the bias between GEOS-4 and ground observations. Recall that the GEOS-4 temperatures represent the average over a 1° by 1° latitude/longitude cell. With this in mind, note that the mountainous regions of western US clearly exhibit the largest differences between the NCDC and GEOS-4 temperatures, particularly for Tmax. We also note that, coastal regions where the 1-degree GEOS-4 cell is too coarse to capture localized ocean/land gradients also tend to exhibit larger differences.

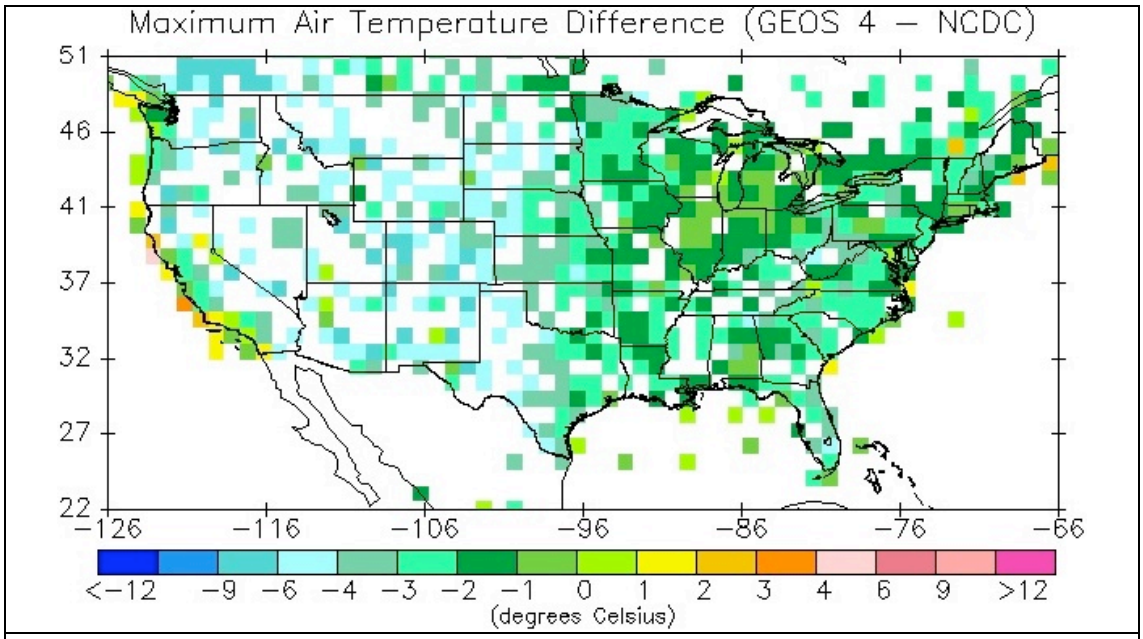

Figure VIII-A.3b: Difference between the mean values of Tmax for the NCDC and GEOS-4 data (2004)

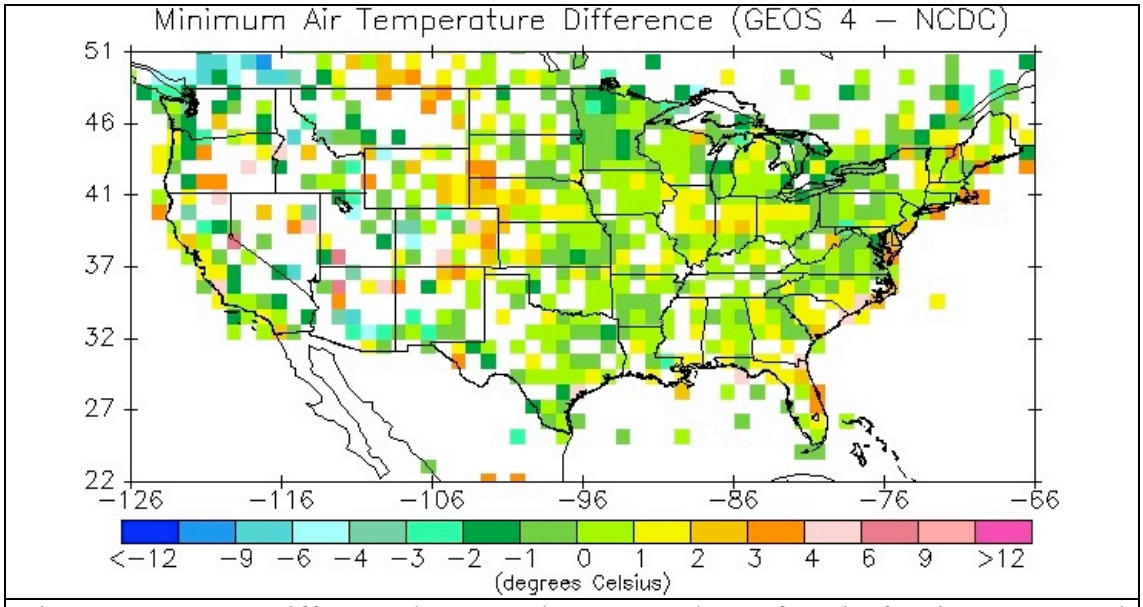

Figure VIII-A.3a: Difference between the mean values of Tmin for the NCDC and GEOS-4 data (2004)

The dependence of the biases between GEOS-4 and ground site observations relative to the elevation difference between the GEOS-4 cell and NCDC ground site stations is examined in more detail for the years 1983 - 2006 in Figure VIII-A.4. Here, the biases between the GEOS-4 and NCDC Tave, Tmax, and Tmin are plotted against the difference in the elevation of the 1-degree GEOS-4 cell and the ground site elevation for all stations meeting our 85% selection criteria. In the left column, the bias and elevation difference for all stations are explicitly plotted. In the right column, the stations have been grouped into elevation difference bins (e.g. 0 to 50m; >50m to 100m; >100m to 150m; etc.) and plotted against the mean bias for the respective elevation bin.

The dependence of the bias between the GEOS-4 and NCDC temperature values on the elevation difference between the GEOS-4 cell and ground elevation is clearly evident in Figure VIII-A.4 and can be attributed to the tropospheric temperature lapse rate. In regions where the average elevation of the GEOS-4 1-degree grid cell is above a ground site the GEOS-4 temperatures will typically be cooler that the values reported at the ground site consistent with the overall GEOS-4 bias relative to the NCDC values seen in Table VIII-A.1. Applying a "correction" to the GEOS-4 temperature based upon the altitude difference and the appropriate lapse rate should remove this elevation difference dependence and bring the GEOS-4 values in closer agreement with ground site observations.

Table VIII-A.2 gives the parameters associated with linear regression fits to the bias between the GEOS-4 values and the NCDC values versus the corresponding elevation difference for each individual year between 1983 and 2006. The regression parameters are for scatter plots of altitude binned data (i.e. See the right hand column of Figure VIII-A.4 as an example of an altitude binned scatter plot.), and is included here to illustrate the yearly consistency in the binned data. Note in particular, that the averaged of all the linear regression slopes in Table VIII-A.2 is approximated equal to the slope of the regression fit to the ensemble of data (see right hand column of Figure VIII-A.4) which, for convenience, is given in the bottom row of Table VIII-A.2. We have taken the average of the Tmax, Tmin, and Tave slopes (e.g. -6.1, -4.7 and -5.3 ^{0}C/kM) as the global lapse rates we recommend for adjusting GEOS-4 Tmax, Tmin, and Tave values to a particular ground site elevation.

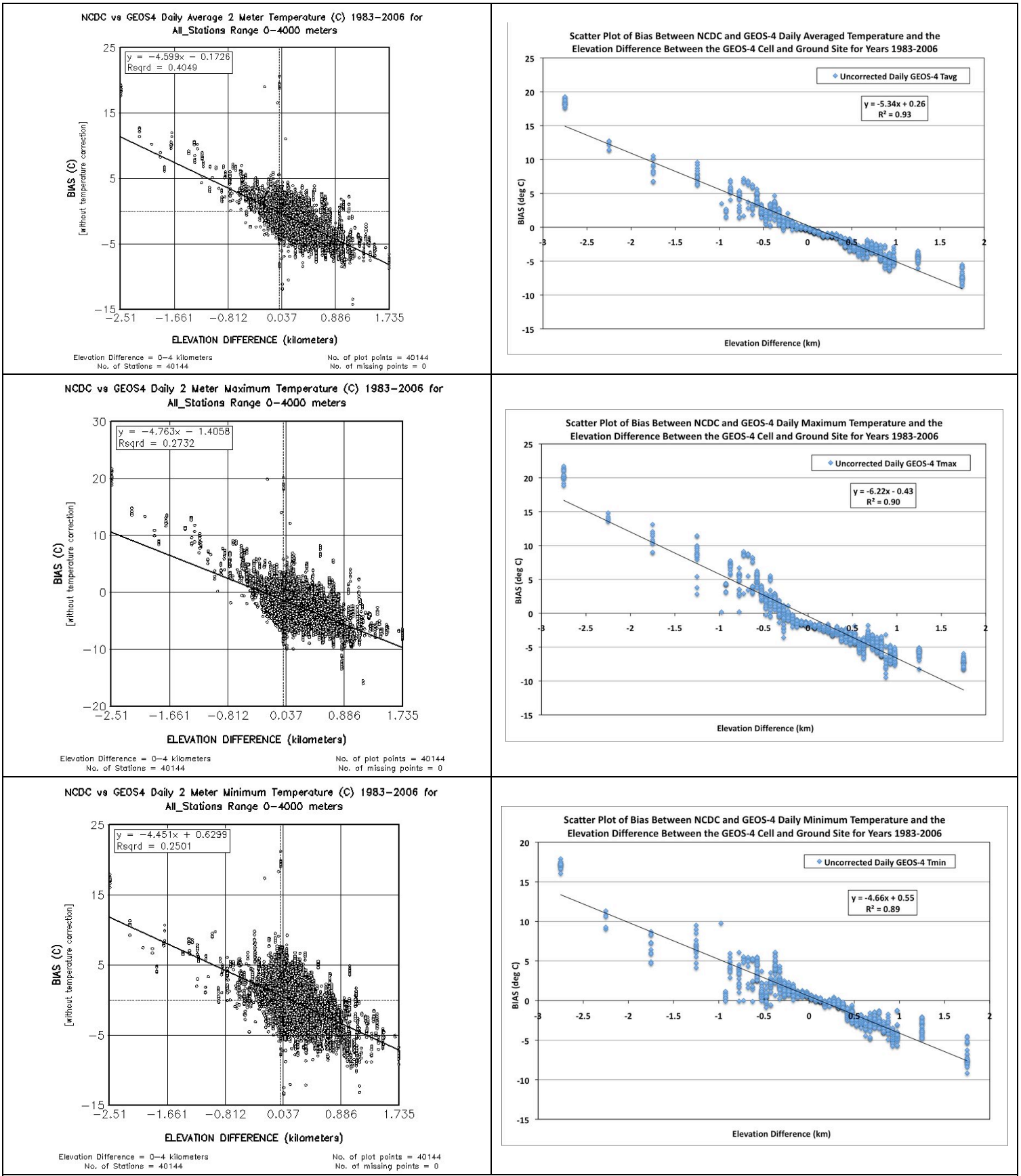

Figure VIII-A.4. The scatter plots in the right and left columns show the dependence of the bias between the GEOS-4 temperatures (T_{ave}, T_{min}, and T_{max}) and values from the NCDC archive on the elevation difference between the GEOS-4 1-degree cell and the ground station elevation for 1983 -2006. In the left column, the bias and elevation difference for all stations are explicitly plotted. In the right column, the stations have grouped into elevation difference bins (e.g. 0 to 50m; >50m to 100m; >100m to 150m; etc.) and plotted against the mean bias for the respective elevation bin.

Table. VIII-A.2. Linear regression parameters associated with the scatter plots of the bias between NCDC and GEOS-4 daily averaged temperatures and the difference in the elevation of the NCDC ground station and the GEOS-4 1-degree grid cell. The bottom row gives the parametes for the altitude binned scatter plots of Figure VIII-A.4.

Year	Tmax			Tmin			Tave		
	Slope (C/km)	Intercept (C)	R^2	Slope (C/km)	Intercept (C)	R^2	Slope (C/km)	Intercept (C)	R^2
2006	-6.09	-0.23	0.88	-4.44	0.27	0.88	-5.15	0.24	0.91
2005	-6.25	-0.38	0.93	-4.33	0.35	0.9	-5.18	0.18	0.94
2004	-6.32	-0.03	0.91	-4.48	0.57	0.9	-5.26	0.41	0.92
2003	-6.15	-0.04	0.93	-4.12	0.49	0.9	-5.03	0.37	0.95
2002	-6.38	-0.12	0.91	-4.5	0.71	0.89	-5.32	0.42	0.93
2001	-5.72	-1.04	0.87	-4.27	0.2	0.82	-4.99	-0.17	0.92
2000	-6.14	-0.24	0.93	-4.5	0.6	0.89	-5.23	0.34	0.94
1999	-6.68	-0.14	0.91	-4.95	0.92	0.93	-5.69	0.53	0.95
1998	-6.39	-0.28	0.91	-4.91	0.69	0.91	-5.5	0.34	0.94
1997	-6.55	-0.05	0.9	-5.18	0.64	0.92	-5.71	0.43	0.93
1996	-6.14	0.04	0.88	-5.24	0.99	0.93	-5.59	0.6	0.94
1995	-6.31	-0.78	0.9	-5.38	1	0.9	-5.71	0.32	0.93
1994	-6.38	-0.41	0.9	-5.42	0.67	0.9	-5.77	0.41	0.93
1993	-6.14	-0.35	0.89	-5.02	0.75	0.89	-5.5	0.48	0.93
1992	-6.29	-0.34	0.89	-5.09	0.75	0.91	-5.49	0.33	0.94
1991	-6.66	-0.41	0.93	-4.94	0.5	0.92	-5.73	0.32	0.96
1990	-6.7	-0.61	0.94	-4.85	0.3	0.9	-5.64	0.13	0.95
1989	-5.37	-1.11	0.87	-3.82	0.15	0.81	-4.5	-0.23	0.9
1988	-5.55	-0.91	0.83	-4.38	0.4	0.84	-4.95	0.04	0.9
1987	-5.01	-1.17	0.82	-4.76	0.55	0.91	-4.84	-0.06	0.94
1986	-5.64	-0.86	0.86	-4.11	0.31	0.84	-4.97	0.03	0.92
1985	-4.96	-1.01	0.85	-4.11	0.3	0.84	-4.71	-0.05	0.94
1984	-5.82	-0.71	0.87	-4.18	0.43	0.89	-4.98	0.1	0.93
1983	-5.56	-0.85	0.85	-3.9	0.37	0.87	-4.71	0.03	0.92
Average	**-6.05**	**-0.50**	**0.89**	**-4.62**	**0.54**	**0.89**	**-5.26**	**0.23**	**0.93**
STDEV	**0.49**	**0.38**	**0.03**	**0.47**	**0.24**	**0.03**	**0.38**	**0.23**	**0.02**
All Years Regression Analysis	**-6.22**	**-0.43**	**0.9**	**-4.66**	**0.55**	**0.89**	**-5.34**	**0.26**	**0.93**

Applying these lapse rate corrections to the GEOS-4 temperature date for the years 1983 through 2006 yields the scatter plots shown in Figures VIII-A.5, where the resulting bias between the lapse rate corrected GEOS-4 data and the corresponding NCDC data is plotted vs the elevation difference between the GEOS-4 grid cell and the ground site data. Note in particular that the ensemble of biases between the lapse rate corrected GEOS-4 and NCDC data exhibits little to no dependency on the difference between the GEOS-4 grid elevation and the ground site elevation.

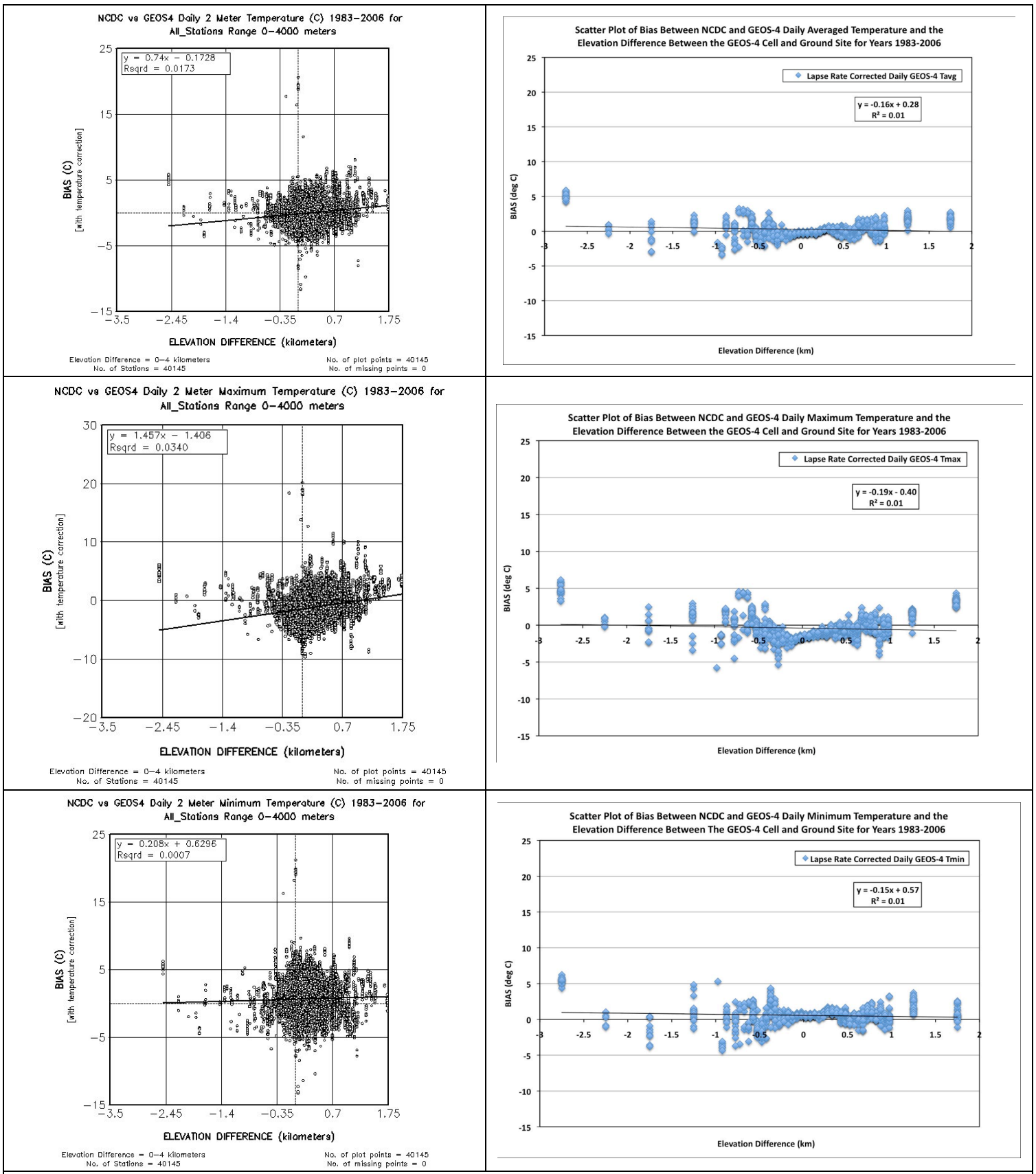

Figure VIII-A.5. The scatter plots in the right and left columns show the dependence of the bias between the GEOS-4 temperatures (T_{ave}, T_{min}, and T_{max}) and values from the NCDC archive on the elevation difference between the GEOS-4 1-degree cell and the ground station elevation for the years 1983 - 2006 after applying the lapse rate adjustments to the GEOS-4 temperatures. In the left column, the bias and elevation difference for all stations are explicitly plotted. In the right column, the stations have grouped into elevation difference bins (e.g. 0 to 50m; >50m to 100m; >100m to 150m; etc.) and plotted against the mean bias for the respective elevation bin.

We have included Table VIII-A.3 to quantify a bias between the lapse-rate corrected GEOS-4 values and the ground site values that continues to be evident and is independent of the elevation difference between GEOS-4 grid and the ground site. Table VIII-A.3 gives the slope, intercept, and correlation coefficient for the linear regressive fit to the lapse rate corrected GEOS-4 values vs. ground site observations for each individual year. Also included for each year is the RMSE and bias between the lapse-rate corrected GEOS-4 values and ground site observations.

Table VIII-A.3. Comparison of NCDC and GEOS-4 Temperatures with lapse rate corrections applied to GEOS-4 values.
(Lapse Rate Correction : Tave -->-5.34 C/km ; Tmax --> -6.22 C/km; Tmin -->-4.66 C/km)

Year	Tmax					Tmin					Tave				
	Slope	Intercept (C)	R^2	RMSE (C)	Bias (C)	Slope	Intercept (C)	R^2	RMSE (C)	Bias (C)	Slope	Intercept (C)	R^2	RMSE (C)	Bias (C)
2006	0.98	-0.85	0.92	3.52	-1.19	1.00	0.47	0.91	3.44	0.50	1.02	-0.37	0.95	2.54	-0.13
2005	0.98	-0.93	0.93	3.61	-1.35	1.00	0.62	0.92	3.46	0.58	1.02	-0.36	0.95	2.52	-0.19
2004	0.98	-0.81	0.92	3.44	-1.20	1.00	0.69	0.92	3.37	0.67	1.01	-0.27	0.95	2.44	-0.11
2003	0.96	-0.57	0.92	3.55	-1.20	0.99	0.84	0.92	3.40	0.78	1.00	-0.10	0.95	2.53	-0.07
2002	0.95	-0.50	0.92	3.64	-1.39	0.98	0.87	0.91	3.45	0.71	0.99	-0.07	0.95	2.54	-0.19
2001	0.97	-1.15	0.93	3.61	-1.61	1.00	0.55	0.91	3.51	0.55	1.01	-0.47	0.95	2.49	-0.31
2000	0.98	-0.72	0.93	3.40	-1.09	1.00	0.68	0.92	3.36	0.70	1.02	-0.21	0.95	2.42	-0.02
1999	0.98	-0.78	0.92	3.40	-1.21	0.99	0.90	0.92	3.28	0.81	1.01	-0.13	0.95	2.35	-0.05
1998	0.98	-0.78	0.93	3.25	-1.10	0.99	0.57	0.91	3.15	0.52	1.01	-0.31	0.95	2.31	-0.15
1997	0.98	-0.76	0.93	3.24	-1.08	1.00	0.41	0.92	3.14	0.38	1.01	-0.27	0.96	2.35	-0.19
1996	0.96	-0.31	0.92	3.34	-0.96	0.99	0.68	0.92	3.19	0.58	1.00	-0.05	0.95	2.39	-0.05
1995	0.98	-0.98	0.93	3.54	-1.36	1.00	0.73	0.93	3.33	0.70	1.01	-0.25	0.96	2.41	-0.13
1994	0.98	-1.04	0.92	3.72	-1.30	1.00	0.45	0.92	3.40	0.43	1.01	-0.32	0.95	2.56	-0.17
1993	0.97	-0.76	0.92	3.60	-1.26	0.99	0.62	0.92	3.32	0.56	1.00	-0.08	0.96	2.45	-0.05
1992	0.96	-0.59	0.92	3.51	-1.23	0.99	0.77	0.91	3.32	0.68	1.00	-0.08	0.95	2.35	-0.03
1991	0.96	-0.70	0.92	3.74	-1.40	0.99	0.69	0.92	3.32	0.63	1.00	-0.10	0.95	2.49	-0.07
1990	0.96	-0.77	0.91	3.78	-1.49	0.99	0.74	0.92	3.37	0.68	1.00	-0.09	0.95	2.49	-0.10
1989	0.96	-0.79	0.92	3.84	-1.45	0.99	0.83	0.92	3.44	0.77	1.00	-0.02	0.95	2.58	-0.07
1988	0.96	-0.70	0.92	3.71	-1.43	0.99	0.90	0.92	3.31	0.82	1.00	0.00	0.95	2.40	-0.02
1987	0.95	-0.53	0.92	3.67	-1.40	0.98	0.82	0.92	3.29	0.72	1.00	-0.05	0.95	2.43	-0.08
1986	0.95	-0.58	0.92	3.71	-1.36	0.98	0.91	0.92	3.30	0.77	0.99	0.08	0.95	2.46	-0.01
1985	0.96	-0.61	0.92	3.71	-1.31	0.99	0.79	0.92	3.52	0.71	0.99	0.02	0.95	2.61	-0.04
1984	0.96	-0.61	0.92	3.65	-1.30	0.99	0.82	0.92	3.38	0.78	1.00	-0.03	0.95	2.54	-0.05
1983	0.97	-0.78	0.92	3.65	-1.28	0.99	0.79	0.92	3.36	0.70	1.00	-0.09	0.95	2.56	-0.10
Average	**0.97**	**-0.73**	**0.92**	**3.58**	**-1.29**	**0.99**	**0.72**	**0.92**	**3.35**	**0.66**	**1.00**	**-0.15**	**0.95**	**2.47**	**-0.10**
STDEV	**0.01**	**0.18**	**0.00**	**0.16**	**0.15**	**0.01**	**0.15**	**0.00**	**0.10**	**0.12**	**0.01**	**0.14**	**0.00**	**0.08**	**0.07**

We note that for each year the bias given in Table VIII-A.3 is independent of altitude (see Figure VIII-A.5) and approximately constant for all years. Similar biases have also been noted when comparing GEOS-4 temperatures to observations from other ground networks suggesting that these biases are most likely associated an "off set" or systematic bias in the GMAO assimilation model.

From Table VIII-A.3 the average of the Tmax, Tmin, and Tave bias is respectively -1.25^{o}C, 0.7^{o}C, and -0.06^{o}C which we take as an additional correction to the GEOS-4 values. Accordingly, the GEOS-4 temperature values can provide a more accurate estimate of the air temperature at a give ground site by applying both a lapse rate adjustment based upon the difference in the GEOS-4 grid cell elevation and the given ground site elevation, and an offset adjustments according to the following equation.

Eq. VIII-1. $$(T^{final})_{GEOS4} = (T^{initial})_{GEOS4} - (H_{GEOS4} - H_{GrdSite})*(LR) + (OffSet)\ ,$$

where $(T^{final})_{GEOS4}$ is the adjusted GEOS-4 Tmin, Tmax, or Tave temperatures; $(T^{initial})_{GEOS4}$ is the corresponding GEOS-4 temperatures initially obtained from the SSE/POWER web site; LR is the respective lapse rate correction for Tmin, Tmax, or Tave; OffSet is the respective values for Tmin, Tmax, and Tave; and H_{GEOS4} and $H_{GrdSite}$ are respectively the elevation of the GEOS-4 grid cell and the ground site in kilometers.

Table VIII-A.4 summarizes the values for LR and OffSet based upon our use of the NCDC meteorological data.

Table VIII-A.4. Lapse rate and offset values for adjusting GEOS-4 temperature to local ground site observations.		
	Lapse Rate ($^oC/km$)	Off Set (^oC)
Tmax	-6.22	-1.29
Tmin	-4.66	+0.66
Tave	-5.34	-0.10

Table VIII-A.5 gives the comparison statistics for the $(T^{final})_{GEOS4}$ temperatures versus the NCDC values after the values in Table VIII-A.4 have been applies to $(T^{initial})_{GEOS4}$ via Equation VIII-A.1. On average the corrections applied to the GEOS-4 data results in a zero bias between GEOS-4 values and those obtained from the NCDC stations, and RMSEs of 3.28^{o}C, 3.25 ^{o}C, and 2.42 ^{o}C for Tmax, Tmin and Tave respectively. Figure VIII-A.6 illustrates that bias between the ground observations and the GEOS-4 values after applying the lapse rate correction and offset values given in Table VIII-A.4 is independent of the elevation difference between the ground site and the GEOS-4 1-degree cell and that the average bias is also near zero.

Table VIII-A.5. Comparison of NCDC and GEOS-4 temperatures after applying lapse rate and offset corrections to GEOS-4 values.
(Lapse rate & offset corrections: Tave -->-5.34 C/km, Offet = -0.10 C ; Tmax --> -6.22 C/km, Offset = -1.29 C; Tmin -->-4.66 C/km. Offset = 0.66 C)

Year	Tmax					Tmin					Tave				
	Slope	Intercept (C)	R^2	RMSE (C)	Bias (C)	Slope	Intercept (C)	R^2	RMSE (C)	Bias (C)	Slope	Intercept (C)	R^2	RMSE (C)	Bias (C)
2006	0.98	0.44	0.92	3.31	0.10	1.00	-0.19	0.91	3.41	-0.16	1.02	-0.27	0.95	2.54	-0.03
2005	0.98	0.36	0.93	3.35	-0.06	1.00	-0.04	0.92	3.41	-0.08	1.02	-0.26	0.95	2.52	-0.09
2004	0.98	0.48	0.92	3.23	0.09	1.00	0.03	0.92	3.31	0.01	1.01	-0.17	0.95	2.43	-0.01
2003	0.96	0.72	0.92	3.35	0.09	0.99	0.18	0.92	3.31	0.12	1.00	0.00	0.95	2.53	0.03
2002	0.95	0.79	0.92	3.37	-0.10	0.98	0.21	0.91	3.37	0.05	0.99	0.03	0.95	2.53	-0.09
2001	0.97	0.14	0.93	3.25	-0.32	1.00	-0.11	0.91	3.46	-0.11	1.01	-0.37	0.95	2.48	-0.21
2000	0.98	0.57	0.93	3.23	0.20	1.00	0.02	0.92	3.29	0.04	1.02	-0.11	0.95	2.43	0.08
1999	0.98	0.51	0.92	3.18	0.08	0.99	0.24	0.92	3.18	0.15	1.01	-0.03	0.95	2.35	0.05
1998	0.98	0.51	0.93	3.07	0.19	0.99	-0.09	0.91	3.11	-0.14	1.01	-0.21	0.95	2.31	-0.05
1997	0.98	0.53	0.93	3.06	0.21	1.00	-0.25	0.92	3.13	-0.28	1.01	-0.17	0.96	2.34	-0.09
1996	0.96	0.98	0.92	3.22	0.33	0.99	0.02	0.92	3.13	-0.08	1.00	0.05	0.95	2.39	0.05
1995	0.98	0.31	0.93	3.27	-0.07	1.00	0.07	0.93	3.26	0.04	1.01	-0.15	0.96	2.41	-0.03
1994	0.98	0.25	0.92	3.49	-0.01	1.00	-0.21	0.92	3.38	-0.23	1.01	-0.22	0.95	2.56	-0.07
1993	0.97	0.53	0.92	3.37	0.03	0.99	-0.04	0.92	3.27	-0.10	1.00	0.02	0.96	2.45	0.05
1992	0.96	0.71	0.92	3.29	0.06	0.99	0.11	0.91	3.25	0.02	1.00	0.02	0.95	2.35	0.07
1991	0.96	0.59	0.92	3.47	-0.11	0.99	0.03	0.92	3.25	-0.03	1.00	0.00	0.95	2.49	0.03
1990	0.96	0.52	0.91	3.48	-0.20	0.99	0.08	0.92	3.30	0.02	1.00	0.01	0.95	2.49	0.00
1989	0.96	0.50	0.92	3.56	-0.16	0.99	0.17	0.92	3.36	0.11	1.00	0.08	0.95	2.57	0.03
1988	0.96	0.59	0.92	3.42	-0.14	0.99	0.24	0.92	3.21	0.16	1.00	0.10	0.95	2.40	0.08
1987	0.95	0.76	0.92	3.40	-0.11	0.98	0.16	0.92	3.21	0.06	1.00	0.05	0.95	2.43	0.02
1986	0.95	0.71	0.92	3.45	-0.07	0.98	0.25	0.92	3.21	0.11	0.99	0.18	0.95	2.46	0.09
1985	0.96	0.68	0.92	3.46	-0.02	0.99	0.13	0.92	3.44	0.05	0.99	0.12	0.95	2.61	0.06
1984	0.96	0.68	0.92	3.41	-0.01	0.99	0.16	0.92	3.29	0.12	1.00	0.07	0.95	2.54	0.05
1983	0.97	0.51	0.92	3.41	0.01	0.99	0.13	0.92	3.28	0.04	1.00	0.01	0.95	2.56	0.00
Average	**0.97**	**0.56**	**0.92**	**3.34**	**0.00**	**0.99**	**0.06**	**0.92**	**3.28**	**0.00**	**1.00**	**-0.05**	**0.95**	**2.46**	**0.00**
STDEV	**0.01**	**0.18**	**0.00**	**0.13**	**0.15**	**0.01**	**0.15**	**0.00**	**0.10**	**0.12**	**0.01**	**0.14**	**0.00**	**0.08**	**0.07**

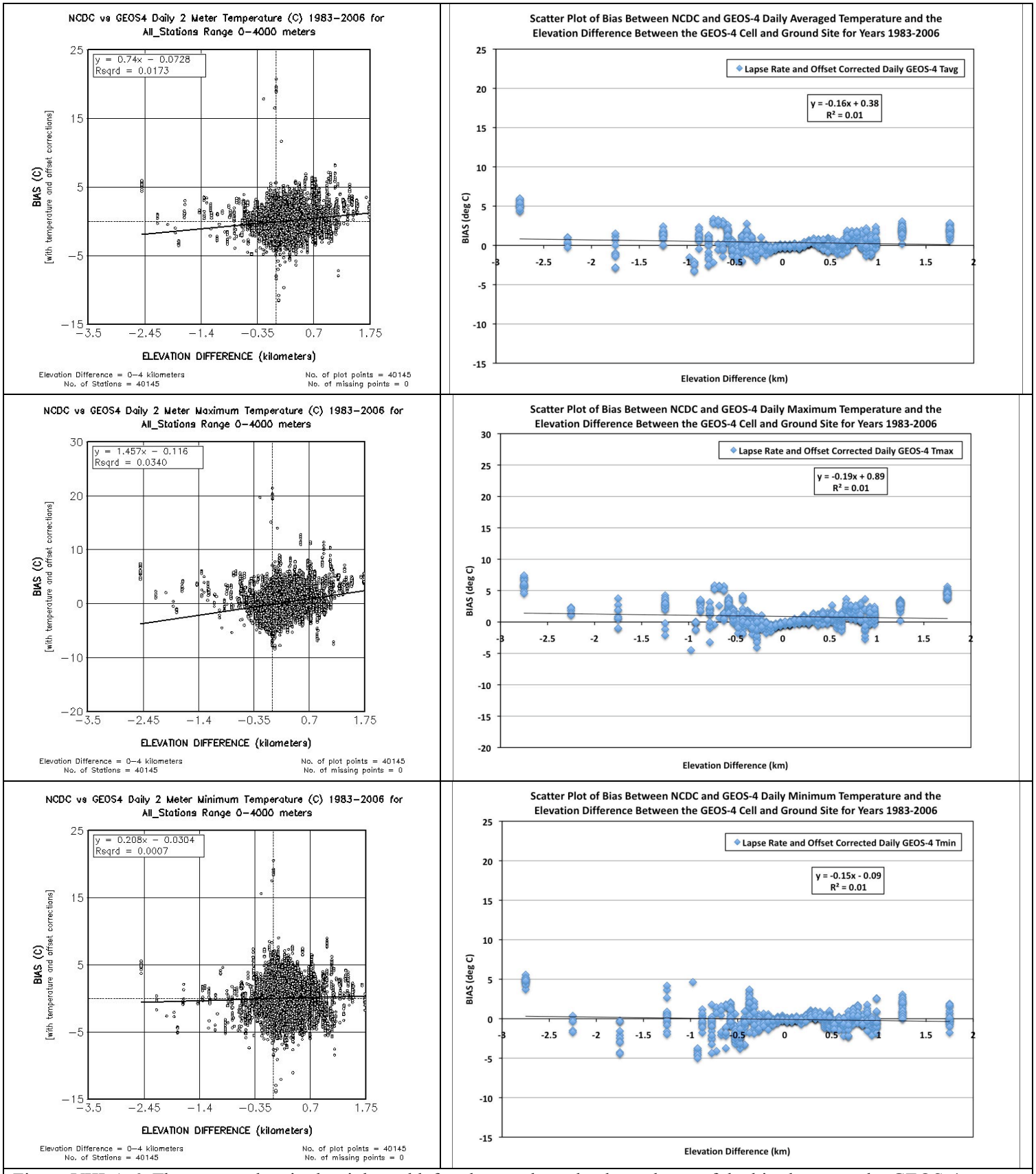

Figure VIII-A.6. The scatter plots in the right and left columns show the dependence of the bias between the GEOS-4 temperatures (T_{ave}, T_{min}, and T_{max}) and values from the NCDC archive on the elevation difference between the GEOS-4 1-degree cell and the ground station elevation for the years 1983 - 2006 after applying the lapse rate adjustments and offset corrections to the GEOS-4 temperatures. In the left column, the bias and elevation difference for all stations are explicitly plotted. In the right column, the stations have grouped into elevation difference bins (e.g. 0 to 50m; >50m to 100m; >100m to 150m; etc.) and plotted against the mean bias for the respective elevation bin.

It's important to recognize that the values given in lapse rates and offset values given in Table VIII-A.4 are based upon the globally distributed ground sites in the NCDC data base. Moreover these values are based upon yearly averaged ground and GEOS-4 data. Results from a number of studies have indicated that tropospheric lapse rates can be seasonally and regionally dependent. Accordingly, for many applications users may be able to provide lapse rate values that are more appropriate for their give location and time of year.

VIII-A.i. ***Climate Zones:*** The analysis and resulting lapse rate and offset corrections to GEOS-4 values are based upon averages of 23 years of near global observations from ground sites contained in the NCDC global "Summary of the Day" (gsod) files. An important consideration is how effective are these correction parameters when applied to more localize regions for a given year. One test of this is to evaluate their applicability in the climate zones shown in Figure VIII-A.i.1. Table VIII-A.i.1 lists the climate zone names and types.

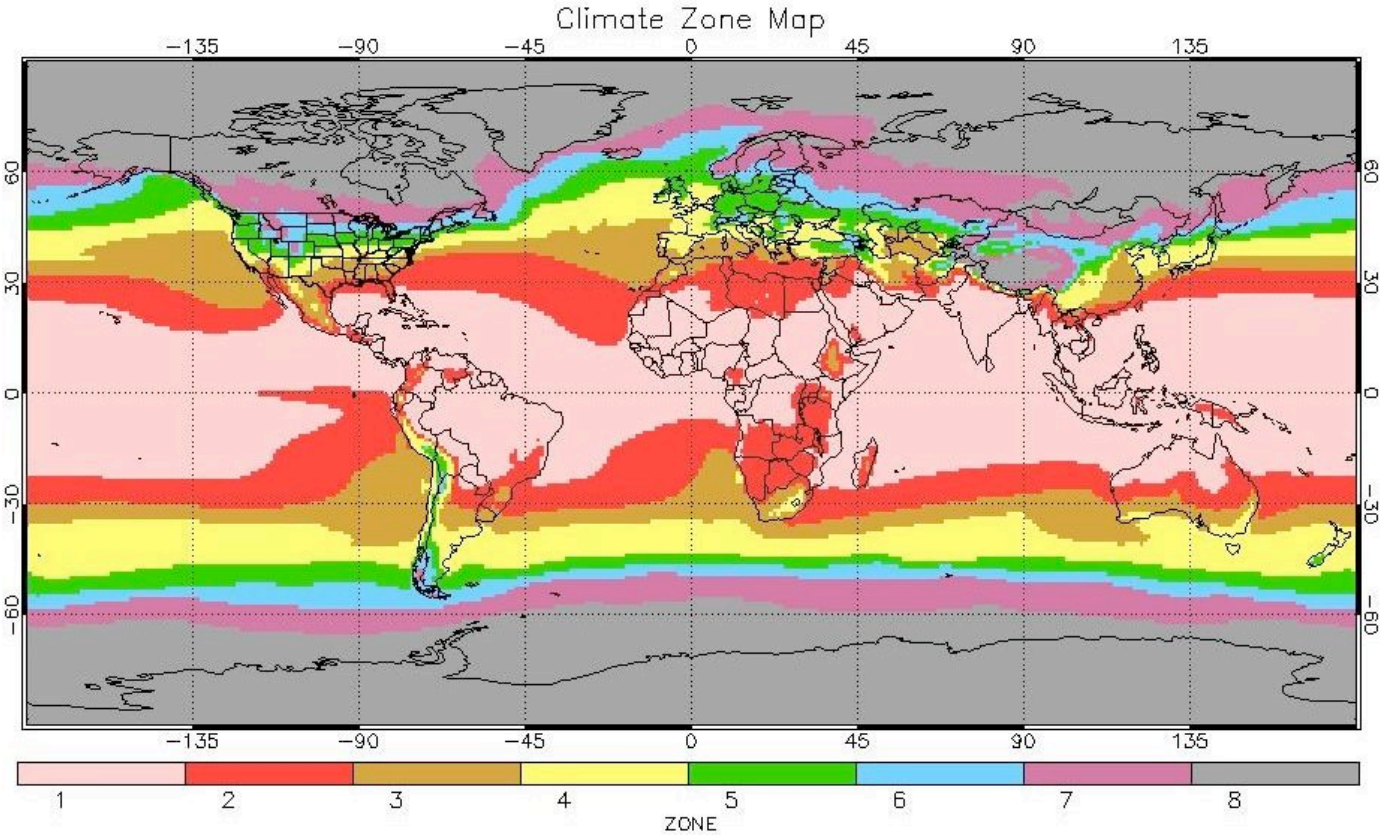

Figure VIII-A.i.1. Global map showing climate zones from GEOS-4 data using the method of Briggs, et al 2002.

Table VIII-A.i.1. Characteristic of climate zones shown in Figure VIII-A.i.1.

Zone #	Climate Zone Name and Type	Zone #	Climate Zone Name and Type
1A	Very Hot – Humid	5A	Cool – Humid
1B	Very Hot – Dry	5B	Cool – Dry
2A	Hot – Humid	5C	Cool – Marine
2B	Hot – Dry	6A	Cold – Humid
3A	Warm – Humid	6B	Cold – Dry
3B	Warm – Dry	7	Very Cold
3C	Warm – Marine	8	Subarctic
4A	Mixed – Humid		
4B	Mixed – Dry		
4C	Mixed – Marine		

Figure VIII-A.i.2a-h shows the distribution of NCDC stations for each of the 8 climate zones. Here again we have used our 85% selection criteria as a filter on the NCDC stations. [Only data from NCDC stations reporting 85% or greater of the possible 1-hourly observations per day and 85% or greater of the possible days per month were used to determine the daily Tmin, Tmax, and Tave included in comparisons with the GEOS-4 derived data.]

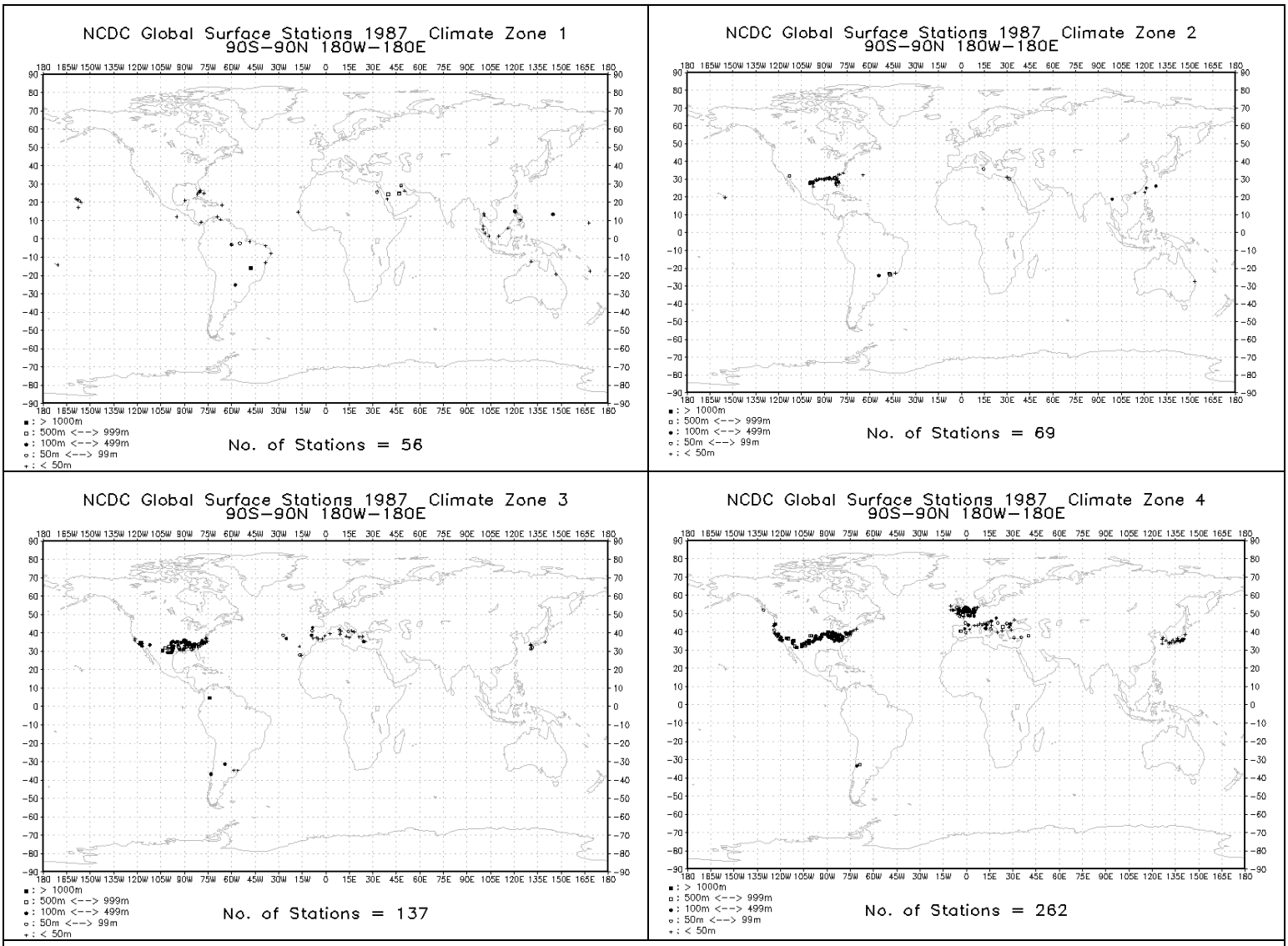

Figure VIII-A.i.2a-d. Global maps showing distribution of NCDC stations in climate zones 1-4 meeting our 85% selection criteria.

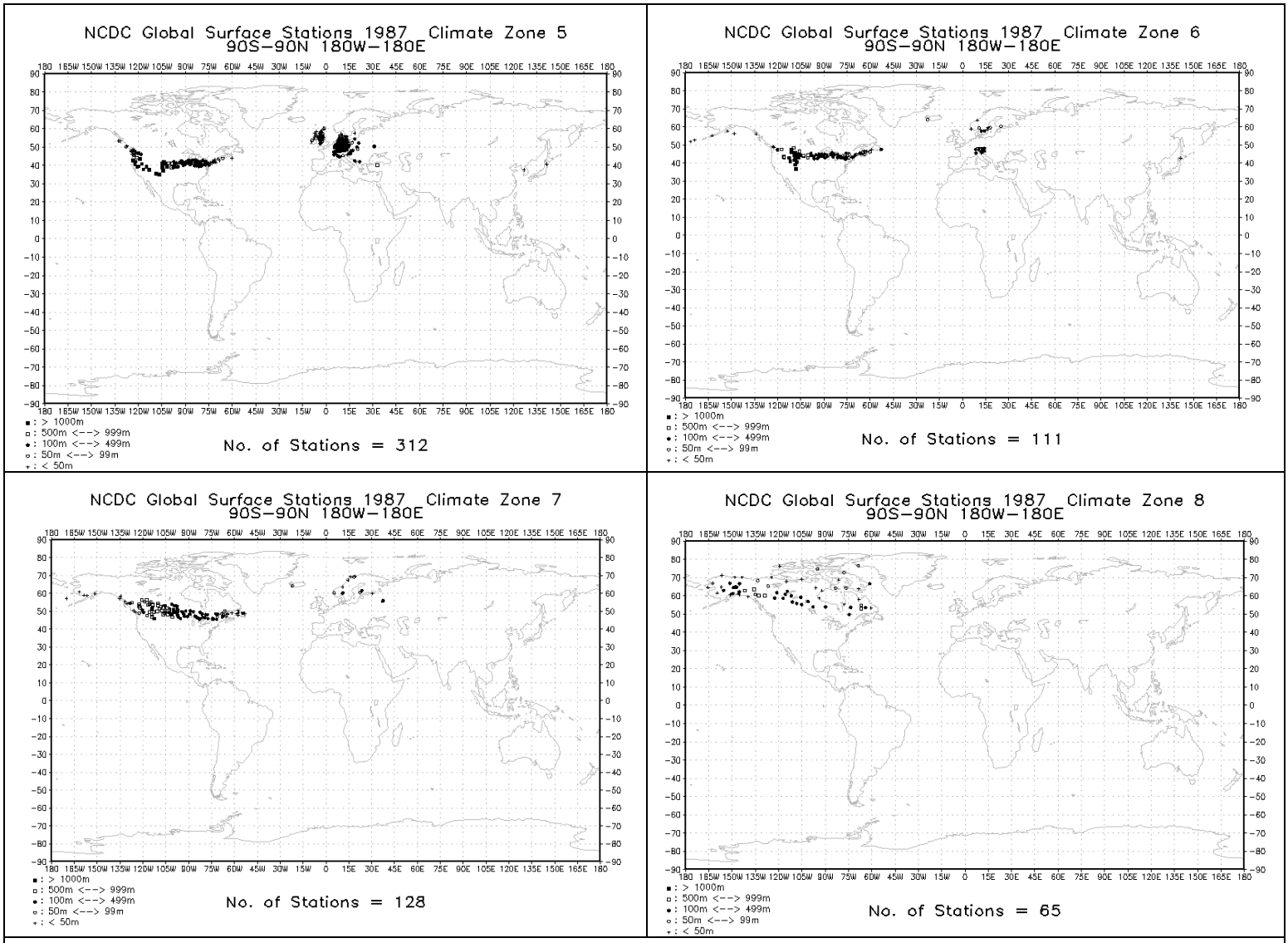

Figure VIII-A.i.2e-h. Global maps showing distribution of NCDC stations in climate zones 5-8 meeting our 85% selection criteria.

The comparison statistics given in Table VIII-A.i.2 illustrate how the biases between the uncorrected 1987 GEOS-4 temperatures and NCDC observations varies with the climate zones 1-8. The slope, intercept, and Rsqd entries are from the linear least squares fit to ensemble of GEOS-4 vs NCDC temperatures contained in each climate zone. Table VIII-A.i.3 provides similar statistics using GEOS-4 temperatures corrected as per equation VIII-A.1 using the parameters given in Table VIII-A.4.

In comparing the biases and RMSE's listed in Tables VIII-A.i.2 and VIII-A.i.3 it is clear the use of the 23 year averaged globally derived correction parameters listed in Table VIII-A.4 significantly improves the agreement between GEOS-4 and ground site observations for 1987. Moreover, since the year 1987 was arbitrarily selected as a test year, we feel justified in using the biases and RMSE values in Table VIII-A.i.2 and VIII-A.i.3 as indicative of the quality of the uncorrected and corrected GEOS-4 daily temperatures.

Table VIII-A.i.2. Comparison Statistics for climate zones shown in Figure VIII-A.i.2 for uncorrected 1987 GEOS-4 temperatures

CLZ1	Bias (C)	Rmse (c)	Slope	Intercept	Rsqd	TotNoPts	NumStns
GEOS-4 Tmax Relative to NCDC Tmax							
ClimateZone1	-2.08	3.18	0.85	2.58	0.71	20050	55
ClimateZone2	-2.08	3.53	0.79	3.45	0.79	25167	69
ClimateZone3	-2.01	3.73	0.89	0.50	0.85	49988	137
ClimateZone4	-1.41	3.49	0.88	0.66	0.89	94804	260
ClimateZone5	-1.22	3.42	0.91	0.08	0.89	113728	312
ClimateZone6	-2.79	4.58	0.94	-1.86	0.89	40466	111
ClimateZone7	-2.96	4.86	0.98	-2.70	0.89	46662	128
ClimateZone8	-3.13	5.65	0.88	-2.93	0.90	23693	65
AVERAGE =	**-2.21**	**4.05**					
GEOS-4 Tmin Relative to NCDC Tmin							
ClimateZone1	0.87	2.59	0.72	7.14	0.69	20025	55
ClimateZone2	1.33	3.21	0.84	3.96	0.83	25162	69
ClimateZone3	0.87	3.02	0.92	1.79	0.87	49988	137
ClimateZone4	0.53	2.94	0.93	1.07	0.87	94815	260
ClimateZone5	0.15	2.92	0.95	0.41	0.87	113758	312
ClimateZone6	-0.06	3.73	0.96	0.05	0.85	40485	111
ClimateZone7	-0.19	4.05	1.00	-0.19	0.86	46677	128
ClimateZone8	-0.42	5.03	0.90	-1.33	0.88	23697	65
AVERAGE =	**0.39**	**3.44**					
GEOS-4 Tave Relative to NCDC Tave							
ClimateZone1	-0.38	1.71	0.82	4.31	0.81	20052	55
ClimateZone2	0.07	2.09	0.86	3.04	0.89	25170	69
ClimateZone3	-0.18	2.21	0.95	0.65	0.92	49997	137
ClimateZone4	-0.24	2.29	0.95	0.36	0.93	94829	260
ClimateZone5	-0.37	2.20	0.97	-0.12	0.94	113777	312
ClimateZone6	-1.07	2.93	0.99	-1.01	0.93	40494	111
ClimateZone7	-1.22	3.25	1.04	-1.43	0.93	46684	128
ClimateZone8	-1.47	4.44	0.91	-1.80	0.91	23698	65
AVERAGE =	**-0.61**	**2.64**					

Table VIII-A.i.3. Comparison Statistics for climate zones shown in Figure VIII-A.i.2 using lapse rate and offset corrected 1987 GEOS-4 temperatures							
CLZ1	**Bias (C)**	**Rmse (C)**	**Slope**	**Intercept**	**Rsqd**	**TotNoPts**	**NumStns**
Corrected GEOS-4 Tmax Relative to NCDC Tmax							
ClimateZone1	-0.58	2.49	0.88	3.15	0.71	20050	55
ClimateZone2	-0.69	2.91	0.80	4.54	0.80	25167	69
ClimateZone3	-0.46	3.23	0.90	1.91	0.84	49988	137
ClimateZone4	0.49	3.02	0.92	1.96	0.90	94804	260
ClimateZone5	0.41	2.96	0.93	1.45	0.91	113728	312
ClimateZone6	-0.54	3.37	0.95	0.13	0.91	40466	111
ClimateZone7	-0.83	3.83	0.98	-0.65	0.90	46662	128
ClimateZone8	-0.53	4.58	0.90	-0.37	0.90	23693	65
AVERAGE =	**-0.34**	**3.30**					
Corrected GEOS-4 Tmin Relative to NCDC Tmin							
ClimateZone1	0.37	2.38	0.73	6.49	0.72	20025	55
ClimateZone2	0.74	2.95	0.85	3.27	0.83	25162	69
ClimateZone3	0.40	2.79	0.93	1.24	0.88	49988	137
ClimateZone4	0.34	2.76	0.95	0.72	0.88	94815	260
ClimateZone5	-0.26	2.79	0.96	-0.05	0.89	113758	312
ClimateZone6	0.01	3.44	0.97	0.10	0.88	40485	111
ClimateZone7	-0.21	3.85	1.01	-0.21	0.87	46677	128
ClimateZone8	-0.08	4.77	0.91	-0.84	0.89	23697	65
AVERAGE =	**0.16**	**3.22**					
Corrected GEOS-4 Tave Relative to NCDC Tave							
ClimateZone1	-0.10	1.58	0.84	4.02	0.83	20052	55
ClimateZone2	0.26	2.05	0.87	3.04	0.90	25170	69
ClimateZone3	0.14	2.14	0.96	0.85	0.92	49997	137
ClimateZone4	0.39	2.08	0.98	0.63	0.94	94829	260
ClimateZone5	0.02	1.88	0.99	0.13	0.95	113777	312
ClimateZone6	-0.14	2.34	1.01	-0.20	0.95	40494	111
ClimateZone7	-0.40	2.80	1.05	-0.65	0.94	46684	128
ClimateZone8	-0.24	3.95	0.93	-0.50	0.92	23698	65
AVERAGE =	**-0.01**	**2.35**					

VIII-A.ii. ***Heating/Cooling Degree Days:***

An important application of the historical temperature data is in the evaluation of heating and cooling degree days. Table VIII-A.1 and VIII-A.2 provide information relative to the use of GEOS-4 temperature corrected and uncorrected versus NCDC values to evaluate the yearly heating degree days (HDD) and cooling degree days (CDD). The HDD and CDD are based upon the daily Tmin and Tmax with a base temperature, Tbase = 18^0C. The HDD and CDD were calculated using the following equations:

Heating Degree Days: For the days of a given time period (e.g. year, month, etc.) sum the quantity [Tbase - (Tmin + Tmax) / 2] when (Tmin + Tmax) / 2 < Tbase

Cooling Degree Days: For the days of a given time period (e.g. year, month, etc.) sum the quantity [((Tmin + Tmax) / 2) - Tbase] when (Tmin + Tmax) / 2 > Tbase.

Values given in Table VIII-A.ii.1 used the uncorrected GEOS-4 temperatures while values in Table VIII-A.ii.2 used GEOS-4 Tmax and Tmin values corrected as per Eq. VIII-A.1. The bottom two rows in each table provide the overall estimates of the agreement between the two data sets for the years 1983 – 2006. The average over the years is the straight average of the values for the individual years listed in the tables. The ensemble average

results by taken the 23 years as a single group. In general, the two approaches agree as expected. It is important to note that the use of the GEOS-4 temperature adjusted for elevation differences between the GEOS-4 grid cell and ground site elevation (e.g. lapse rate correction) and the appropriate offsets result in a significant improvement in the agreements between the GEOS-4 and NCDC based HDD and CDD, particularly in the bias values.

Table VIII-A.ii.1

Table VIII-A.ii.1. Comparison of the yearly heating and cooling degree days based upon NCDC vs GEOS-4 temperature data. No corrections to GEOS-4 values.

	Heating Degree Days (Tmax, Tmin)							Cooling Degree Days (Tmax, Tmin)						
Year	Bias (HDD)	Bias %	RMSE (HDD)	RMSE %	Slope	Intercept (HDD)	R^2	Bias (CDD)	Bias %	RMSE (CDD)	RMSE %	Slope	Intercept (CDD)	R^2
1983	15.99	6.32	68.92	27.24	1.03	9.61	0.94	-4.63	-8.65	29.02	54.25	0.86	2.87	0.91
1984	16.19	6.27	64.58	25.02	1.03	8.27	0.95	-4.16	-8.18	27.32	53.67	0.86	2.97	0.92
1985	15.74	5.87	65.22	24.31	1.03	8.99	0.96	-5.81	-10.91	28.49	53.52	0.85	2.01	0.92
1986	13.91	5.49	85.47	33.75	0.98	18.07	0.91	-6.51	-12.34	28.04	53.14	0.84	2.01	0.93
1987	17.07	6.82	55.59	22.20	1.04	7.67	0.96	-6.09	-11.78	27.49	53.16	0.85	1.88	0.93
1988	14.85	6.06	65.86	26.87	1.03	6.55	0.95	-5.36	-9.80	27.96	51.09	0.86	2.42	0.93
1989	14.37	5.71	67.15	26.70	1.03	7.30	0.95	-6.12	-11.60	29.50	55.87	0.84	2.56	0.91
1990	16.48	6.94	66.99	28.20	1.04	7.47	0.95	-6.48	-11.65	29.18	52.47	0.83	2.85	0.92
1991	14.69	6.03	78.74	32.33	1.01	11.89	0.92	-6.93	-11.60	30.28	50.71	0.84	2.59	0.92
1992	12.68	5.08	79.89	32.03	1.00	11.93	0.91	-4.81	-10.33	26.01	55.84	0.85	1.95	0.92
1993	17.53	6.84	71.68	27.96	1.03	9.99	0.94	-5.18	-9.71	26.95	50.55	0.88	1.27	0.93
1994	22.63	9.14	72.58	29.31	1.05	11.43	0.95	-6.00	-10.54	28.38	49.83	0.87	1.51	0.92
1995	17.41	7.05	70.69	28.64	1.03	9.70	0.95	-5.31	-9.01	28.27	47.95	0.87	2.37	0.93
1996	9.98	4.56	99.76	45.63	0.93	25.18	0.84	-6.57	-10.56	30.59	49.14	0.86	2.20	0.92
1997	19.50	8.51	62.23	27.16	1.05	6.97	0.95	-6.33	-11.21	28.46	50.44	0.85	2.09	0.92
1998	24.65	11.56	68.35	32.06	1.09	5.74	0.94	-5.19	-8.91	27.48	47.17	0.87	2.30	0.93
1999	18.45	8.47	61.74	28.35	1.06	6.19	0.95	-3.87	-6.44	29.08	48.46	0.88	3.08	0.92
2000	17.56	7.30	67.00	27.87	1.05	6.20	0.95	-3.21	-6.02	28.05	52.57	0.88	3.13	0.92
2001	24.28	9.92	65.32	26.69	1.06	8.66	0.96	-7.06	-12.70	30.25	54.41	0.84	1.80	0.92
2002	16.61	6.92	68.13	28.38	1.03	9.81	0.94	-7.94	-13.78	30.13	52.28	0.83	1.62	0.92
2003	14.76	6.24	66.51	28.11	1.04	6.39	0.94	-5.83	-9.95	31.04	52.99	0.84	3.26	0.91
2004	16.48	6.86	90.58	37.69	1.00	17.38	0.90	-6.13	-11.64	28.19	53.52	0.84	2.23	0.92
2005	20.28	8.26	67.33	27.44	1.05	7.64	0.95	-5.73	-9.82	29.61	50.80	0.86	2.52	0.92
2006	16.38	6.69	126.99	51.82	0.91	39.46	0.81	-4.81	-8.76	29.52	53.77	0.87	2.52	0.91
Average of Individual Years	**17.02**	**7.04**	**73.22**	**30.24**	**1.02**	**11.19**	**0.93**	**-5.67**	**-10.25**	**28.72**	**51.98**	**0.86**	**2.33**	**0.92**
Ensemble Average of All Years	**17.28**		**77.20**		**1.02**	**12.47**	**0.93**	**-5.65**		**28.89**		**0.86**	**2.36**	**0.92**

Table VIII-A.ii.2

Table VIII-A.ii.2. Comparison of the yearly heating and cooling degree days based upon NCDC vs GEOS-4 temperature data. GEOS-4 values have been lapse rate and offset corrected with values listed in Table VIII-A.4.

	Heating Degree Days (Tmax, Tmin)							Cooling Degree Days (Tmax, Tmin)						
Year	Bias (HDD)	Bias %	RMSE (HDD)	RMSE %	Slope	Intercept (HDD)	R^2	Bias (CDD)	Bias %	RMSE (CDD)	RMSE %	Slope	Intercept (CDD)	R^2
1983	-0.88	-0.35	56.38	22.28	1.00	-1.84	0.96	2.75	5.13	27.08	50.62	0.95	5.29	0.92
1984	-1.33	-0.51	51.45	19.93	1.01	-3.00	0.96	2.27	4.46	25.69	50.46	0.94	5.13	0.92
1985	-2.42	-0.90	53.77	20.04	1.00	-2.87	0.97	0.79	1.48	24.42	45.92	0.94	4.24	0.93
1986	-4.31	-1.70	77.40	30.56	0.96	5.21	0.92	0.38	0.72	24.09	45.65	0.92	4.76	0.94
1987	-2.71	-1.07	58.45	23.13	0.99	-1.35	0.95	0.26	0.50	23.71	45.82	0.92	4.18	0.94
1988	-2.12	-0.87	53.74	21.92	1.01	-4.85	0.96	1.13	2.07	24.95	45.59	0.93	4.70	0.94
1989	-1.92	-0.76	56.41	22.43	1.01	-4.22	0.96	0.29	0.54	25.60	48.49	0.91	4.84	0.92
1990	0.70	0.30	51.27	21.58	1.02	-3.69	0.96	0.20	0.35	24.73	44.46	0.91	5.12	0.93
1991	-1.13	-0.46	66.52	27.31	0.99	0.45	0.94	0.64	1.07	26.54	44.43	0.93	4.73	0.93
1992	-2.79	-1.12	68.58	27.49	0.99	0.15	0.93	1.62	3.49	21.44	46.03	0.95	3.94	0.94
1993	0.54	0.21	60.03	23.42	1.01	-2.49	0.95	1.40	2.63	24.19	45.36	0.96	3.73	0.94
1994	4.73	1.91	56.80	22.94	1.03	-1.94	0.96	1.37	2.40	26.31	46.19	0.95	4.05	0.93
1995	0.43	0.17	58.03	23.51	1.01	-2.68	0.96	2.17	3.68	26.48	44.90	0.95	5.32	0.93
1996	-5.18	-2.37	92.31	42.22	0.91	14.19	0.86	2.25	3.61	28.95	46.50	0.94	5.90	0.92
1997	3.38	1.47	45.23	19.74	1.03	-4.30	0.97	1.66	2.94	24.81	43.98	0.94	4.91	0.93
1998	8.27	3.88	51.59	24.20	1.06	-5.29	0.96	2.72	4.66	25.86	44.37	0.96	5.18	0.93
1999	2.90	1.33	45.45	20.87	1.03	-4.27	0.97	3.74	6.23	27.15	45.22	0.96	6.10	0.93
2000	1.51	0.63	49.49	20.59	1.03	-6.10	0.97	3.72	6.97	25.83	48.41	0.96	5.77	0.93
2001	6.65	2.72	48.17	19.68	1.04	-3.38	0.97	0.47	0.85	27.45	49.38	0.93	4.58	0.92
2002	1.72	0.71	52.52	21.87	1.02	-2.23	0.96	-0.91	-1.59	26.17	45.40	0.91	4.09	0.93
2003	1.06	0.45	52.02	21.99	1.02	-4.52	0.96	1.70	2.89	27.26	46.53	0.93	5.66	0.93
2004	1.22	0.51	79.73	33.17	0.99	4.78	0.91	1.15	2.19	24.33	46.19	0.93	4.87	0.93
2005	4.27	1.74	50.91	20.75	1.04	-4.79	0.97	1.07	1.84	26.15	44.86	0.94	4.84	0.93
2006	1.24	0.51	119.76	48.87	0.89	27.55	0.82	2.07	3.77	26.49	48.23	0.95	4.96	0.93
Average of Individual Years	**0.58**	**0.27**	**60.67**	**25.02**	**1.00**	**-0.48**	**0.95**	**1.45**	**2.62**	**25.65**	**46.38**	**0.94**	**4.87**	**0.93**
Ensemble Average of All Years														

B. Surface Pressure:

Recognizing that improvement in the GEOS-4 temperatures can be achieved through adjustments associated with differences in the average elevation of the GEOS-4 1-degree cell and that of the ground site of interest suggest that other altitude dependent parameters, such as pressure, might also benefit in similar altitude related adjustments. Figures VIII-B.1(a-c) illustrate significant improvements in the GEOS-4 surface pressure values (p) by using the hypsometric equation (VIII-B.1), relating the thickness (h) between two isobaric surfaces to the mean temperature (T) of the layer.

(VIII-B.1) $h = z_1 - z_2 = (RT/g)\ln(p_1/p_2)$ where:
z_1 and z_2 are the geometric heights at p_1 and p_2,
R = gas constant for dry air, and
g = gravitational constant.

Figure VIII-B.1a shows the scatter plot of the GEOS-4 pressure at 2-meters versus the observations reported in the NCDC archive for 2004. Figure VIII-B.1b shows the agreement with the application of equation 1, using the 2m daily mean temperature with no correction to the GEOS-4 temperatures (e.g. no lapse rate or offset correction). Figure VIII-B.1c shows the scatter plot where the GEOS-4 surface pressure and temperature have been corrected for elevation differences. Clearly, adjustment to the GEOS-4 surface pressures using equation 1 results in significant improvements to the estimates of the NCDC station pressures.

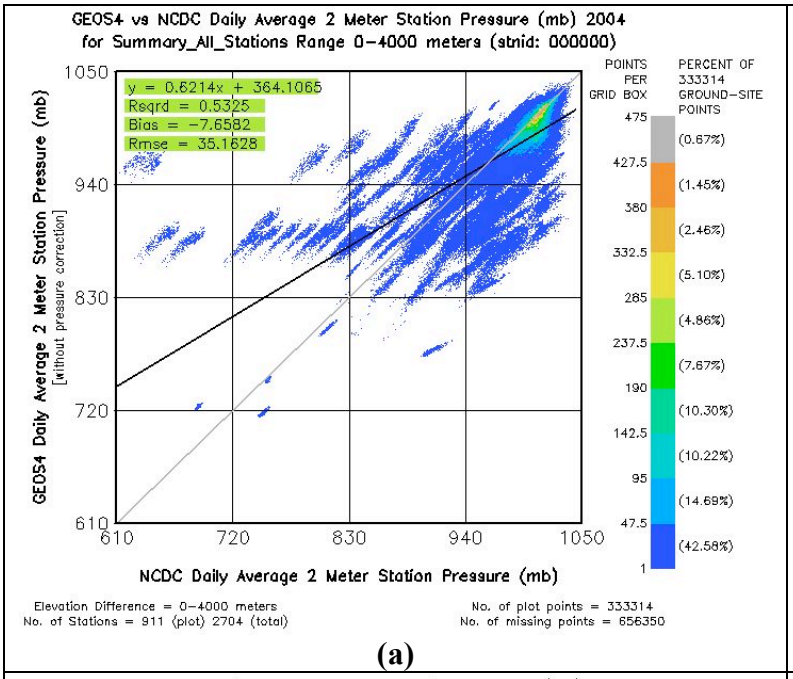

(a)

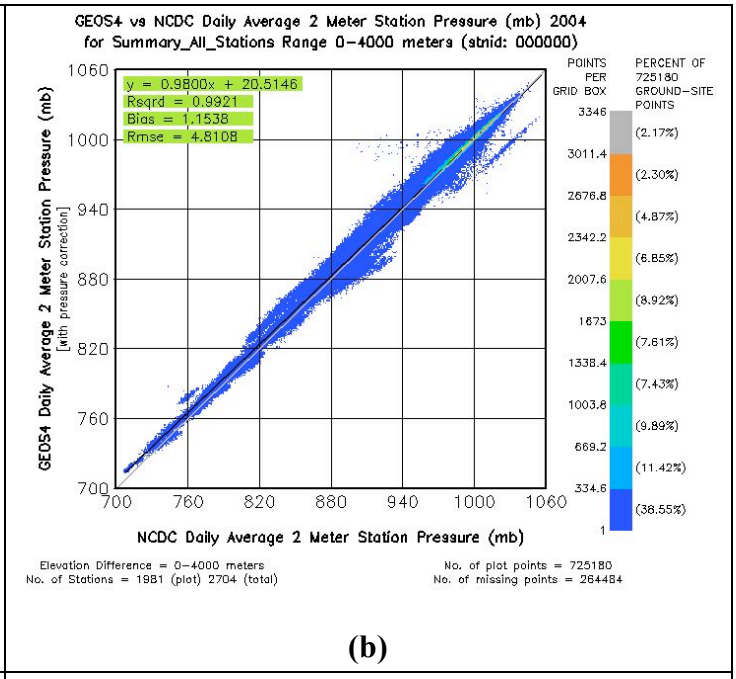

(b)

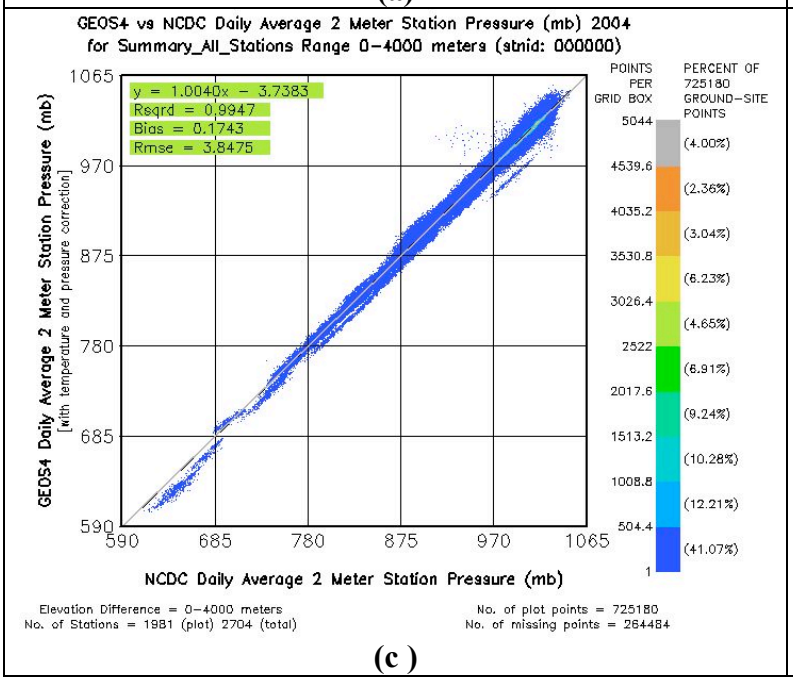

(c)

Figure VIII-B.1. Panel (a) is a scatter plot of the uncorrected GEOS-4 pressures vs. ground observation in the NCDC gsod-files. Panel (b); Panel (b) is the scatter plot of the NCDC pressures vs the GEOS-4 pressure corrected according to Eq. VIII-B.1 and the GEOS-4 2m temperature; Panel (c) is the scatter plot of the NCDC pressure and the GEOS-4 pressure according to Eq. VIII-B.1 where now the GEOS-4 temperature is also corrected according to Eq. VIII-A.1

C. Humidity (Dew Point/Frost Point) [Validation in Progress]

D. Precipitation: The precipitation data in SSE Release 6.0 has been obtained from the Global Precipitation Climate Project (GPCP - http://precip.gsfc.nasa.gov) and the Tropical Rainfall Measurement Mission (TRMM) Daily Global and Regional Rainfall derived data sets (TMPA-RT-3B42RT http://trmm.gsfc.nasa.gov/). The GPCP precipitation data product is a global 1-degree daily combination of observations from multiple platforms. Specifically,

1. Special Sensor/Microwave Imager (SSM/I; 0.5°x0.5° by orbit, GPROF algorithm) provides fractional occurrence of precipitation, and
2. GPCP Version 2 Satellite-Gauge (SG) combination (2.5°x2.5° monthly) data provides monthly accumulation of precipitation as a "scaling constraint" that is applied to the algorithms use to estimate precipitation values from :

a. geosynchronous-orbit IR (geo-IR) T_b histograms (1°x1° grid in the band 40°N-40°S, 3-hourly),
b. low-orbit IR (leo-IR) GOES Precipitation Index (GPI; same time/space grid as geo-IR),
c. TIROS Operational Vertical Sounder (TOVS; 1°x1° on daily nodes, Susskind algorithm), and
d. Atmospheric Infrared Sounder (AIRS; 1°x1° on daily nodes, Susskind algorithm).

The use of the multiple platforms enumerated above to construct the GPCP 1-Degree Daily Combination data files, in general, provides global coverage for the precipitation estimates, however missing data are not uncommon within the GPCP files. Where available, TRMM data is used to provide precipitation values for the grid points having missing data. In general, the TRMM orbital characteristics provide coverage from 40N to 40S latitude with a ¼-degree resolution. The TRMM data is taken from the ¼-degree daily averaged files, 3B42RT, and averaged to 1-degree to be compatible with the GPCP resolution, and used to fill in missing data in the GPCP file from 40S to 40N. No averaging of the GPCP and TRMM data in common grid cells is performed. Evaluation of the resulting precipitation data is discussed below.

In the remainder of this section the precipitation values provided through the SSE Release 6.0 archive for a 1-degree cell are compared with measurements made at ground sites within the same 1-degree cell. We also compare the averaged rainfall over the Continental United States (CONUS) to NCDC ground sites within the CONUS . In general, precipitation often tends to be a rather localized and short duration event. Consequently, accurately capturing the amount of precipitation even in terms of mean daily amounts from satellite observation is challenging. The precipitation data in SSE release 6.0 results are GPCP 1-degree daily mean values augmented with TRMM observations to fill in missing values in the GPCP data. The GPCP data were used as the base precipitation source since it is derived from inputs from multiple platforms and therefore was deemed to have a better chance of capturing rainfall events. The TRMM data, while having a higher spatial resolution (e.g. ¼ - degree) its polar orbit provides limited coverage of a given ground site.

Figure VIII-D.1 shows the location of three ground sites in Louisiana all within a 1-degree grid cell bounded by on the North and South by 32N and 31S latitudes respectively and on the East and West by 92W and 93W longitudes respectively. Daily mean precipitation data measured at these three sites over a 9-year period beginning in 1997 were compared to daily mean values available from the POWER/SSE Release 6.0. Figures VIII-D.2a, b, and c show the comparison of the POWER/SSE values to ground site measurements for the accumulation over 1-day and for a 5-day accumulation and for a 30-day accumulation.

Figure VIII-D.3 Illustrate the dependence of the mean bias error (MBE) and the root mean square error (RMSE) for each ground site relative to the average precipitation values from the GPSP/TRMM satellite based estimates on the number of accumulation days for this grid cell. Note that the values for the three ground sites relative to the GPCP/TRMM data are virtually identical indicating that similar rain fall was observed at each of the three sites.

Figure VIII-D.1 Location of the three ground sites in Louisiana used in the precipitation comparative study and the 1-degree grid cell over which the GPCP/TRMM precipitation is averaged.

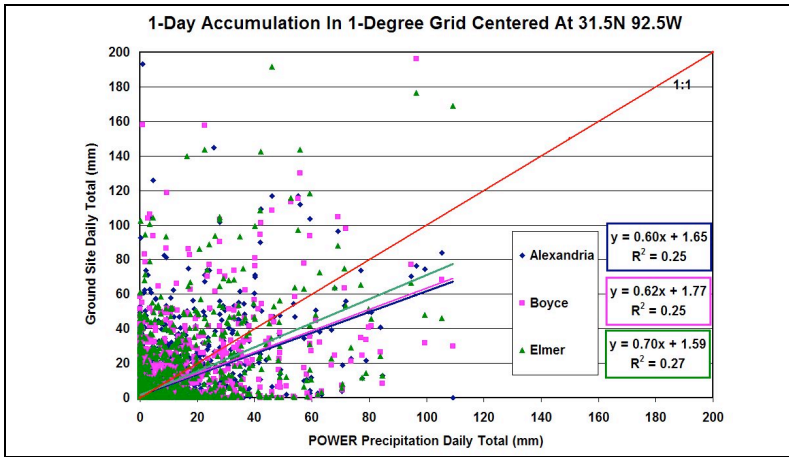

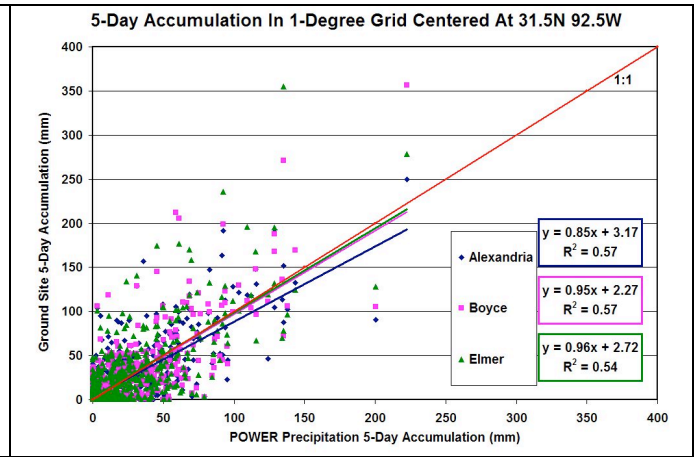

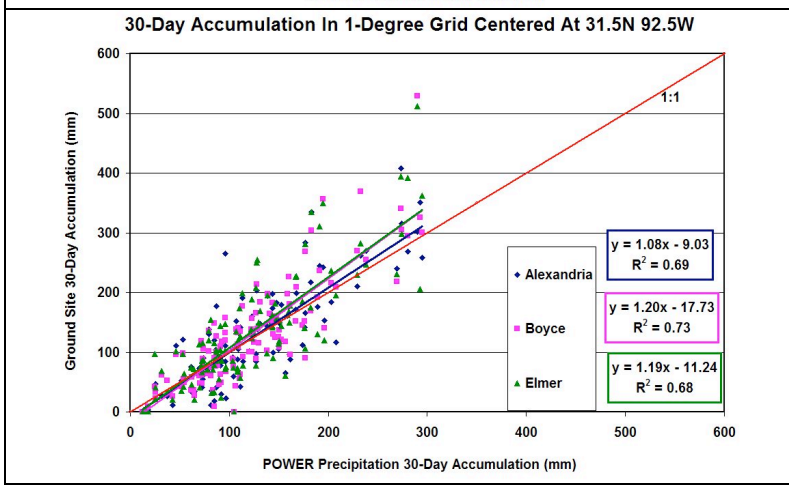

Figures VIII-D.2. Scatter plots of ground site measurements and GPCP/TRMM data for the accumulation over (a) 1-day, (b) 5-day, and (c) 30-day accumulation periods computed from precipitation data covering the 1997 – 2005 years.

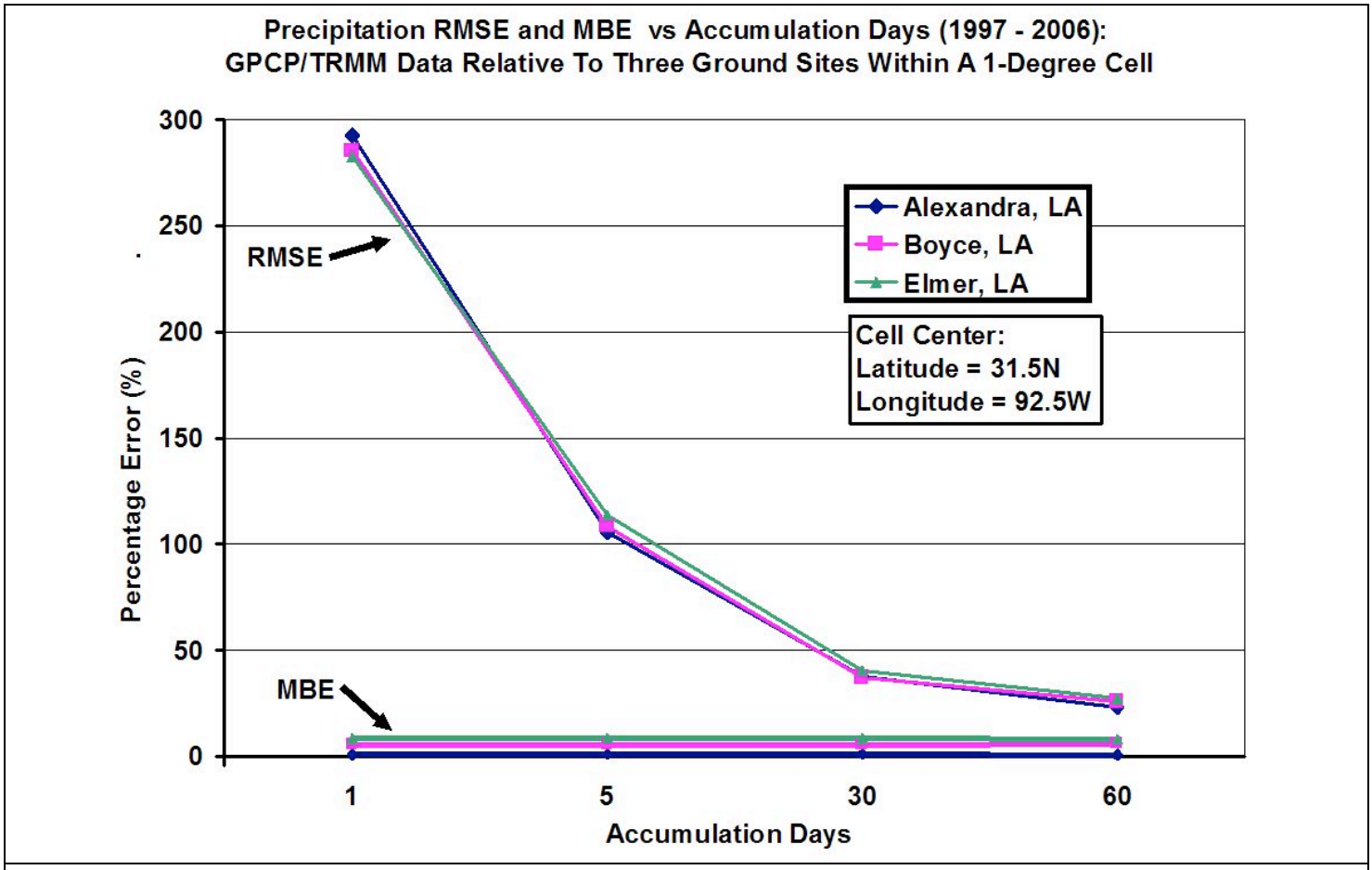

Figure VIII-D.3 The mean bias error (MBE) and root mean square error (RMSE) between ground site precipitation measurements and values from GPCP/TRMM satellite observations versus accumulation days.

IX. Wind Speed: The main focus of the wind parameters in POWER/SSE Release 6.0 continues to be applications related to power generation via wind. Accordingly, the primary emphasis was place on providing accurate winds at 50 m above the Earth's surface. Based upon analysis of the winds in GEOS-4 relative to winds provided in the previous release of SSE (i.e. Release 5.1), Release 6.0 winds continue to be based on the Version 1 GEOS (GEOS-1) reanalysis data set described in Takacs, Molod, and Wang (1994). In particular, the 50-meter velocities were derived from GEOS-1 layer 1 values using equations provided by GEOS project personnel. Adjustments were made in a few regions based on science information from Dorman and Sellers (1989) and recent vegetation maps developed by the International Geosphere and Biosphere Project (IGBP) (Figure IX-1). GEOS-1 vegetation maps were compared with IGBP vegetation maps. Significant differences in the geographic distribution of crops, grasslands, and savannas were found in a few regions. In those regions, airport data were converted to new 50-m height velocities based on procedures in Gipe (1999). GEOS-1 50-m values were replaced with the new Gipe-derived estimates in those regions. The scenes provided in SSE Release 6.0 are compared with surface observations below.

Ten-year annual average maps of 50-m and 10-m "airport" wind speeds are shown in Figure IX.2. Velocity magnitude changes are now consistent with general vegetation heights that might be expected from the scene types in Figure IX.1. Note that SSE heights are above the soil, water, or ice surface and not above the "effective" surface in the upper portion of vegetation canopies.

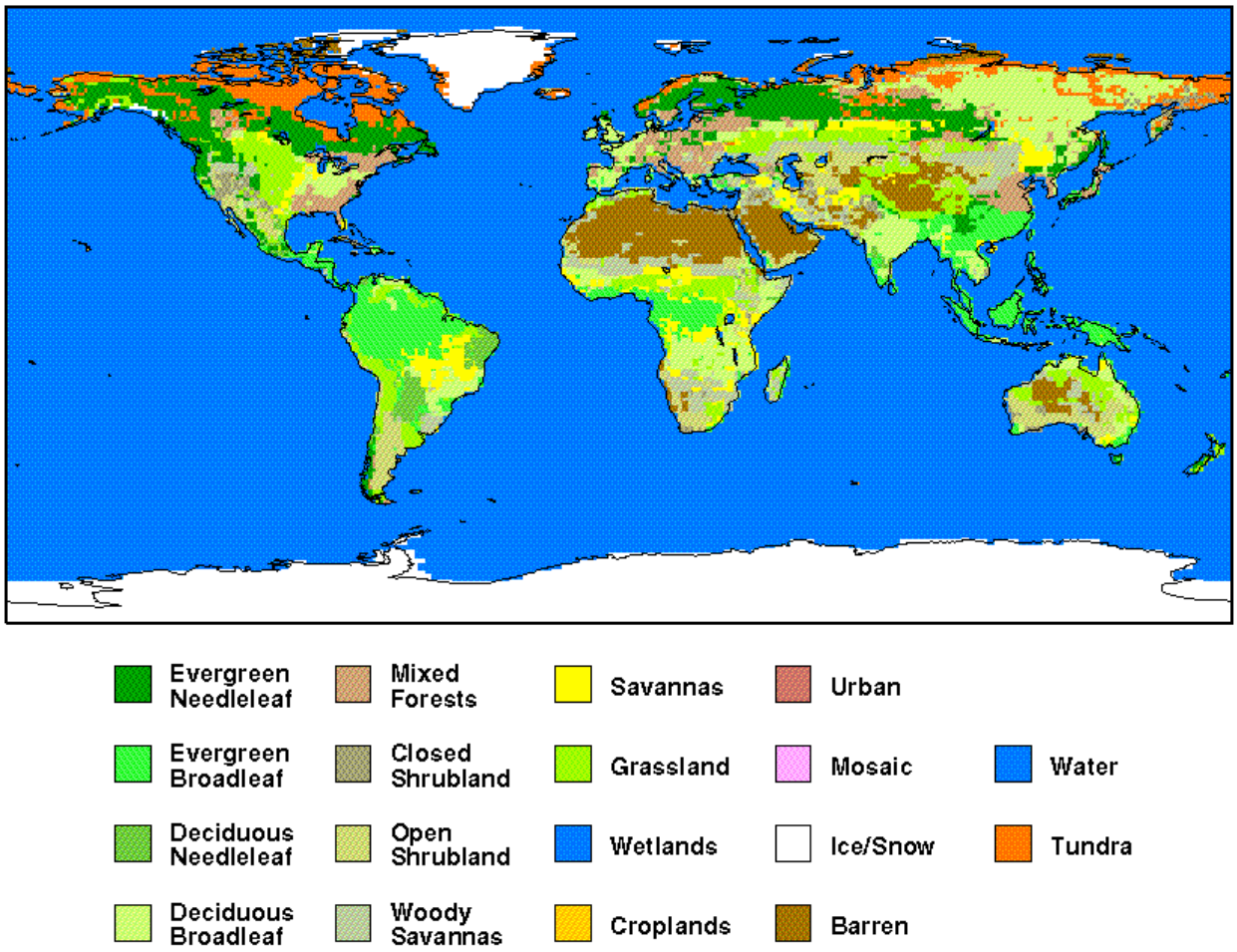

Figure IX-1. International Geosphere and Biosphere Project (IGBP) scene types.

Ten-year average SSE "airport" estimates were compared with 30-year average airport data sets over the globe furnished by the RETScreen project. In general, monthly bias values varied between ±0.2 m/s and RMS (including bias) values are approximately 1.3 m/s (Fig. IX.3). This represents a 20 to 25 percent level of uncertainty relative to mean monthly values and is about the same level of uncertainty quoted by Schwartz (1999). Gipe (1999) notes that operational wind measurements are sometimes inaccurate for a variety of reasons. Site-by-site comparisons at nearly 790 locations indicate SSE 10-m "airport" winds tend to be higher than airport measurements in remote desert regions in some foreign countries. SSE values are usually lower than measurements in mountain regions where localized accelerated flow may occur at passes, ridge lines or mountain peaks. One-degree resolution wind data is not an accurate predictor of local conditions in regions with significant topography variation or complex water/land boundaries.

Designers of "small-wind" power sites need to consider the effects of vegetation canopies affecting wind from either some or all directions. Trees and shrub-type vegetation with various heights and canopy-area ratios reduce near-surface velocities by different amounts. GEOS-1 calculates 10-m velocities for a number of different vegetation types. Values are calculated by parameterizations developed from a number of "within-vegetation" experiments in Canada, Scandinavia, Africa, and South America. The ratio of 10-m to 50-m velocities (V10/V50) for 17 vegetation types is provided in Table IX.1. All values were taken from GEOS-1 calculations except for the "airport" flat rough grass category that was taken from Gipe.

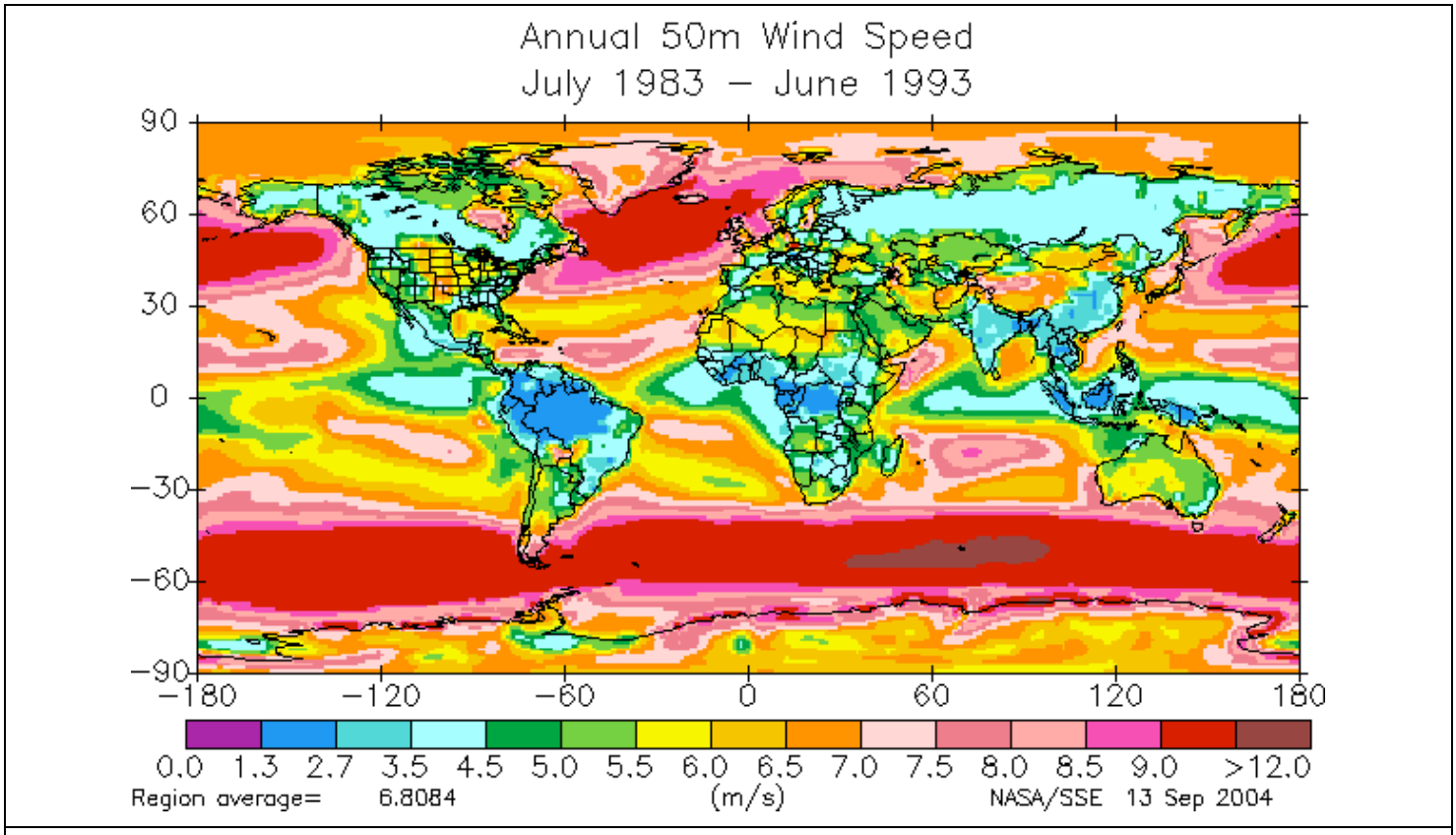

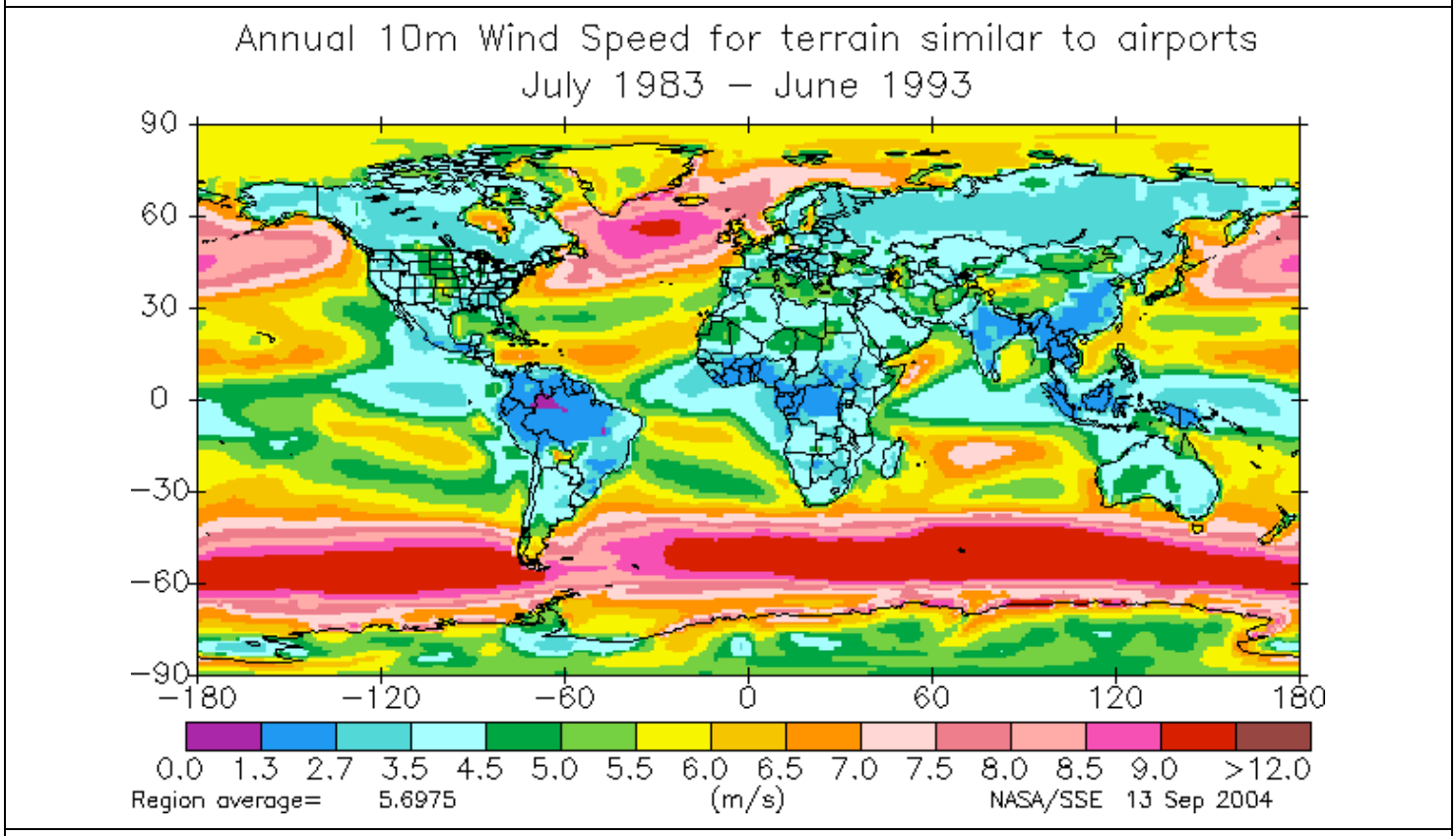

Figure IX.2. SSE Release 6.0 estimates of wind velocity at 50 and 10 meters above the ground, water, or snow/ice surface.

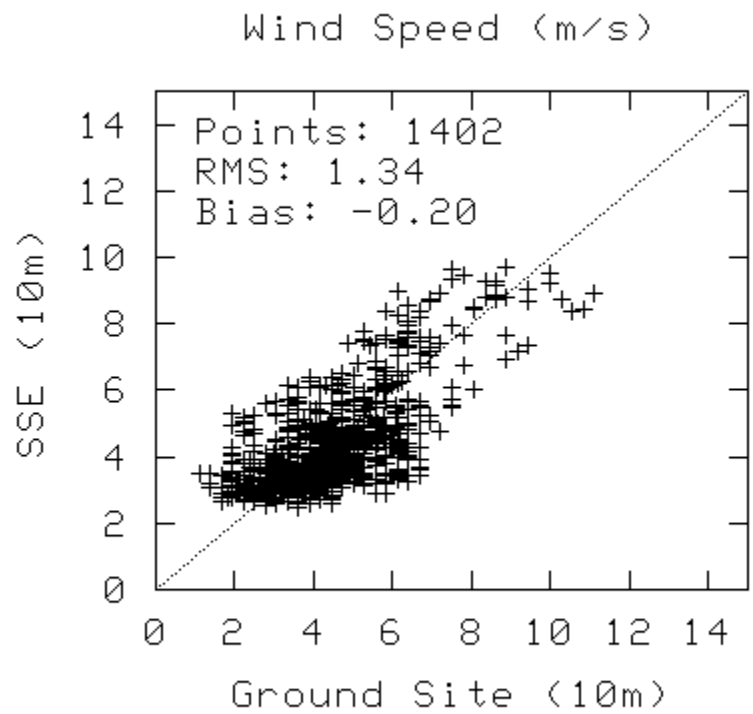

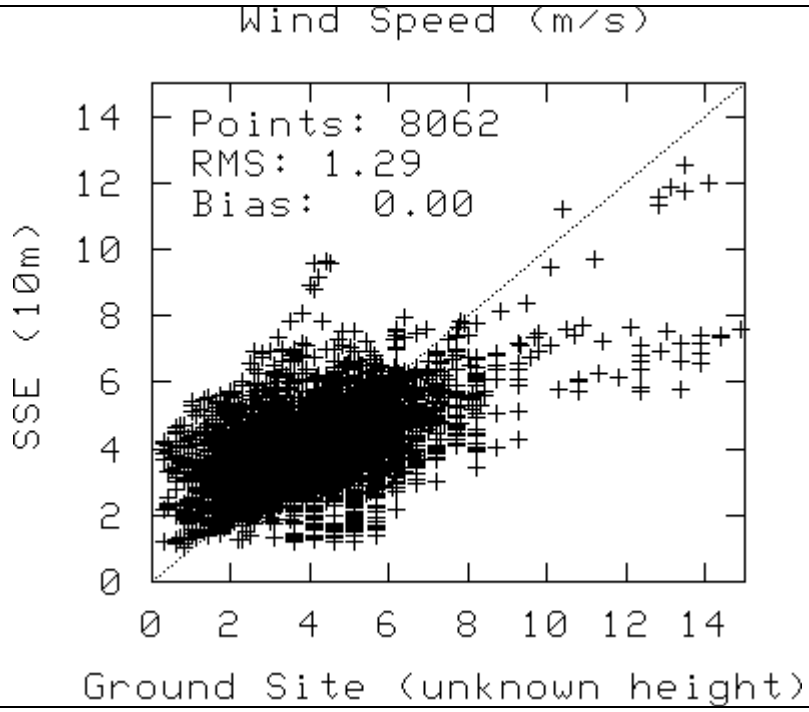

Figure IX.3. Comparison of monthly means based upon 10-year Release 6 SSE 10-m wind speed with monthly means based upon 30-year RETScreen site data.

Table IX.1. Wind Velocity V10/V50 Ratio for Various Vegetation Types.												
Northern hemisphere month	**1**	**2**	**3**	**4**	**5**	**6**	**7**	**8**	**9**	**10**	**11**	**12**
35-m broadleaf-evergreen trees (70%) small type	0.47	0.47	0.47	0.47	0.47	0.47	0.47	0.47	0.47	0.47	0.47	0.47
20-m broadleaf-deciduous trees (75%)	0.58	0.57	0.56	0.55	0.53	0.51	0.49	0.51	0.53	0.55	0.56	0.57
20-m broadleaf & needleleaf trees (75%)	0.44	0.47	0.50	0.52	0.53	0.54	0.54	0.52	0.50	0.48	0.46	0.45
17-m needleleaf-evergreen trees (75%)	0.50	0.53	0.56	0.58	0.57	0.56	0.55	0.55	0.55	0.54	0.53	0.52
14-m needleleaf-deciduous trees (50%)	0.52	0.53	0.55	0.57	0.57	0.58	0.58	0.54	0.51	0.49	0.49	0.50
18-m broadleaf trees (30%)/groundcover	0.52	0.52	0.52	0.52	0.52	0.52	0.52	0.52	0.52	0.52	0.52	0.52
0.6-m perennial groundcover (100%)	0.65	0.65	0.65	0.65	0.65	0.65	0.65	0.65	0.65	0.65	0.65	0.65
0.5-m broadleaf (variable %)/groundcover	0.65	0.65	0.65	0.65	0.65	0.65	0.65	0.65	0.65	0.65	0.65	0.65
0.5-m broadleaf shrubs (10%)/bare soil	0.65	0.65	0.65	0.65	0.65	0.65	0.65	0.65	0.65	0.65	0.65	0.65
0.6-m shrubs (variable %)/groundcover	0.65	0.65	0.65	0.65	0.65	0.65	0.65	0.65	0.65	0.65	0.65	0.65
Rough bare soil	0.70	0.70	0.70	0.70	0.70	0.70	0.70	0.70	0.70	0.70	0.70	0.70
Crop: 20-m broadleaf-deciduous trees (10%) & wheat	0.64	0.62	0.69	0.57	0.57	0.57	0.57	0.57	0.57	0.59	0.61	0.63
Rough glacial snow/ice	0.57	0.59	0.62	0.64	0.64	0.64	0.64	0.64	0.62	0.59	0.58	0.57
Smooth sea ice	0.75	0.78	0.83	0.86	0.86	0.86	0.86	0.82	0.78	0.74	0.74	0.74
Open water	0.85	0.85	0.85	0.85	0.85	0.85	0.85	0.85	0.85	0.85	0.85	0.85
"Airport": flat ice/snow	0.85	0.85	0.85	0.85	0.85	0.85	0.85	0.85	0.85	0.85	0.85	0.85
"Airport": flat rough grass	0.79	0.79	0.79	0.79	0.79	0.79	0.79	0.79	0.79	0.79	0.79	0.79
Note: 10-m and 50-m heights are above soil, water, or ice surfaces, not above the "effective" surface near the tops of vegetation.												

X. References

Bloom, S., A. da Silva, D. Dee, M. Bosilovich, J.-D. Chern, S. Pawson, S. Schubert, M. Sienkiewicz, I. Stajner, W.-W. Tan, M.-L. Wu, Documentation and Validation of the Goddard Earth Observing System (GEOS) Data Assimilation System - Version 4, Technical Report Series on Global Modeling and Data Assimilation, NASA/TM—2005–104606, Vol. 26, 2005

Braun, J. E. and J. C. Mitchell, 1983: Solar Geometry for Fixed and Tracking Surfaces. Solar Energy, Vol. 31, No. 5, pp. 439-444.

Briggs, Robert S., R. G. Lucas, Z. T. Taylor, 2003: Climate Classification for Building Energy Codes and Standards. Technical Paper, Pacific NW National Laboratory, March 26, 2002. Continue to use original climate zone definitions.

Collares-Pereira, M. and A. Rabl, 1979: The Average Distribution of Solar Radiation- Correlations Between Diffuse and Hemispherical and Between Daily and Hourly Insolation Values. Solar Energy, Vol. 22, No. 1, pp. 155-164.

Dorman, J. L. and P. J. Sellers, 1989: A Global Climatology of Albedo, Roughness Length and Stomatal Resistance for Atmospheric General Circulation Models as Represented by the Simple Biosphere Model (SiB). Journal of Atmospheric Science, Vol. 28, pp. 833-855.

Erbs, D. G., S. A. Klein, and J. A. Duffie, 1982: Estimation of the Diffuse Radiation Fraction for Hourly, Daily and Monthly average Global Radiation. Solar Energy, Vol. 28, No. 4, pp. 293-302.

Gipe, Paul, 1999: Wind Energy Basics, Chelsea Green Publishing, 122 pp.

Gupta, S. K., D. P. Kratz, P. W. Stackhouse, Jr., and A. C. Wilber, 2001: The Langley Parameterized Shortwave Algorithm (LPSA) for Surface Radiation Budget Studies. NASA/TP-2001-211272, 31 pp.

Klein, S.A., 1977: Calculation of monthly average insolation on tilted surfaces. Solar Energy, Vol. 19, pp. 325-329.

Liu, B. Y. H. and R. C. Jordan, 1960: The Interrelationship and Characteristic Distribution of Direct, Diffuse, and Total Solar Radiation. Solar Energy, Vol. 4, No. 3, pp. 1-19.

RETScreen: Clean Energy Project Analysis: RETScreen® Engineering & Cases Textbook, Third Edition, Minister of Natural Resources Canada, September 2005. (http://www.retscreen.net/ang/12.php, Engineering e-Textbook, Version 4, RETScreen Photovoltaic Project Analysis Chapter, pp. PV.15-PV.21, ISBN: 0-662-35672-1, Catalogue no.: M39-99/2003E-PDF).

Schwartz, Marc, 1999: Wind Energy Resource Estimation and Mapping at the National Renewable Energy Laboratory. NREL Conf. Pub. NREL/CP-500-26245.

Surface Weather Observations and Reports, Federal Meteorological Handbook No. 1, FCM-H1-2005, Washington, D.C., 2005

Takacs, L. L., A. Molod, and T. Wang, 1994: Volume 1: Documentation of the Goddard Earth Observing System (GEOS) general circulation model - version 1, NASA Technical Memorandum 104606, Vol. 1, 100 pp.

White, J.W. et al., Evaluation of NASA satellite- and assimilation model-derived long-term daily temperature data over the continental US, Agric. Forest Meteorol. (2008), doi:10.1016/j.agrformet.2008.05.017